

Selective Oxidation of Hydrocarbons Using Supported Gold, Silver, Copper and Bimetallic Catalysts

Thesis submitted in accordance with the requirement of Cardiff
University for the degree of Doctor of Philosophy

By

Yi-Jun Xu

September 2006

UMI Number: U584136

All rights reserved

INFORMATION TO ALL USERS

The quality of this reproduction is dependent upon the quality of the copy submitted.

In the unlikely event that the author did not send a complete manuscript and there are missing pages, these will be noted. Also, if material had to be removed, a note will indicate the deletion.



UMI U584136

Published by ProQuest LLC 2013. Copyright in the Dissertation held by the Author.
Microform Edition © ProQuest LLC.

All rights reserved. This work is protected against
unauthorized copying under Title 17, United States Code.



ProQuest LLC
789 East Eisenhower Parkway
P.O. Box 1346
Ann Arbor, MI 48106-1346

Acknowledgements

I would like to express my cordial gratitude to my supervisor, Professor Graham J. Hutchings, for his constant encouragement and advice during my PhD journey that consisted of challenges and interests. I feel very honoured to learn a lot from him, not only his broad knowledge and sharp scientific instinct on heterogeneous catalysis, but also his optimistic and kind personality.

Especially, I would like to thank Dr. Philip Landon and Dr. Dan Enache for their valuable and warmhearted suggestions on my thesis and PhD research. I would like to thank Dr. Stuart Taylor and Dr. Albert Carley for their help during my PhD research. I wish to thank Dr. Paul McMorn and Mr. Mathew Hughes for their initial work and help at the beginning of my PhD research. Thanks go to all the members of Professor Hutchings' research group and the technical staff of the School of Chemistry.

I would like to thank EPSRC for funding of the ATHENA project and the Committee of Vice-Chancellors and Principals of the Universities of the United Kingdom for providing me with an ORS Award during my PhD study at Cardiff University.

Finally, I want to express my earnest thanks to my wife, Ms. Zi-Rong Tang, and my family for their support.

Abstract (Microfiche)

Supported gold catalysts can provide tuneable activity for liquid phase selective oxidation of alkenes, in particular cyclohexene and cis-cyclooctene, using molecular oxygen from air under mild conditions. Selective oxidation can be readily kick-started using a nano-crystalline gold catalyst supported on carbon along with a small amount of TBHP as initiator. Extremely high selectivity, *ca.* 98%, for partial oxidation products with significant conversion has been obtained using a bismuth-modified gold catalyst for selective oxidation of cyclohexene. In the case of cis-cyclooctene oxidation, high selectivity to partial oxidation products has also been achieved at a high rate of reaction, without the use of solvent, which is a major tenet of green chemistry. Gold catalysts are also active for the selective oxidation of cyclohexane to cyclohexanol and cyclohexanone.

The gas-phase epoxidation of propene to propene epoxide (PO) has been studied using only molecular oxygen as oxidant over a series of supported Ag, Cu, Au and bimetallic (Au-Cu, Cu-Ag and Au-Ag) catalysts. It has been found that the support has an important effect on the catalyst performance. A Au-Cu catalyst exhibited very high selectivity to PO, *ca.* 96%, at a propene conversion, *ca.* 0.14%, at relatively low temperature, 200⁰C. The intrinsic instability of PO leads to the observation of high selectivity to PO only at low temperature.

Abstract

The liquid phase selective oxidation of alkenes, in particular cyclohexene and cis-cyclooctene, has been studied using supported gold catalysts. The results have shown that supported gold catalysts can provide tuneable activity for selective oxidation of alkenes using molecular oxygen from air under mild conditions. Selective oxidation can be readily kick-started using a nano-crystalline gold catalyst, typically gold supported on carbon, along with a small amount of TBHP as initiator. The selectivity to target partial oxidation products can be finely tuned by carefully choosing the solvent. Significantly, extremely high selectivity, *ca.* 98%, for partial oxidation products with high conversion has been obtained using a Bi-modified gold catalyst for selective oxidation of cyclohexene. In addition, an analogous effect of enhancing selectivity for partial oxidation products has been found over supported gold catalyst modified by Sn, Sb or Pb. This suggests that there is a significant scope to design and optimize supported gold catalysts with appropriate promoters in order to obtain highly selective supported gold catalysts for selective oxidation.

In the case of cis-cyclooctene oxidation, high selectivity to partial oxidation products has also been achieved at a high rate of reaction, without the use of solvent, which is a major tenet of green chemistry. Gold catalysts are also highly selective for the oxidation of cyclohexane to cyclohexanol and cyclohexanone under mild conditions.

The gas-phase direct epoxidation of propene to propene epoxide (PO) has been

investigated using only molecular oxygen as oxidant over a series of supported Ag, Cu, Au and bimetallic (Au-Cu, Cu-Ag and Au-Ag) catalysts. It has been found that the support has an important influence on the catalyst performance for selective propene epoxidation.

Over supported Ag catalysts, PO selectivity is typically lower than 40%; only in the case of Ag/SiO₂ nanopowder catalyst has high selectivity to PO, *ca.* 74%, been obtained. Supported Cu catalysts are also active for selective propene epoxidation and can exhibit either comparable or better catalytic performance than Ag catalysts. The most selective catalyst (*ca.* 81% PO selectivity with 0.36% propene conversion) comprises Cu supported on SiO₂ nanopowder. This suggests that there is a broad scope to explore Cu-based materials as inexpensive potential catalysts for propene epoxidation. Supported Au catalysts generally exhibit poor selectivity to PO.

Among the supported bimetallic catalysts, Au-Cu/ZnO can show stable performance and high selectivity to PO, *ca.* 96%, at propene conversion, *ca.* 0.14%, at low temperature. The catalytic performance is better than supported Cu or Au alone. Supported Cu-Ag catalysts give higher PO yields compared to supported Ag or Cu alone. However, supported Au-Ag catalysts are poorly active for propene epoxidation. Finally, it should be noted that the intrinsic instability of PO leads to the observation of high selectivity for all these catalysts only at low temperature (200⁰C~250⁰C).

Table of Contents

Chapter One: Introduction

1.1. History of catalysis.....	1
1.2. Definitions of catalyst and catalysis	2
1.3. Role of catalysis in chemistry	3
1.4. Categories of catalysis	4
1.4.1 Homogeneous catalysis	4
1.4.2 Heterogeneous catalysis	5
1.4.3 Enzymatic catalysis	8
1.5. Heterogeneous catalytic oxidation.....	8
1.6. Catalysis by gold, a novel catalyst.....	11
1.6.1. Historical perspective.....	11
1.6.2. Pioneering breakthroughs.....	12
1.6.2.1 Acetylene hydrochlorination over Au/C catalysts	12
1.6.2.2 Mechanism of acetylene hydrochlorination over Au/C catalyst	13
1.6.2.3 Low temperature CO oxidation over Au catalysts	16
1.6.2.4 Mechanism of CO oxidation over Au catalysts	16
1.6.3. Preparation methods of supported Au catalysts.....	22
1.6.4. Reactions catalysed by gold.....	23

1.6.4.1 Selective oxidation of alcohols	23
1.6.4.2 Water gas shift reaction and CO removal from H ₂ for fuel cell applications	28
1.6.4.3 Selective epoxidation of propene.....	31
1.6.4.4 Production of hydrogen peroxide	35
1.6.4.5 Selective hydrogenation	39
1.6.4.6 Other reactions	41
1.6.4.7 Outlook of gold catalysts	41
1.7. Catalysis by silver and copper	42
1.7.1 Catalysis by silver	42
1.7.2 Mechanism of ethene epoxidation catalyzed by Ag.....	43
1.7.3 Catalysis by copper.....	45
1.8 Objectives and outline of this thesis.....	46
1.9 References and notes	50

Chapter Two: Experimental Techniques

2.1. Introduction.....	55
2.2. X-ray powder diffraction (XRD).....	55
2.2.1 Introduction to XRD	55
2.2.2 Theoretical principles	56
2.3. BET method.....	59
2.4. Scanning Electron Microscopy (SEM).....	60

2.5. Transmission Electron Microscopy (TEM).....	63
2.6. X-ray photoelectron spectroscopy (XPS).....	65
2.7. Atomic Absorption Spectrophotometry (AAS).....	68
2.8. Reactors used in the present work	71
2.9. References and notes	72

Chapter Three: Heterogeneous Selective Oxidation of Alkenes over Supported Gold Catalysts

3.1. Introduction.....	73
3.2. Experimental.....	74
3.2.1 Preparation of gold and Bi, Sn, Sb or Pb-doped gold catalysts	74
3.2.2 Characterisation of supports and catalysts	75
3.2.3 Catalyst testing.....	75
3.3. Results and discussions	76
3.3.1 Characterisation of supports and catalysts	76
3.3.2 Selective oxidation of cyclohexene	79
3.3.2.1 Initial experiments for cyclohexene oxidation	79
3.3.2.2 Solvent effect on cyclohexene oxidation over Au/G catalyst	82
3.3.2.3 Time online studies for cyclohexene oxidation over Au/G catalyst	86
3.3.2.4 Cyclohexene oxidation over Bi-doped Au/G catalyst.....	89

3.3.2.5 Cyclohexene oxidation over Sn, Sb or Pb-doped Au/G catalyst	93
3.3.3 Selective oxidation of cis-cyclooctene.....	95
3.3.3.1 Three purposes of study of cis-cyclooctene oxidation	95
3.3.3.2 Selective oxidation of cis-cyclooctene with solvents	95
3.3.3.3 Time online studies for selective oxidation of cis-cyclooctene using solvents.....	98
3.3.3.4 Selective oxidation of cis-cyclooctene in the absence of solvent	100
3.3.4 Reaction mechanism	101
3.4. Conclusions.....	104
3.5. References and notes	105

Chapter Four: Selective Oxidation of Cyclohexane over Supported Gold Catalysts

4.1. Introduction.....	106
4.2. Experimental.....	108
4.2.1 Catalyst preparation.....	108
4.2.2 Catalyst testing.....	109
4.3. Results and discussions	110
4.3.1 Cyclohexane oxidation in the presence of solvents	110
4.3.2 Cyclohexane oxidation without solvents	112

4.3.2.1 Glass reactor reactions	112
4.3.2.2 Autoclave reactions.....	117
4.3.2.3 Reactions over Au/pretreated-graphite catalysts	118
4.3.2.4 Comparison with supported Pd or Pt catalysts.....	122
4.4. Conclusions.....	123
4.5. References and notes	124

Chapter Five: Heterogeneous Gas-phase Selective Epoxidation of Propene to Propene Oxide

5.1. Introduction.....	126
5.2. Experimental.....	131
5.2.1 Supports used for catalyst preparation	131
5.2.2 Characterisation of supports.....	132
5.2.3 Catalyst preparation.....	132
5.2.3.1 Preparation of supported Ag, Cu or Au catalysts	132
5.2.3.2 Preparation of supported Ag-Cu, Ag-Au or Cu-Au bimetallic catalysts	133
5.2.4 Reaction conditions	134
5.3 Results and discussions	136
5.3.1 Characterisation of supports.....	136
5.3.1.1 XRD analysis.....	136
5.3.1.2 BET analysis of supports	139

5.3.1.3 SEM images of supports	140
5.3.2 Propene oxidation over supported Ag catalysts	145
5.3.3 Propene oxidation over supported Cu catalysts	158
5.3.4 Propene oxidation over supported Au catalysts	170
5.3.5 Propene oxidation over supported Au-Cu catalysts	179
5.3.6 Propene oxidation over supported Cu-Ag catalysts	193
5.3.7 Propene oxidation over supported Au-Ag catalysts	205
5.4. Conclusions	210
5.5. References and notes	212

Chapter Six: Summary, Conclusion and Future Work

6.1. Summary and conclusion	215
6.2. Future work	218

Chapter One

Introduction

1.1. History of catalysis

The earliest examples of catalysis can be dated back to the dawn of civilization, at a date lost in time when mankind began to produce alcohol by fermentation. The work done during this period was sporadically documented without any effort to explain these phenomena [1]. This period in the history of catalysis ended when Berzelius systematically investigated the recorded observations and classified them as catalysis in 1835 [1]. Thereafter, more systematic research and discoveries of new catalytic processes made it quite clear that catalysis was applicable to most chemical processes and there could be significant financial gains by implementing or improving catalysis in an industrial process [2,3].

As the understanding of the process has developed, more accurate definitions have been made. For instance, Sabatier (Nobel laureate in chemistry, 1912) defined catalysis as a mechanism whereby some substances are involved in the process of accelerating a chemical reaction without being products of the reaction.

Nowadays, it is well known that catalysis plays a pivotal role in many aspects of human progress, such as in the efficient manufacture of many kinds of materials, from fuels to plastics, the creating of new energy sources, protecting the environment, and the development of effective, safer medicines [1-3].

1.2. Definitions of catalyst and catalysis

Catalysts are substances that change the rate of a reaction without being used up during the reaction. Catalysis is the word used to describe the action of the catalyst. Catalysts function by providing a reaction pathway with an alternative mechanism and low activation energy barrier, or by inhibiting the one already present. As a consequence, the rate of the reaction is increased.

For example, a hypothetical exothermic chemical reaction with or without a catalyst that leads to the same product is shown in **Figure 1.1**, wherein it can be seen that the catalyzed reaction pathway has much lower activation energy barrier than that of the uncatalyzed reaction pathway.

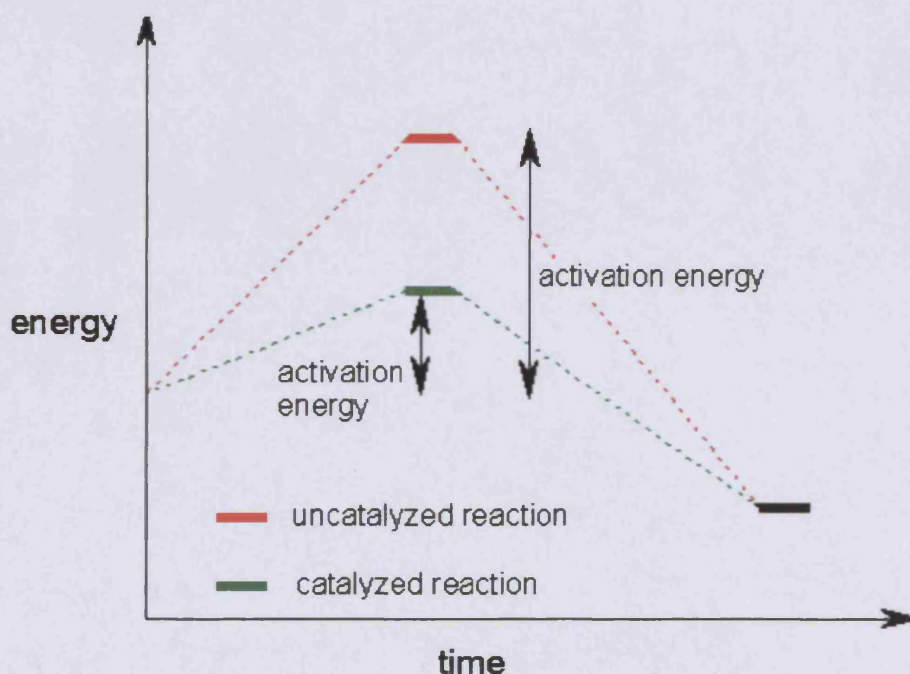


Fig. 1.1 Generic graph for the effect of a catalyst on a chemical reaction

1.3. Role of catalysis in chemistry

Catalysis is of central importance for chemistry, particularly for the modern chemical industry. 90% of the processes in the chemical industry use catalysts. Since the chemical industry is one of the most important and competitive sectors for all developed economies, it is not surprising that catalysis is an extremely active research area.

Catalysts are big business. The British agency Frost and Sullivan reported in 1998 that the European catalyst had a turnover of 3.7 billions dollars [4]. With 4% growth per year, it should approach 5 billion dollars in 2005. Catalysis in chemistry represents about a quarter of the market [4].

Catalysts have an enormous impact on the chemical industry because they:

- a. enable reactions to take place;
- b. make processes more efficient;
- c. an increase of selectivity 0.5% to 1% can lead to a up to 1 million dollar increase in operating profit;
- d. make processes environmentally friendly.

Hence, the chemical industry heavily depends on catalysis. The identification and design of new catalysts and catalysed reactions are of key importance, not only for industrial technological applications, but also from a fundamental research viewpoint. In the 21st century, catalysis will have a tremendous effect on our life.

1.4. Categories of catalysis

According to the physical state of catalyst in the reaction, catalysis can roughly be classified into two types: homogeneous catalysis and heterogeneous catalysis. In homogeneous catalysis, the catalyst and reactants are in the same phase, usually liquid. For example, the hydrolysis of an ester catalyzed by base proceeds in a homogeneous liquid phase. Whereas, in heterogeneous catalysis, the catalyst and reactants are in different phases. Heterogeneous catalysis is of considerable industrial importance and underlies major processes for the productions of fine chemicals. As well as these two kinds of catalysis, catalysis by enzymes belongs to an important type of catalysis in the biological field.

1.4.1 Homogeneous catalysis

With respect to homogeneous catalysis, one advantage is that there is good contact between the catalyst and reactants, so there is a much greater effective concentration of catalyst compared with heterogeneous catalysts. This means that to achieve the same rate milder conditions can be used and so it is possible to achieve greater selectivity. Generally, at the research and development stage it is often quicker and simpler to work with homogeneous catalysts, and then hydrogenising the system for industrial application. The big disadvantage for homogeneous catalysis is that the catalyst and the product need to be separated after reaction. The separation often involves distillation. In some cases, this makes catalyst recovery difficult because the high temperature needed for the distillation may destroy the catalyst.

1.4.2 Heterogeneous catalysis

For heterogeneous catalysis, it is clear that the advantage is that there is little difficulty in separating and recycling the catalyst. In fact, heterogeneous catalysis is used in most industrial chemical processes, for example, the Haber process for producing ammonia using hydrogen and nitrogen with a catalyst often iron catalyst, and Fischer-Tropsch process for the synthesis of hydrocarbons and other aliphatic compounds using a mixture of hydrogen and carbon monoxide with a catalyst usually containing iron or cobalt.

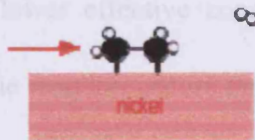
Most examples of heterogeneous catalysis generally involve the stages as described in the following:

- a. One or more of the reactants are adsorbed on to the surface of the catalyst at active sites. Simply speaking, an active site is a part of the surface which is particularly good at adsorbing molecules and facilitating reaction.
- b. There is some sort of interaction between the surface of the catalyst and the reactant molecules, which makes them more reactive. This might involve an actual reaction with the surface, or some weakening of the bonds in the attached molecules.
- c. The reaction happens. At this stage, both of the reactant molecules might be attached to the surface, or one might be attached and hit by the other one moving freely in the gas or liquid.
- d. The product molecules are desorbed. Desorption simply means that the

product molecules break away. This leaves the active site available for new molecules to attach and react.

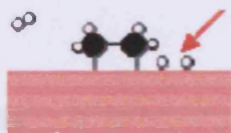
A simple example is shown in **Figure 1.2**, i.e., the hydrogenation of ethene by hydrogen in the presence of a nickel (Ni) catalyst. *A good catalyst* needs to adsorb the reactant molecules strongly enough for them to react, but not so strongly that the product molecules could not stick permanently to the surface.

Ethene molecule
adsorbed to the
surface of the nickel



Step 1

Hydrogen molecule
adsorbed and broken
into atoms



Step 2

Hydrogen atom
forms a bond with
one of the carbons



Step 3

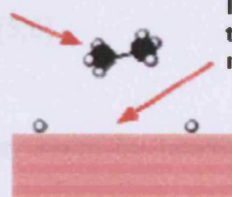
Another hydrogen
molecule adsorbed
and split into atoms



Step 4

This end breaks free

The product molecule
is now entirely free



Step 5

leaving space on the surface
to adsorb more ethene
molecules and hydrogens

Fig. 1.2 The hydrogenation of ethene using a nickel catalyst

It should be noted that there is a lower effective concentration of catalyst in heterogeneous catalyzed reactions since the reaction occurs only on the exposed active surface. Thus, to design highly active, selective and stable heterogeneous catalysts has been a great challenge in the heterogeneous catalysis community.

1.4.3 Enzymatic catalysis

In addition to heterogeneous and homogeneous catalysis, enzymatic catalysis is an important area in the field of catalysis. Virtually all living processes depend on biological catalysts called enzymes. In recent years, enzymes and enzyme-like materials have become increasingly used as catalysts for industrial processes.

1.5. Heterogeneous catalytic oxidation

Heterogeneous catalytic oxidation is a key technique used in the large-scale production of useful organic chemicals and intermediates as well as for environmental clean-up and pollution abatement [5,6].

Oxidation processes that are driven by heterogeneous catalysts can be broadly divided into two groups. The first contains selective oxidation, ammoxidation and oxychlorination, where the desired reaction product is not the most thermodynamically stable, and secondly, total oxidation, where the desired reaction products (carbon dioxide and water in the case of hydrocarbon oxidation) are the most thermodynamically stable [6]. In general, the former type of reaction is practised for the

production of bulk organic chemicals whereas the latter is practised for energy conversion or for pollution abatement.

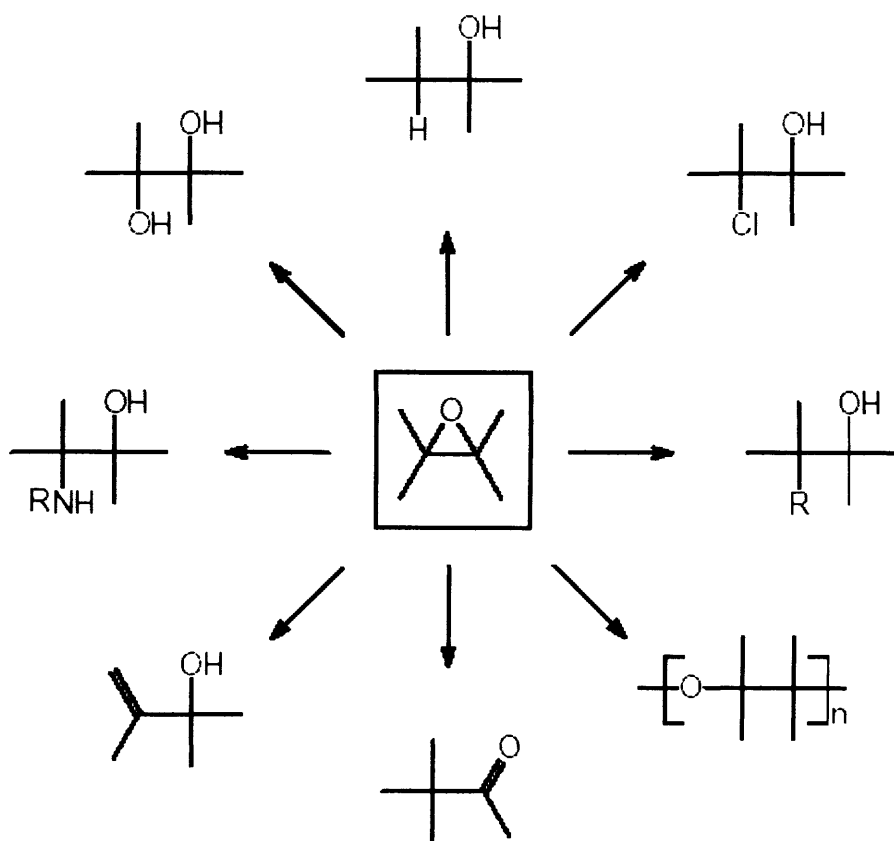
The common oxidation reactions and catalysts that are used for them are summarized in **Table 1.1**.

Table 1.1. Common oxidation processes and catalysts used [5]

Common oxidation processes			
	reaction		catalyst
total oxidation			
carbon monoxide	→	carbon dioxide	CuMnO ₂ , Au·MO _x at 25 °C, Pt·MO _x > 200 °C
sulfur dioxide	→	sulfur trioxide	Pt, V ₂ O ₅
hydrocarbons, carbon monoxide and nitrogen oxides	→	carbon dioxide, water and nitrogen	three way car exhaust catalyst, Pt, Pd
CO, VOCs	→	CO ₂ , H ₂ O	Pt, Pd/Al ₂ O ₃
selective oxidation			
butane	→	maleic anhydride	vanadium phosphates
propene	→	acrolein	MoOBi ₂ O ₇ , USb ₂ O ₇ , FeSb ₂ O ₇
propene	→	acrylonitrile	MoBi ₂ O ₇ , USb ₂ O ₇ , FeSb ₂ O ₇
o-xylene	→	phthalic anhydride	V ₂ O ₅
methanol	→	formaldehyde	iron molybdate, Ag
ethene	→	ethylene oxide	Ag
ethyl benzene	→	styrene	V ₂ O ₅ /TiO ₂
butene	→	butadiene	BiMo ₇ O ₂₀
benzene	→	phenol	Fe-ZSM-5
propene	→	propene oxide	TS-1
toluene	→	benzaldehyde	vanadium phosphates
isobutene	→	methacrylic acid	molybdophosphoric heteropolyacids
ethene	→	acetic acid	Pd-silicotungstic heteropolyacid

Selective oxidation of hydrocarbons to produce oxygen-containing organic compounds, such as alcohols, aldehydes, ketones, epoxides and acids, is of key importance for modern chemistry processes, which is also a key goal of the work presented in this thesis. The so-formed products can be used as a starting point for further chemical functionalization and can also be used to produce plastics, detergents,

paints, cosmetics and food additives. For example, the selective epoxidation of alkenes represents a major area of research because epoxides are an important and versatile class of organic compounds [7]. By means of reduction, rearrangement or ring-opening reactions with various nucleophiles, epoxides can further be transformed into diols, aminoalcohols, allylic alcohols, ketones, polyethers etc. as depicted in **Scheme 1.1**.



Scheme 1.1. Possible transformations of epoxides (R=alkyl or aryl)

1.6. Catalysis by gold, a novel catalyst

1.6.1. Historical perspective

Historically, gold has always been regarded as being catalytically inactive. The intrinsic catalytic capabilities of group VIII metals (Cu, Ag and Au) can be ascribed to the optimum degree of d-band vacancy [8]. The elements of Cu, Ag and Au have fully occupied d-bands. Because of their relatively low ionisation potentials, Cu and Ag readily lose electrons to yield d-band vacancies, therefore indicating they are potentially able to be catalytically active. As a matter of fact, in the chemical industry, Cu is used for methanol synthesis and Ag is used for ethylene oxide synthesis. In contrast, Au has a high ionisation potential and accordingly has a poor affinity towards molecules. It was demonstrated by early surface science studies and density functional calculations that no dissociative adsorption of H₂ and O₂ occurs below 473K, indicating that Au should be catalytically inactive for hydrogenation and oxidation reactions [9,10]. For these reasons, gold received very little attention in the catalysis community.

In the 1970s [11], Bond and co-workers reported the hydrogenation of alkenes and alkynes using the catalyst Au/SiO₂ and this work can be regarded as the first hint that Au might not always be poorly active when dispersed as small particles, but until recently the use of gold as a selective hydrogenation catalyst has received little attention while considerable interest and effort have been devoted to oxidation reactions catalyzed by supported gold [12].

Two important observations in the 1980s completely changed the general perception of gold and highlighted the special attributes of gold as a heterogeneous catalyst, namely:

- a. Hutchings successfully predicted that gold would be the best catalyst for acetylene hydrochlorination [13].
- b. Haruta discovered that supported Au nanoparticles are very active for low temperature CO oxidation reaction [14].

1.6.2. Pioneering breakthroughs

1.6.2.1 Acetylene hydrochlorination over Au/C catalysts

In 1982, Hutchings discovered that gold is the catalyst of choice for acetylene hydrochlorination [13]. In the early 1980s, one of the routes to the synthesis of vinyl chloride was based on acetylene hydrochlorination using mercuric chloride supported on carbon as a catalyst. This catalyst suffers from deactivation because of sublimation of the active component and therefore a replacement catalyst that was more stable was an important research goal [13,15].

The attention of Hutchings was drawn to a paper by Shinoda in which it was observed that a range of metal chlorides, over 30, supported on carbon gave a spectrum of activities for this reaction [15]. Most of the metal chlorides were divalent and the reaction of acetylene hydrochlorination could be considered as a two-electron process; hence, the decision was made to plot the data presented by Shinoda against the standard

electrode potential (**Figure 1.3**). The plot of conversion against the standard electrode potential gives a smooth curve and this predicts that gold, and more importantly Au^{3+} , will be the best catalyst for this reaction, and this hypothesis was confirmed in subsequent research reported by Hutchings [15].

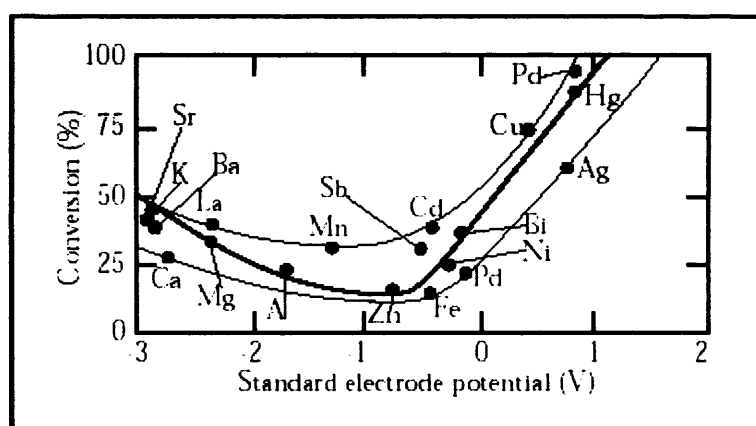


Fig. 1.3 Correlation of catalytic activity for acetylene hydrochlorination with the standard electrode potential [16]

1.6.2.2 Mechanism of acetylene hydrochlorination over Au/C catalyst

It was found that, although the gold catalysts were much more stable than the supported mercuric chloride catalysts, they still deactivated slowly with time and the rate of deactivation depended on temperature (**Figure 1.4**). The deactivation rate was at a minimum at $100\text{ }^{\circ}\text{C}$, but at this temperature the catalyst was not sufficiently active and temperatures of *ca.* $180\text{ }^{\circ}\text{C}$ are preferred. At temperatures below $100\text{ }^{\circ}\text{C}$, the deactivation was caused by deposition of polymeric carbonaceous materials and at higher temperatures the deactivation was caused by reduction of Au^{3+} to Au^0 as shown

in detailed ^{197}Au Mössbauer spectroscopy (Figure 1.5). This was a significant observation and meant that deactivation could be arrested by co-feeding dilute NO in with the reactor feedstock [15,16]. This had no effect on catalyst selectivity but prevented deactivation. Hutchings' pioneering work was the first demonstration of *in situ* reactivation of gold catalysts as well the first clear demonstration that cationic gold (Au^{3+}) can be an effective heterogeneous catalyst. Au^{3+} is the active species for acetylene hydrochlorination reaction over supported gold catalysts [15,16].

Current research in Hutchings' group has further demonstrated that supported Au catalyst exhibits unique high activity towards acetylene hydrochlorination compared to other metals or metal alloys, such as Rh, Pt, Pd, Au-Pd and Au-Pt. This suggests that there is great scope to develop supported Au catalysts for this important chemical reaction.

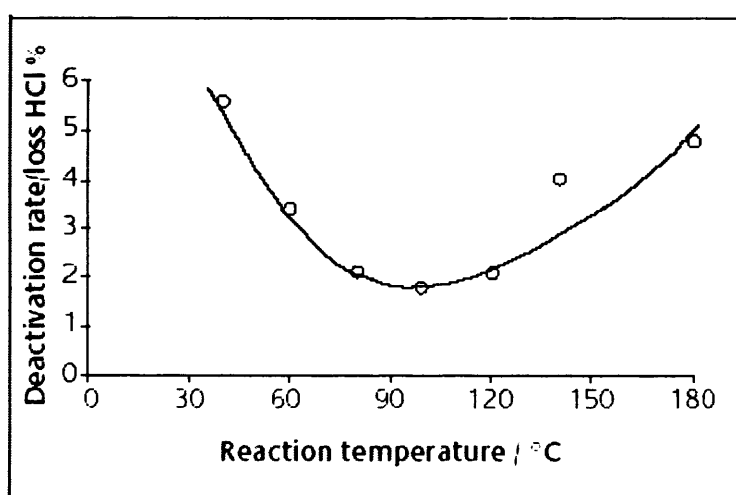


Fig. 1.4 Deactivation rate of Au/carbon catalysts for acetylene hydrochlorination as a function of temperature (0.0005 mol Au/100g catalyst, C_2H_2 : HCl = 1:1.2) [16]

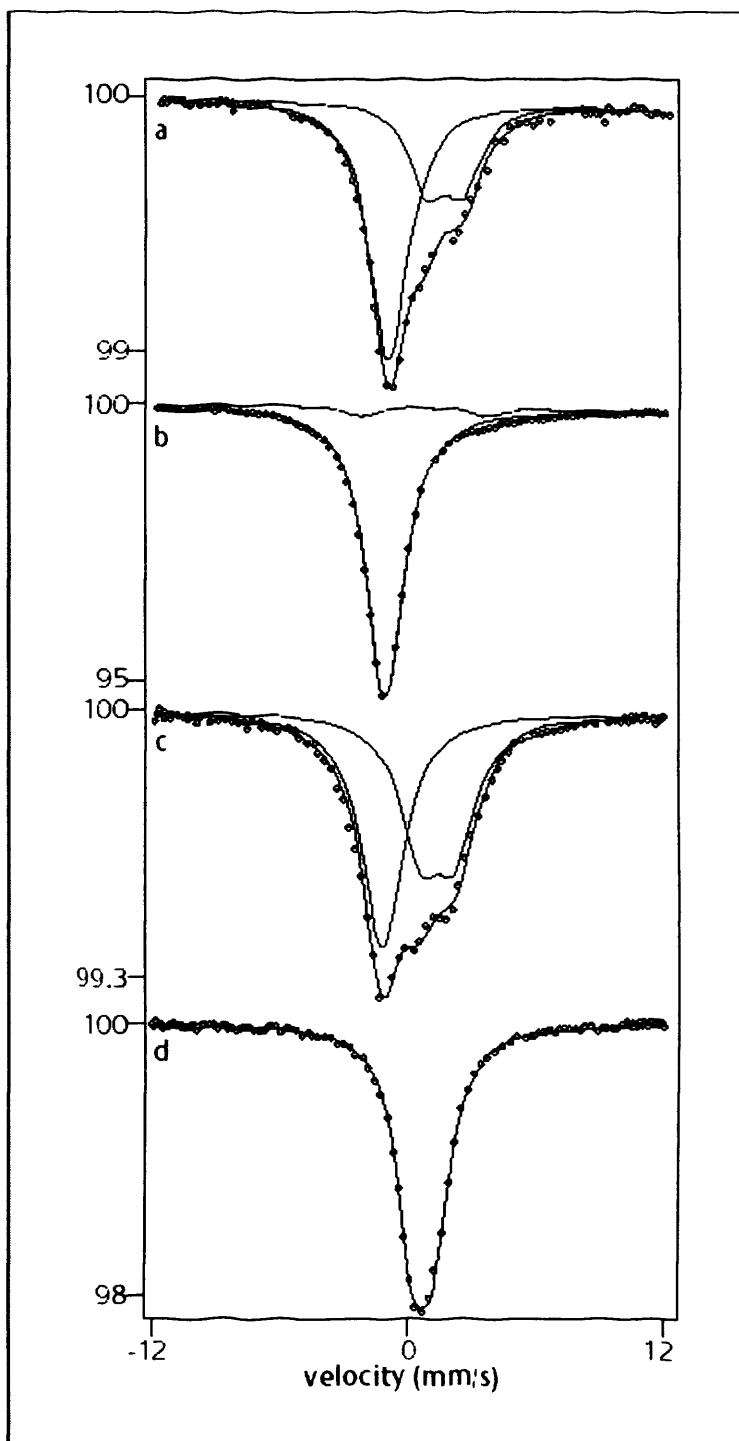


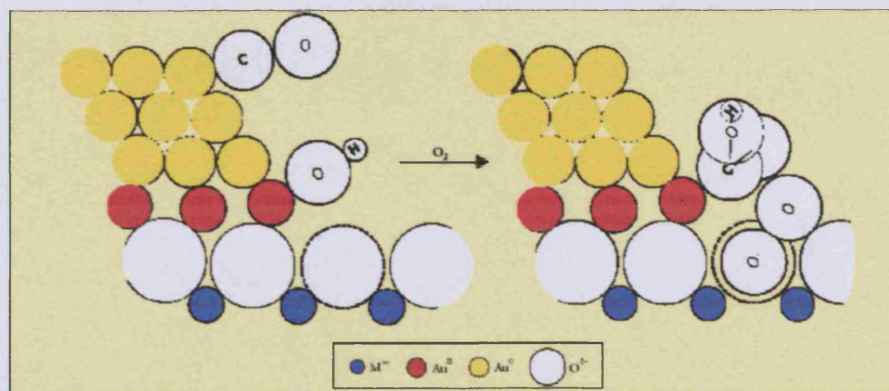
Fig. 1.5 ^{197}Au Mössbauer spectra of: (a) 2% HAuCl_4/C adsorbed on activated carbon from an aqua regia solution, (b) the catalyst after deactivation at 180°C for 6 h ($\text{GHSV} = 1140 \text{ h}^{-1}$, $\text{C}_2\text{H}_2 : \text{HCl} = 1:1.1$), (c) a sample of the same type after reactivation by boiling in aqua regia, and (d) crystalline $\text{HAuCl}_4 \cdot x\text{H}_2\text{O}$ [16]

1.6.2.3 Low temperature CO oxidation over Au catalysts

Also, in the early 1980s, Haruta recognised that supported gold nano-particles could be surprisingly highly active catalysts for the oxidation of CO at very low temperatures and in particular at temperatures below 0 °C [14]. This represents extremely high activity and is not able to be replicated by other metals. This significant discovery spurred a great deal of the research interest that is being performed in the area of gold catalysis today. More importantly, this early research indicated that gold catalysts must be prepared in an appropriate manner. Many of the active catalysts are typically found to comprise small crystallites, 2–4nm in diameter, of gold supported on an oxide. What is more, CO oxidation is now being used by many researchers as a standard test reaction to explore the fundamental reaction mechanism and, therefore, to understand the active sites of gold catalysts.

1.6.2.4 Mechanism of CO oxidation over Au catalysts

For acetylene hydrochlorination using Au/C catalyst, Hutchings demonstrated that Au³⁺ is the active species responsible for the reaction [15,16]. However, there has been much debate concerning the nature of the active site for CO oxidation using gold catalysts. Bond and Thompson proposed a model where they suggested that Au atoms at the interface between the Au particle and the oxide are the active centres for CO oxidation over supported Au catalysts (Scheme 1.2) [17].



Scheme 1.2. Bond-Thompson mechanism for CO oxidation [17]

This model implies an important role for the interface between the gold particles and the support, which has been partly confirmed by subsequent studies. Nevertheless, in this model, it still remains unclear whether Au^{3+} or Au is the active form of gold.

Using a model system in combination with STM and STS spectroscopy (**Figure 1.6**), Goodman group reported an unusual size dependence of gold clusters on TiO_2 for the low-temperature catalytic oxidation of CO and suggested this observed reactivity could be attributed to the quantum size effect of the very small gold nanoparticles [18]. Only particles in the range of 2 to 3 nm are active. This effect has been ascribed to oxidation of the Au atoms that are in contact with the support, hence illustrating the importance of tuning the electronic properties of the gold nanoparticles to achieve high catalytic activity.

Furthermore, the Goodman group recently reported that the well-ordered bi-layer Au films on TiO_2 show unprecedented catalytic activity for CO oxidation as compared to the monolayer Au film model system that is significantly less active [19]. In this

paper, they reported that gold is no longer in the form of nano-particles, but as a supported bi-layer film on TiO_2 and has a catalytic activity for CO oxidation about 45 times higher than that of Au clusters supported on TiO_2 .

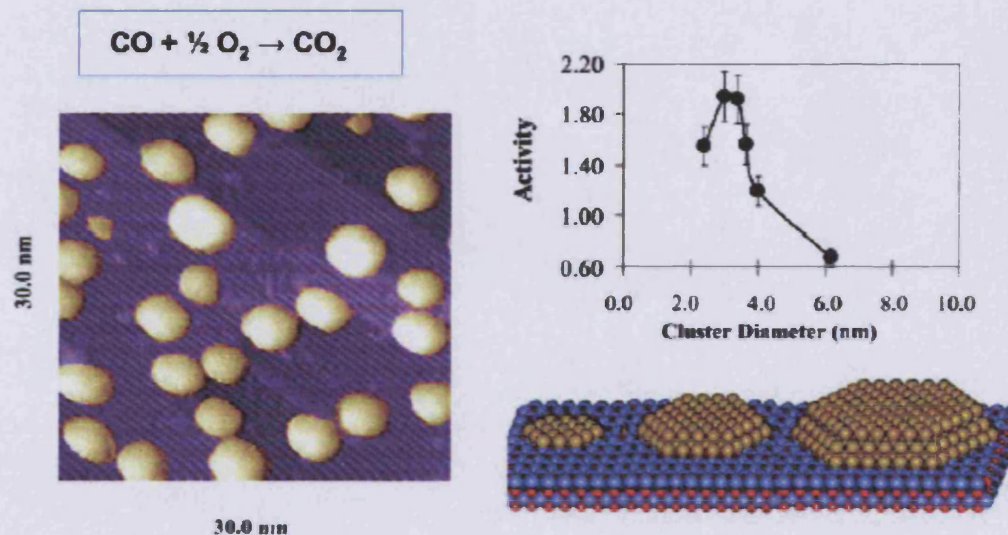


Fig. 1.6 Effect of Au particle size of Au/ TiO_2 catalysts for CO oxidation [20]

Nørskov *et al* reported using a ten gold atom model cluster coupled with density functional calculations and showed that the activation of CO was energetically favoured on Au particles containing 10 atoms (**Figure 1.7**) [21]. In both reaction pathways, the reaction barriers are less than 0.4eV, indicating that CO oxidation should be possible well below room temperature. Nørskov's study suggests that having small particles is not enough, and that the size and shape of the particles are both important parameters for CO activation and oxidation. Boyen and co-workers suggested that Au particles containing 55 atoms that are 1.4nm in diameter are very stable and could be the active site for CO oxidation [22].

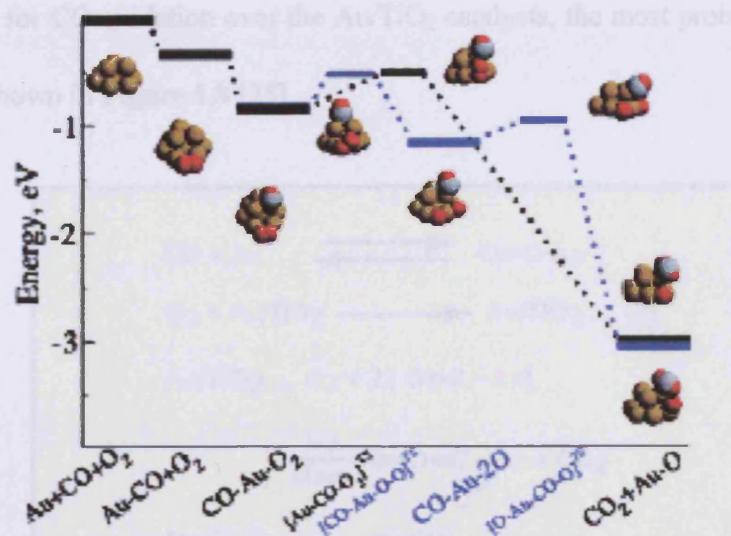


Fig.1.7 Reaction profiles for CO oxidation on Au₁₀ particles. Thicker lines represent stable states, while thinner lines correspond to transition states. Yellow spheres represent Au atoms, red spheres represent O atoms, and grey spheres represent C atoms.

Black colour: direct path where the adsorbed O₂ directly reacts with CO;

Blue colour: indirect path where the O₂ is dissociated at first and then react with molecular CO [21]

By using density functional theory with a slab model, Liu *et al* reported that the interface between Au and the oxide can oxidize CO with a very low activation barrier, with the TiO₂ support enhancing the electron transfer from the Au to the antibonding states of O₂, supporting the model proposed by Bond and Thompson [23]. That is, the peripheries act as primary reaction zones. Hammer *et al* and Yoon *et al* have also found analogous support effects in Au/MgO systems [24].

To date, for CO oxidation over the Au/TiO₂ catalysts, the most probable pathway suggested is shown in **Figure 1.8** [25].

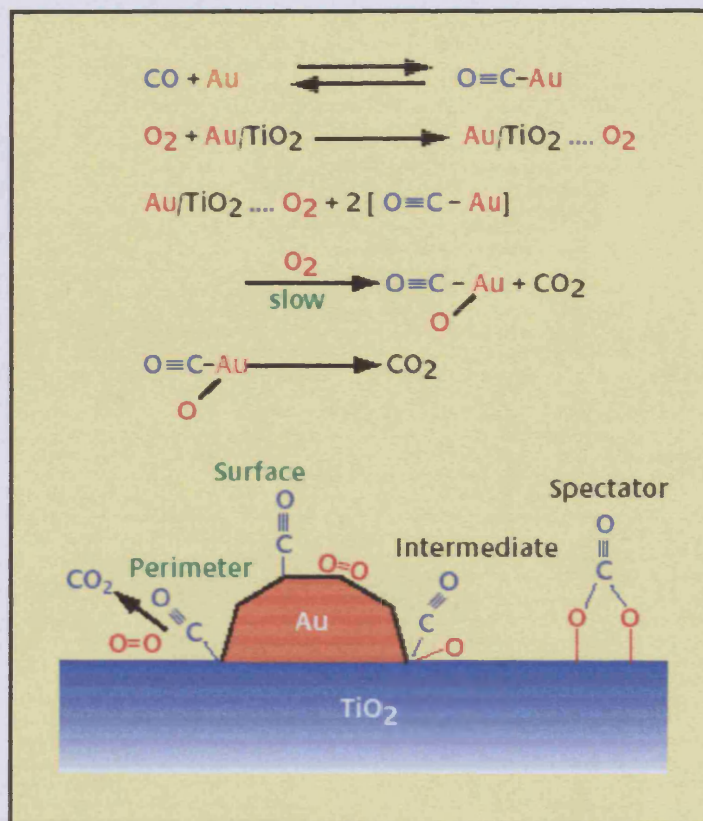


Fig.1.8 Possible pathways for CO oxidation over Au/TiO₂ [25]

Recently, a direct correlation has been found for the catalytic CO oxidation and the concentration of F-centres of a MgO support (**Figure 1.9**), implying a critical role of surface F-centers in the activation of Au in Au/MgO catalysts [26]. Corma's group has shown that nanocrystalline CeO₂ support is able to increase the activity of Au nanoparticles for CO oxidation by two orders of magnitude as compared to the regular support, suggesting that a strong synergetic effect between the metal oxide support and Au exists at the interface and that a support with special morphology and structure can

influence the catalytic properties of the as-prepared supported gold catalyst [27]. Guzman *et al.* used extended X-ray adsorption fine structure (EXAFS) and X-ray absorption near-edge spectroscopy (XANES) to characterize the average particle size and the oxidation states of Au on MgO catalyst for CO oxidation, and reported that the catalytic activity of supported gold increased with an increase in the ratio of cationic gold (Au^+) to metallic gold up to 60% and then levelled off (Figure 1.10) [28].

Hutchings and co-workers showed that Au^{3+} in $\text{Au}/\text{Fe}_2\text{O}_3$ was an important component of very active catalysts for CO oxidation, strongly suggesting that the active site for heterogeneous catalysts may vary with the composition of the as-prepared catalyst [29].

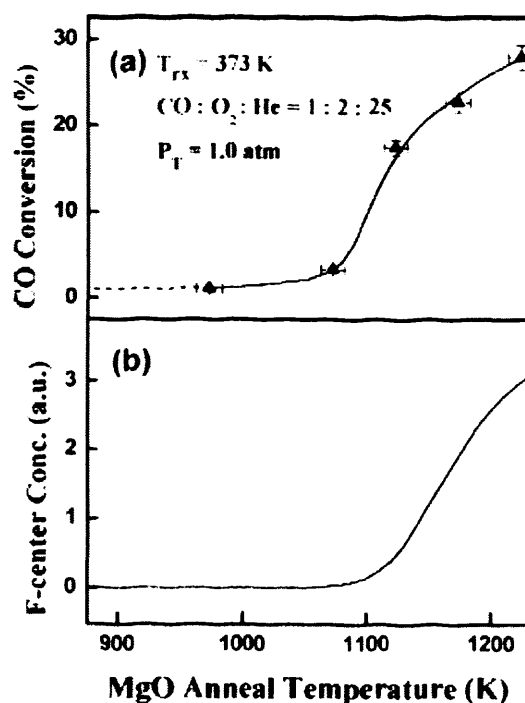


Fig. 1.9. Conversion of CO to CO_2 by Au/MgO as a function of annealing temperature [26]

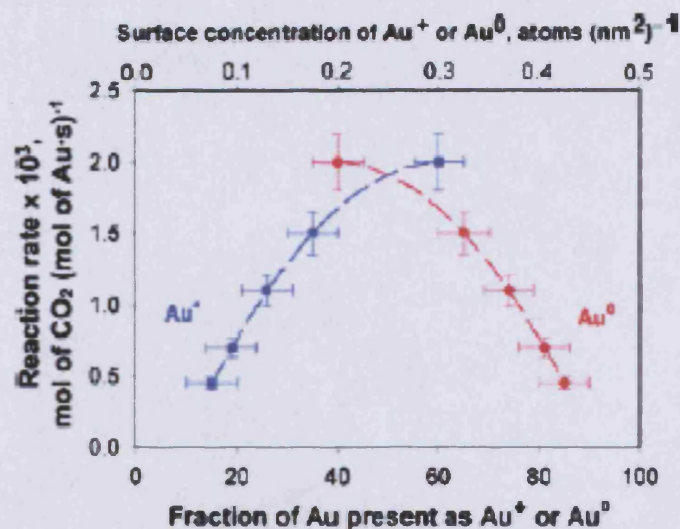


Fig. 1.10. Correlation of the catalytic activity with the percentage and surface concentration of cationic and zero-valent Au (the concentrations of Au were calculated on the basis of the approximate surface area of MgO) [28]

1.6.3. Preparation methods of supported Au catalysts

It has now been well demonstrated that heterogeneous gold catalysts, when prepared in an appropriate manner (Table 1.2 showing four categories of preparation techniques that lead to the deposition of Au nanoparticles with diameters below 10nm), are highly active and selective for a number of reactions, often at lower temperatures than existing commercial catalysts [30,31].

The particle size, support materials, structure, and preparation methods are important properties for creating a good supported gold catalyst [30,31]. Through appropriate preparation of supported gold catalysts, gold is expected to contribute much to the development of highly selective and green chemical processes.

Table 1.2. Preparation techniques for nanoparticles gold catalysts [31]

Categories	Preparation techniques	Support materials
Preparation of mixed precursors of Au and the metal component of supports	coprecipitation (hydroxides or carbonates) CP	Be(OH) ₂ , TiO ₂ *, Mn ₂ O ₃ , Fe ₂ O ₃ , Co ₃ O ₄ , NiO, ZnO, In ₂ O ₃ , SnO ₂
	amorphous alloy (metals) AA	ZrO ₂
	co-sputtering (oxides) in the presence of O ₂ CS	Co ₃ O ₄
Strong interaction of Au precursors with support materials	deposition-precipitation (HAuCl ₄ in aqueous solution) DP	Mg(OH) ₂ *, Al ₂ O ₃ , TiO ₂ , Fe ₂ O ₃ , Co ₃ O ₄ , NiO, ZnO, ZrO ₂ , CeO ₂ , Ti-SiO ₂
	liquid phase grafting (organogold complex in organic solvents) LG	TiO ₂ , MnOx, Fe ₂ O ₃
	gas phase grafting (organogold complex) GG	all kinds, including SiO ₂ , Al ₂ O ₃ -SiO ₂ , and activated carbon
Mixing colloidal Au with support materials	colloid mixing CM	TiO ₂ , activated carbon
Model catalysts using single crystal supports	vacuum deposition VD (at low temperature)	Defects are the sites for deposition, MgO, SiO ₂ , TiO ₂

* The addition of Mg citrate during or after co-precipitation or deposition-precipitation is important for depositing Au as nanoparticles

1.6.4. Reactions catalysed by gold

Heterogeneous supported Au catalysts can catalyse many reactions other than low temperature CO oxidation and acetylene hydrochlorination as mentioned above. Some typical reactions catalysed by supported gold nanoparticles in the open literatures are listed below.

1.6.4.1 Selective oxidation of alcohols

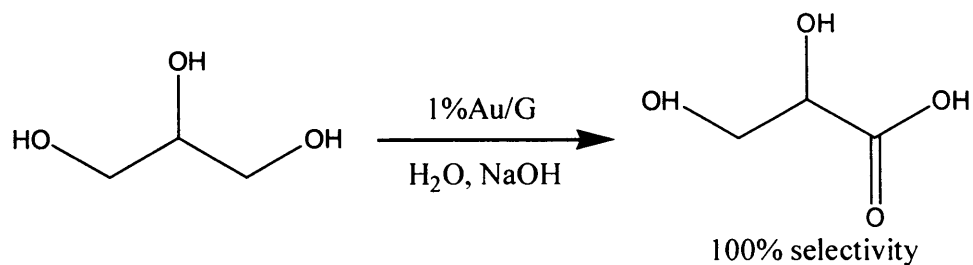
The selective oxidation of alcohols to chemical intermediates and fine chemicals represents an important and demanding target in green chemistry [32]. The use of stoichiometric inorganic reagents, though decreasing, is still widespread. The present stringent ecological standards increase the pressure to develop new and environmentally

benign catalytic processes. From a viewpoint of industrial application, identifying and designing new heterogeneous catalysts for selective oxidation of alcohols using oxygen or air is clearly an attractive choice.

Prati's group showed that gold supported on carbon catalysts can be used for selective oxidation of alcohols and polyols [33,34]. In particular, gold on carbon catalysts are very selective towards primary alcohols in the presence of a base. Gold catalysts appear to be more resistant to oxygen poisoning than supported platinum-based catalysts, allowing a higher oxygen partial pressure to be used. Moreover, with gold catalysts, a very high selectivity to target products can be achieved. For example, Prati reported that 92% selectivity to glycerate at full conversion was obtained by oxidising glycerol at 30⁰C over gold-on-carbon catalysts in the presence of base. Rossi and co-workers found that supported gold catalysts are effective for the gas-phase oxidation of volatile alcohols to the corresponding aldehydes and ketones [35].

Hutchings's research group showed that gold supported on graphite catalysts can oxidise glycerol to glyceric acid with 100% selectivity using dioxygen as the oxidant in the presence of base under relatively mild conditions (**Scheme 1.3**) [36,37]. For comparison, supported Pd and Pt on graphite catalysts were also studied. However, it was found that supported Pd and Pt catalysts always gave other C₃ and C₂ products in addition to glyceric acid and, in particular, also gave some C₁ by-products. Hence, supported gold catalysts exhibit unique selectivity for the selective oxidation of glycerol

to glyceric acid by careful control of reaction conditions, as compared to supported Pd and Pt catalysts.



Scheme 1.3 Selective oxidation of glycerol to glyceric acid using 1% Au/Graphite catalyst

It should be noted that a base, such as NaOH, is necessary in alcohol oxidations over gold catalysts. For glycerol oxidation to glyceric acid over gold supported on graphite catalysts, it is proposed that, in the presence of base, H⁺ is readily abstracted from one of the primary hydroxyl groups of glycerol to form glycerate, thereby overcoming the rate-limiting step of the alternative oxidation pathway [36,37].

Recently, Corma and co-workers have shown that a gold/nanocrystalline CeO₂ catalyst is highly active and selective for the oxidation of alcohols [38]. Gold nanoparticles are able to transform nano-crystalline cerium oxide from a stoichiometric oxidant into a catalytic material for the selective oxidation of primary and secondary alcohols to aldehydes and ketones in the presence of oxygen at atmospheric pressure but without solvent and base. High turnover frequencies (TOFs) and selectivities were observed (**Table 1.3**). This process is interesting from both an economic and environmental viewpoint.

Table 1.3 Selective oxidation of alcohols using molecular oxygen catalyzed by Au/nanocrystalline-CeO₂ [38]

Substrate	t [h]	Conversion [%]	Product	Selectivity [%]
3-octanol	3.5	97	3-octanone	> 99
3-octanol	2.5	89	3-octanone	96
2-phenylethanol	2.5	92	acetophenone	97
2,6-dimethylcyclohexanol	2.5	78	2,6-dimethylcyclohexanone	94
1-octen-3-ol	3.5	80	1-octen-3-one	> 99
cinnamyl alcohol	7	66	cinnamaldehyde	73
3,4-dimethoxybenzyl alcohol	7	73	3,4-dimethoxybenzaldehyde	83
3-phenyl-1-propanol	6	70	3-phenylpropyl 3-phenylpropanoate	98
vanillin alcohol	2	96	vanillin	98
2-hydroxybenzyl alcohol	2	> 99	2-hydroxybenzaldehyde	87
3,4-dimethoxybenzyl alcohol	2	> 99	3,4-dimethoxybenzoic acid	> 99
cinnamyl alcohol	3	> 99	cinnamic acid	98
n-hexanol	10	> 99	hexanoic acid	> 99
2-phenylethanol	5	> 99	acetophenone	51

Most recently, Hutchings and co-workers have shown that, using a Au/TiO₂ catalyst, benzyl alcohol can be selectively oxidised to benzaldehyde with oxygen in the absence of solvents [39]. In particular, they have found, by analysis using x-ray photoelectron spectroscopy (XPS) in combination with scanning transmission electron microscopy (STEM), that the introduction of Au to Pd produces a highly selective Au-Pd/TiO₂ catalyst featuring a Pd-rich shell surrounding a Au rich core (**Figure 1.11**). This Au-Pd/TiO₂ catalyst can give nearly 100% selectivity to benzaldehyde and very high turn over frequencies (TOFs) of up to 270,000 turnovers per hour. This finding represents great scope for selective oxidation of alcohols to aldehydes, particularly for oxidation of primary alkyl alcohols, with O₂ in place of traditional stoichiometric oxygen donors. Further detailed work to optimize the catalytic reaction system is in progress in Hutching's research group.

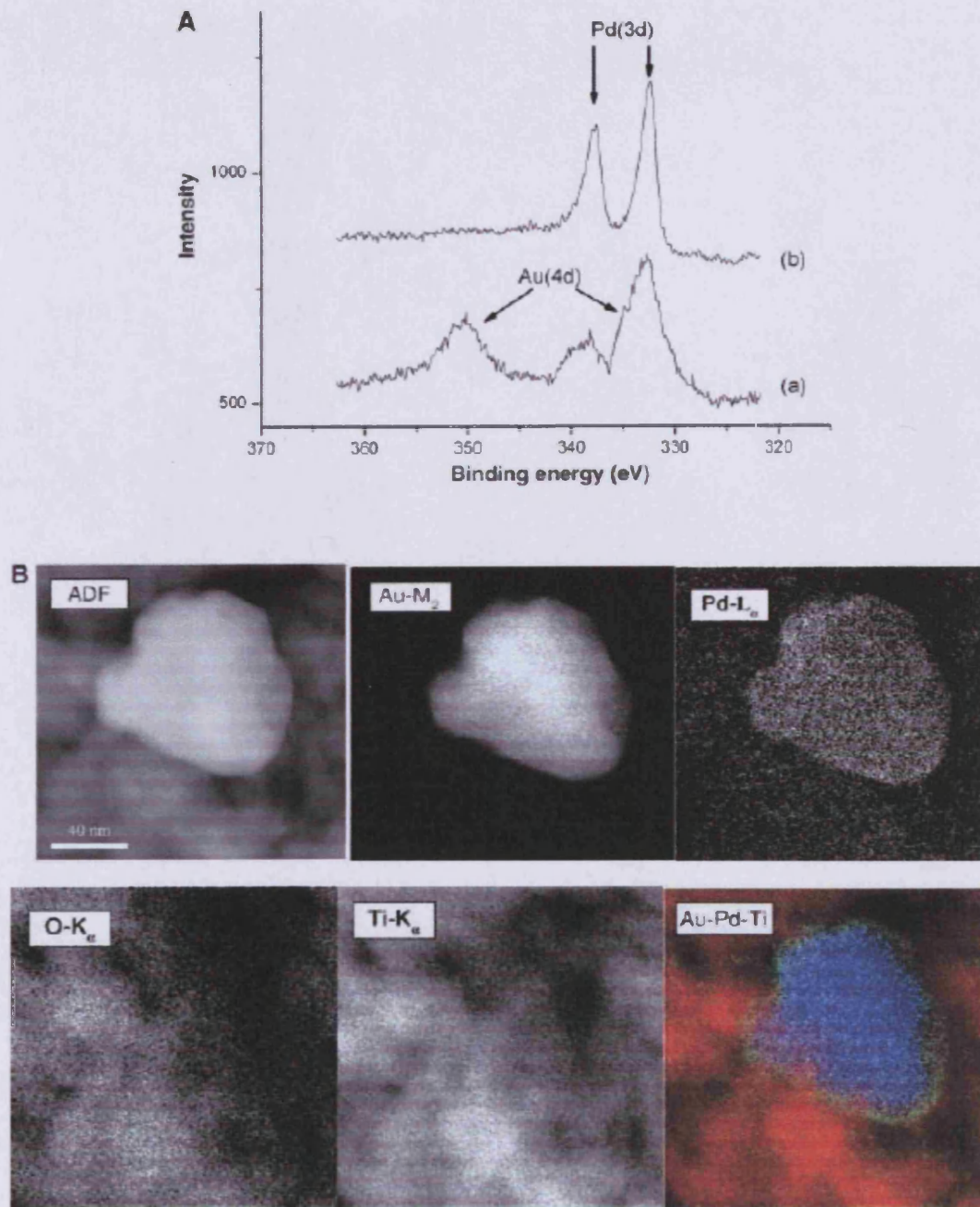
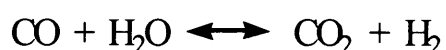


Fig. 1.11. (A) Au (4d) and Pd (3d) spectra for a 2.5%Au–2.5Pd%/TiO₂ catalyst after different heat treatments: (a) uncalcined or (b) calcined at 673 K in air. (B)

Montage showing the ADF-STEM image of a bimetallic particle and the corresponding MSA-processed STEM-XEDS maps of the Au-M₂, Pd-L_α, O-K_α, and Ti-K_α signals. Also shown is a reconstructed MSA-filtered Au-Pd-Ti composition map (Ti, red; Au, blue; and Pd, green) [39]

1.6.4.2 Water gas shift reaction and CO removal from H₂ for fuel cell applications

The water gas shift (WGS) reaction, as shown below, is a very important process employed in the chemical industry.



This reaction provides an economic route for the production of hydrogen and it is a principal step in the production of ammonia and ammonia-based fertilizers. Owing to the increasing application of polymer electrolyte fuel cells for automobiles and to residential electricity-heat delivery systems, low temperature WGS reaction is attracting renewed interest. Furthermore, the WGS reaction plays a key role in automobile exhaust processes since the hydrogen produced is effective for NO_x reaction. In comparison with commercial catalysts based on Ni or Cu, which operate at 900K or at 600K respectively, supported Au catalysts appear to be advantageous in that they operate at temperatures as low as 473K [40]. **Figure 1.12** summarizes the catalytic activity of supported gold catalysts for the WGS reaction (degree of CO conversion) at 473K. As a support, TiO₂, ZrO₂ and Fe₂O₃ are especially effective, and the crystallinity of these metal oxides appreciably affects the catalytic activity. Supported Au/NaY catalyst was reported to be active for the WGS reaction at 373K although stability may be a problem [40].

Based on the research reported in the open literature [40], several basic factors should be considered in order to achieve highly active and stable catalysts for the WGS reaction, namely:

- High WGS activity is displayed by gold particles with an optimum size of 3-5nm.
- Appropriate supports provide a good interaction between gold particles and the support as well as a highly stable dispersion of gold particles on it.
- The support can modify the electronic properties of nano gold particles and this interaction defines the precise nature of the structure and properties at the gold/support interface.

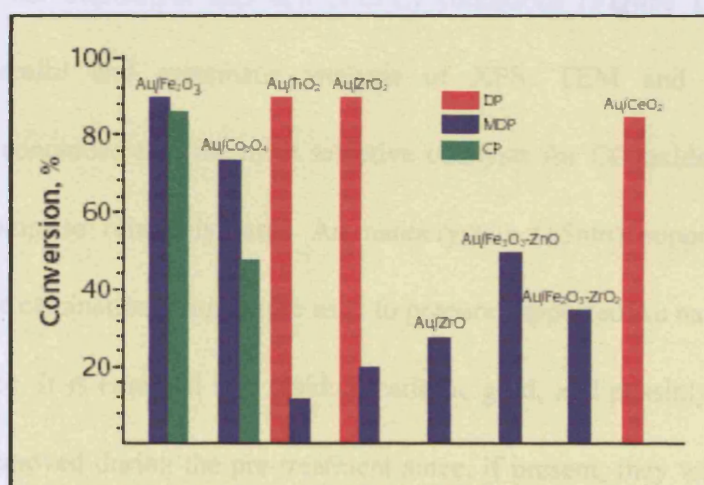


Fig.1.12. Catalytic activity of WGS reaction (degree of CO conversion) for supported gold catalysts at 473K. DP: deposition-precipitation; MDP: modified version of deposition-precipitation; CP: coprecipitation [40]

Regarding selective CO removal in a H₂ stream, supported Au catalysts are potentially advantageous over other noble metal catalysts because supported Au catalysts can be more active for CO oxidation compared to H₂ oxidation. It has been reported that Au/Mn₂O₃ and Au/Fe₂O₃ catalysts exhibit particularly good stability, high catalytic activity and selectivity [40].

Most recently, Landon *et al.* reported a significant and fascinating work on selective oxidation of CO in the presence of H₂, H₂O and CO₂ using Au/Fe₂O₃ catalysts with a single-stage reactor [41,42]. They reported that a gold catalyst supported on Fe₂O₃ prepared using co-precipitation, followed by a two-stage calcination process up to 550^oC, created a catalyst with high CO oxidation activity but low H₂ oxidation activity under typical polymer electrolyte fuel cell (PEFC) conditions (**Figure 1.13**). More importantly, by careful and systematic analysis of XPS, TEM and Mössbauer spectroscopy, they concluded that the most selective catalysts for CO oxidation in the presence of H₂ comprise relatively large Au nanocrystals (>5nm) supported on a reducible oxide. The calcination temperature used to prepare supported Au nanoparticles is key of importance. It is essential that residual cationic gold, and possibly small Au nanoparticles are removed during the pre-treatment since, if present, they will catalyse the reverse WGS reaction thereby decreasing CO conversion.

This work reported by Landon *et al.* represents a successful example catalysed by supported gold catalysts for selective oxidation of CO in a typical fuel cell conditions.

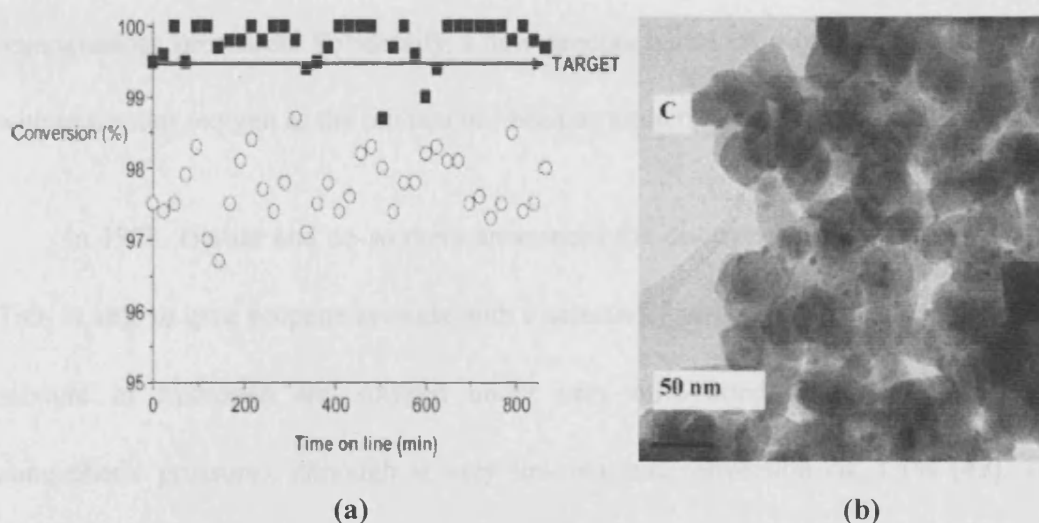


Fig.1.13. (a) Variation of CO (■) and O₂ (○) conversion with time-on-line for a 5% Au/Fe₂O₃ catalyst calcined in air at 400 + 550⁰C. Reaction conditions: 80⁰C, 0.9% CO, 0.9% O₂, 50% H₂, 22% CO₂, 4.7% H₂O with the balance N₂; 100 mg of catalyst were used with a total flow rate of 20 ml min⁻¹, GHSV = 12 000 h⁻¹. (6)

Bright filed TEM image of the catalyst used in the reaction [42]

1.6.4.3 Selective epoxidation of propene

Apart from low temperature CO oxidation by supported nano-sized gold particles, the selective epoxidation of propene represents another characteristic reaction catalyzed by gold. It is well known that the heterogeneous epoxidation of alkenes other than ethene is very difficult. This difficulty is often ascribed to the presence of labile allylic H atoms, whose facile abstraction results in combustion rather than selective oxidation. Hence, silver catalysts are very inefficient in propene epoxidation although silver catalysts are widely used for ethene epoxidation to ethene oxide in industry. As a consequence, the commercial production of propene oxide (PO) proceeds by one of two

homogeneous processes. To identify a new process based on a heterogeneous catalyst with molecular oxygen as the oxidant has been an attractive goal for many chemists.

In 1998, Haruta and co-workers announced the discovery that gold supported on TiO_2 is able to give propene epoxide with a selectivity up to 100% in the presence of a mixture of hydrogen and oxygen under very mild conditions (323K-373K and atmospheric pressure), although at very low reactant conversion *ca.* 1.1% [43]. This report generated significant interest in propene epoxidation by supported gold catalysts. It was disclosed that the epoxidation of propene to PO using gold catalysts is strongly sensitive to the contact structure of nano-sized gold particles. The strong contact of Au particles is indispensable for the epoxidation of propene using gas phases containing O_2 and H_2 . As shown in **Figure 1.14**, Haruta suggests that spherical nano-sized gold particles loaded onto TiO_2 need higher temperatures to promote the epoxidation of propene and often cause complete oxidation to produce only CO_2 and H_2O , the yield of H_2O is higher than that of CO_2 [31]. In contrast, hemispherical Au particles, which are strongly attached to the TiO_2 support, produce PO with almost 100% selectivity at a lower temperature, 323K. The consumption of H_2 is about three times that of propene conversion and appreciably less than that over spherical supported Au particles catalysts. The strong sensitivity of propene epoxidation to the contact structure of gold particles suggests that the reaction takes place at the perimeter interfaces around the nano-sized gold particles. Subsequent research reported by Liu *et al.* and Haruta *et al.* has confirmed this hypothesis [31].

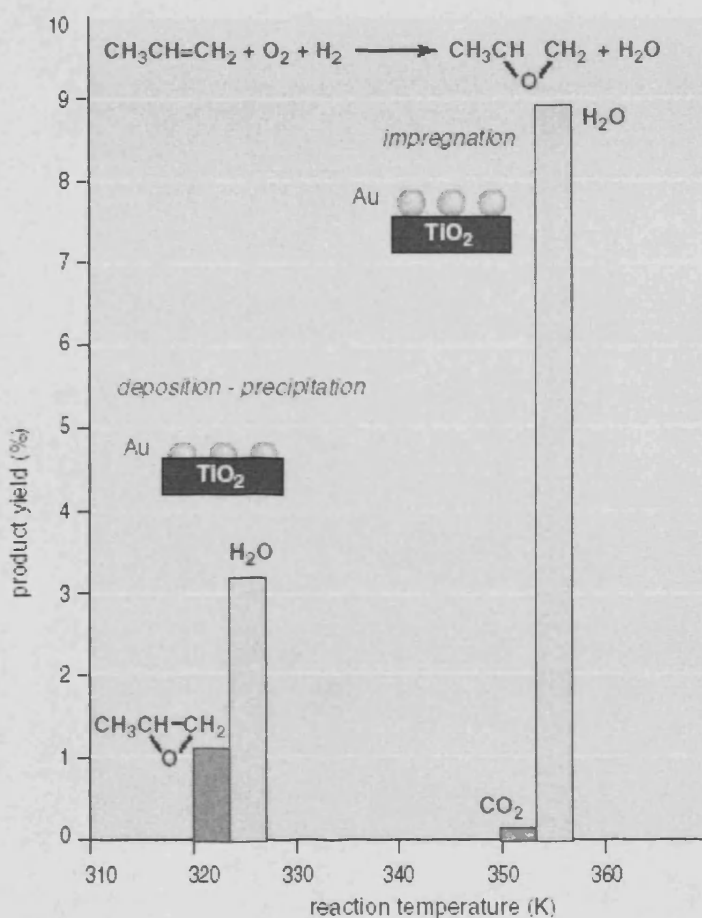


Fig. 1.14. Product yields for the reaction of propylene, oxygen and hydrogen over Au/TiO₂ catalysts prepared by deposition-precipitation and impregnation methods [31]

In addition, it was reported that, as for other reactions catalyzed by gold, catalyst preparation methods, selection of the support material and the size of nano-gold particles are three important factors for propene epoxidation for non-promoted gold catalysts [43,44]. For example, only supported gold particles with the size between 2nm to 5nm are efficient catalysts for propene epoxidation. Recently, Haruta *et al.* demonstrated that highly dispersed gold nanoparticles supported on 3D mesoporous,

silylated titanosilicates with large pores in the presence of $\text{Ba}(\text{NO}_3)_2$ as a promoter are very efficient catalysts for the epoxidation of propene to PO with molecular O_2 and H_2 . Conversions of up to 10% with 93% PO selectivity have been achieved, however the H_2 efficiency is still low, typically 30% [45].

In the meantime, it should be mentioned that the mode of operation of supported gold catalysts for propene epoxidation is still not clear. The fact that both hydrogen and oxygen are needed for propene epoxidation has triggered speculation that a peroxide species could be an important reaction intermediate for the reaction, which is supported by the fact that titania is capable of epoxidizing propene using hydrogen peroxide in the liquid phase [46], and the fact that gold has been observed to produce hydrogen peroxide directly from hydrogen and oxygen [47]. However, no evidence exists that shows this is occurring during propene epoxidation, which makes the peroxide mechanism speculative.

Research reported by Nijhuis and co-workers demonstrated that the role of supported gold nanoparticles in the epoxidation of propene to PO is more than that generally assumed, namely, that gold merely provides a peroxide species, which subsequently epoxidizes propene on the titania sites [48]. Infrared spectroscopy showed that gold nanoparticles on titania catalyze a reaction between propene and the titania sites. A bidentate propoxy species is produced, similar to that formed when propene epoxide is adsorbed on titania. The gold particles also catalyze a consecutive oxidation of the bidentate propoxy species to form carbonate/carboxylate species, which is

possibly the cause of catalyst deactivation. In the presence of hydrogen and oxygen the bidentate propoxy species can desorb from the catalyst surface. Accordingly, they propose the following reaction mechanism. Propene reacts with titania to produce an adsorbed bidentate propoxy species. This reaction is catalyzed by the gold nanoparticles present on the titania. Hydrogen and oxygen produce a hydroperoxide species on gold. The peroxide species aids in the desorption of the bidentate propoxy species from the catalyst, producing propene oxide and water and restoring the titania to its original state.

In addition, it has been concluded that over Au/TiO₂ catalysts, water plays an important role [49], which is similar to the observation that moisture enhances the catalytic activities of CO oxidation using supported gold catalysts [50]. Propene epoxidation and water production have a strong influence each other. Water addition to the feed gas stream was recommended as it suppressed the catalyst deactivation by lowering the concentration of propene oxide adsorbed on the titania through competitive adsorption [49].

1.6.4.4 Production of hydrogen peroxide

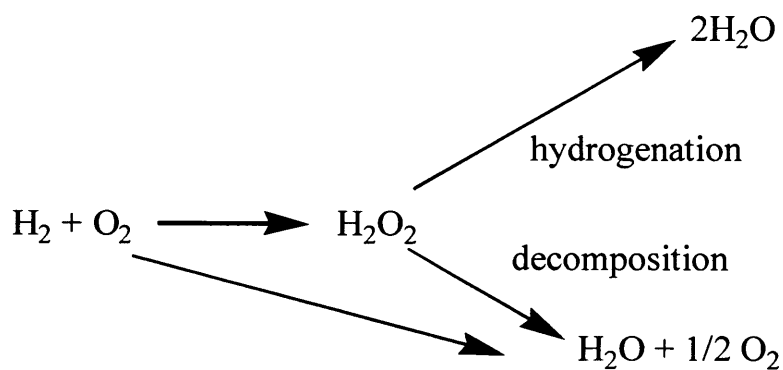
Hydrogen peroxide (H₂O₂) is one of a large number of liquid-phase oxygen donors, which are widely used as oxidants for selective oxidation under ambient conditions. Currently, hydrogen peroxide is produced by the sequential hydrogenation and oxidation of an alkyl anthraquinone and global production is *ca.* 1.9×10⁶ tonnes per annum [47,51]. However, there are problems associated with the anthraquinone route

and these include the cost of the quinone solvent system and the requirement for periodic replacement of anthraquinone due to its hydrogenation. Besides, the process is only economically viable on a relatively large scale ($4-6 \times 10^4$ tpa) and this necessitates the transportation and storage of concentrated solutions of hydrogen peroxide.

The identification of a direct route for the synthesis of hydrogen peroxide from the reaction of dioxygen and hydrogen would be highly beneficial. For example, this presents the possibility of small-scale distributed synthesis. In view of this, there is considerable interest in the direct manufacture of hydrogen peroxide from the catalysed reaction of hydrogen and oxygen, which presents significant scope for the production of hydrogen peroxide by an environmentally benign way. To date, some success has been obtained using supported Pd catalysts, particularly when halides are used as promoters [52]. Meanwhile, it is worthwhile to note that supported Au catalysts have been widely studied for propene epoxidation to PO using a mixture of hydrogen and oxygen and it is deemed that a surface hydroperoxy species may be formed, suggesting that gold catalysts can potentially be used for the synthesis of hydrogen peroxide.

Hutchings' research group have found that supported Au catalysts can be very effective for the synthesis of hydrogen peroxide (**Scheme 1.4**) and, furthermore, the rate of hydrogen peroxide formation can be significantly enhanced by the use of a supported Au/Pd alloy as can be clearly seen in **Figure 1.15** [47,51]. The supported Au-Pd catalyst produces significantly more hydrogen peroxide than the pure supported Au catalyst or the supported Pd catalyst, indicating there is a synergetic effect of Pd acting as a

promoter for the Au catalyst. In addition, the use of supercritical CO₂ as a reaction medium for the formation of hydrogen peroxide has been shown to have a beneficial effect, for example, overcoming the H₂ diffusion limitation. However, in general, the rate of hydrogen peroxide decomposition is too rapid at temperatures above the critical temperature, 31.1^oC. Hence, the inherent instability of hydrogen peroxide at the elevated temperature required to achieve supercritical conditions mitigates against the use of this medium.



Scheme 1.4 Reaction involved in the synthesis of H₂O₂

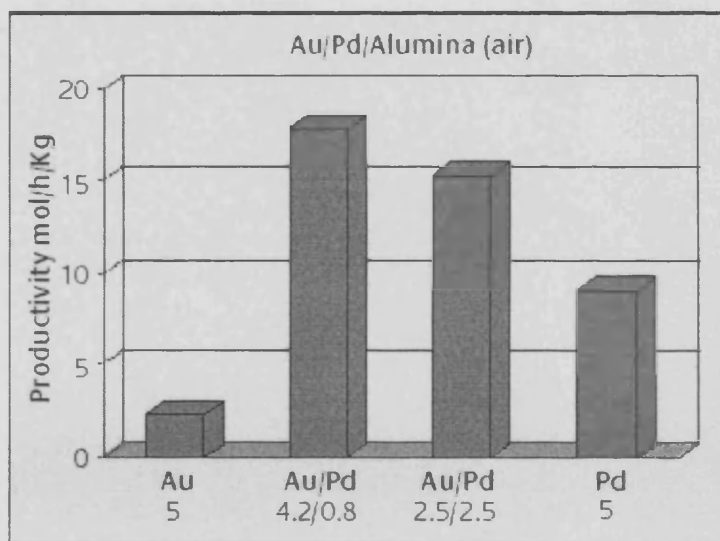


Fig. 1.15. Production of hydrogen peroxide from the reaction of H_2 and O_2 over Au and Au/Pd catalysts at $2^{\circ}C$ in an autoclave reactor using aqueous methanol (CH_3OH , 5.6 g; H_2O 2.9 g) as solvent with catalyst (0.05 g), the reactor was purged three times with CO_2 (3 MPa) and then filled with 5% H_2/CO_2 and 25% O_2/CO_2 [16]

This suggests that supported Au catalysts, particularly Au-Pd alloy, are effective for the direct synthesis of hydrogen peroxide from hydrogen and oxygen. Supported Au catalysts may provide a significant improvement over Pd catalysts that have previously been investigated. Most recently, Hutchings' research group reports that TiO_2 -supported Au-Pd catalysts are very effective for hydrogen peroxide synthesis, and the highest selectivity reached 93%, suggesting there is great scope to improve the catalyst function by choosing alternative supports and reaction conditions [53,54].

More interestingly, it was found that the active site for hydrogen peroxide synthesis is different from that for low temperature CO oxidation catalyzed by

supported gold catalysts, indicating that selective oxidation with supported Au catalysts requires a significantly different structure than the catalysts that are most active for CO oxidation. Clearly, the real active sites for reactions catalyzed by gold for different reactions are complicated. In fact, as yet there is no absolute consensus for the case of CO oxidation over supported gold catalysts in the open literatures, which can be attributed to the inherent complexity and nature of different real supported Au catalysts [53].

The interesting and pioneering work initiated by Hutchings' research group illustrates that gold can be used as a highly effective catalyst for hydrogen peroxide synthesis and also represents an exciting new reaction catalyzed by Au.

1.6.4.5 Selective hydrogenation

In contrast to the use of supported Au catalysts for oxidation reactions, it seems that the capabilities of supported Au catalysts in hydrogenation reactions have been less well explored. The first study of the hydrogenation reaction using supported Au catalysts was made by Bond and co-workers, namely 1,3-butadiene hydrogenation [11]. They found that a Au/SiO₂ catalyst was selective for partial hydrogenation to form butenes. However, these Au catalysts prepared by an impregnation method were significantly less active than the Pd and Pt catalysts. Due to its low melting point and poor affinity for oxygen, Au could not be highly dispersed over the metal oxide supports using the impregnation method. Lately, Hutchings *et al.* reported that

supported Au catalysts with sulfur as additives exhibit high activity and selectivity for crotonaldehyde hydrogenation [55].

Since supported gold catalysts are widely used for oxidation reactions, it should be reasonable to expect that the activities of supported Au catalysts could also be appreciably improved for hydrogenation if they are properly prepared. Over the last few years, there have been many studies of hydrogenation over supported gold catalysts. Claus has recently given an overview of the field of heterogeneously catalyzed hydrogenation using supported gold catalysts [56].

One characteristic feature of supported Au catalysts for the hydrogenation of unsaturated hydrocarbons is that partial hydrogenation of unsaturated hydrocarbons takes place very selectively: butadiene to butane and acetylene to ethylene. Apart from this, the other main advantage of supported Au catalysts is their ability to selectively catalyze the hydrogenation of the C=O group of α,β unsaturated aldehydes producing allyl-type unsaturated alcohols. For example, the selectivity for the hydrogenation of C=O versus that of C=C was reported to reach 40~50% when using supported Au on TiO₂ or ZrO₂ catalysts in the hydrogenation of α,β unsaturated aldehyde [56]. Hutchings and co-workers reported recently that a Au/ZnO catalyst exhibits a selectivity of *ca.* 80% to C=O hydrogenation to the unsaturated alcohol [57].

1.6.4.6 Other reactions

The reduction of NO with hydrocarbons to N₂ in the presence of excess O₂ and H₂O is an important reaction in the treatment of exhaust gases in gasoline and diesel engines. This reaction can take place over some supported Au catalysts. Alkenes such as ethene and propene are more effective as reductants than are alkanes because the former adsorb to a greater degree on Au surfaces. The optimum temperature and maximum efficiency for NO reduction depend on the kind of metal oxide supports and increase in the order of ZnO (523K, 49%), α -Fe₂O₃ (523K, 12%), MgO (623K, 42%), TiO₂ (623K, 30%) and Al₂O₃ (673K, 80%) [31]. Over a Au/Al₂O₃ catalyst, the NO conversion to N₂ in the presence of 5% oxygen and 10% water is comparatively higher than over the other catalysts reported so far. When using a mechanical mixture of Au/Al₂O₃ with MnO_x, an enhanced activity has been achieved.

Besides, supported Au/Co₃O₄ catalysts have been reported to be active for N₂O decomposition to N₂ and O₂ [58]. Supported Au on Co₃O₄ or Fe₂O₃ catalysts have been used for oxidative decomposition of chlorofluorocarbon, o-chlorophenol and dioxin [59].

1.6.4.7 Outlook of gold catalysts

In short, ongoing and potential applications of heterogeneous supported gold catalysts can be summarized in **Table 1.4**. With further technology developments, the future for catalysis by gold should be exceptional and potential applications for catalysis

by Au may involve the following commercially areas: pollution and emission control; chemical processing of a range of bulk and speciality chemicals; the emerging hydrogen economy for clean hydrogen production and fuel cell systems; sensors to detect poisonous or flammable gases or substances in solution.

Table 1.4. Ongoing and potential applications of gold catalysts [25]

Fields of applications	Reactants or Reactions	Support materials
Indoor air quality control	odour (commercialized), CO sick house gases	Fe ₂ O ₃ TiO ₂
Pollutant abatement	dioxin oxidation-decomposition NO reduction N ₂ O decomposition	Fe ₂ O ₃ Al ₂ O ₃ Co ₃ O ₄
H ₂ energy carrier	water-gas shift CO removal fuel cell anode	ZrO ₂ , CeO ₂ Al ₂ O ₃ , Mn ₂ O ₃ , Fe ₂ O ₃ carbon black
Chemical process	hydrochlorination hydrogenation [C=C, C=O + C=C, C-OH] liquid-phase selective oxidation propylene epoxidation	AuCl ₃ / activated carbon ZnO activated carbon TiO ₂ (anatase) and Ti-SiO ₂

1.7. Catalysis by silver and copper

1.7.1 Catalysis by silver

In industry, Ag catalysts have been used worldwide for the selective epoxidation of ethene to ethene oxide using dioxygen (pure oxygen or air) as the oxidant, which represents an economic and environmentally benign process [60]. One of the most important uses of ethene oxide is the production of ethene glycol. However, it should be noted that the scope of this epoxidation chemistry catalyzed by Ag is still limited to ethene epoxidation. Industrial preparation of other epoxides, such as propene epoxide, must go through a different and more costly route [61].

1.7.2 Mechanism of ethene epoxidation catalyzed by Ag

Two primary reaction mechanisms have been proposed for the production of ethene oxide [62]. One mechanism involves the adsorption of molecular oxygen as the active species in the epoxidation reaction, while the other involves the adsorption of atomic oxygen as the active species. Both of these mechanisms seek to explain how different types of adsorbed oxygen species may affect the selectivity of the reaction.

The molecular mechanism states that molecular oxygen is active in epoxidation, while atomic oxygen is active in combustion. This remaining oxygen atom participates in a combustion reaction with ethene. Hence, according to this mechanism, it would be advantageous to utilize inhibitors to prevent the adsorption of atomic oxygen.

The atomic mechanism states that atomic oxygen is the active species in both epoxidation and combustion, while molecular oxygen plays no part. Epoxidation occurs when one oxygen atom reacts with the double bond of one adsorbed molecule of ethene; combustion occurs when one oxygen atom abstracts the slightly acidic hydrogen atom of one adsorbed molecule of ethene, which results in complete oxidation. Similarly, one oxygen atom can react with and completely oxidize a newly produced ethene oxide molecule. Therefore, according to this mechanism, it would be desirable to use promoters or inhibitors to activate the atomic oxygen towards epoxidation rather than combustion.

In fact, industrial processes do use inhibitors and promoters to improve selectivity to ethene oxide [63]. Chlorine is adsorbed onto the silver as an inhibitor, and alkali metals, such as cesium, are dispersed in the bulk of silver as promoters. The amount of chlorine added must be tightly controlled because high coverage of chlorine will deactivate the catalyst. The appropriate amount of inhibitors can increase selectivity by altering the electronic properties of the adsorbed oxygen atom and activating it for epoxidation. Electron-withdrawing species, such as adsorbed chlorine, act to decrease the electron density of the oxygen atom. The electron-deficient oxygen favours an attack on the electron-rich double bond of ethene. Although alkali-metal promoters are electron-donating species, their presence also increases the selectivity of the epoxidation. Electron-donors, such as cesium, might be thought to increase oxygen electron density, thereby favouring combustion. However, research has also found that cesium promoters do not affect the electronic properties of the oxygen, but they instead affect the electronic properties of the ethene. Cesium can prevent both ethene and ethene oxide from isomerising to an isomer that is more active for combustion.

Currently, most researchers favour the atomic oxygen mechanism over the molecular oxygen mechanism. The research supporting the atomic oxygen mechanism is more persuasive, although the molecular oxygen mechanism presents a selectivity barrier that seems to be encountered in industrial practise.

The main drawback to using silver catalyst is that, although its initial selectivity ranges 79~85%, as it ages its selectivity deteriorates, and there are no generally

applicable methods of regeneration. Silver catalyst may age due to abrasion, deposition of carbon-containing compounds, and recrystallization of the silver. The life span of the catalyst is 2-5 years, and due to this limitation new technologies are being investigated. Increases in the cost of ethene could mean that only significant increases in catalyst selectivity and life-span could maintain an economically viable ethene oxide process.

1.7.3 Catalysis by copper

Copper is industrially employed for methanol synthesis and the water gas shift reaction, and is also well known to be active for steam reforming of methanol [64,65]. Currently, methanol synthesis catalysts are prepared by co-precipitation of Cu, Zn and Al as hydroxides or carbonates, which are then decomposed to mixed oxides (e.g., Cu/ZnO/Al₂O₃) by treatment in air and reduced in H₂ before use.

Methanol is an alternative hydrogen source for fuel cell applications. For the methanol steam reforming reaction (MSR) (**Scheme 1.5**), high yields of hydrogen can be achieved at relatively low temperatures. Methanol fulfils some important criteria concerning availability and handling, such as low hazardous level, inexpensive and easy distribution. Very advantageous is the low concentration of CO produced via the MSR process and the absence of other harmful gases.



Scheme 1.5 The methanol steam reforming reaction (MSR)

Copper alloy catalysts, such as Cu-Ni, Cu-Pt, Cu-Pd and Cu-Ir, are also used for selective hydrogenation of oils and a variety of hydrocarbons [64]. In addition, copper also plays an important role in the microelectronics industry as copper and copper-oxide-based components gain popularity.

Notably, in recent years, it has been shown that copper can be used as a potential catalyst for alkene epoxidation and copper may be intrinsically more selective than silver. For example, Lambert showed that copper could be an inexpensive potential catalyst for propene epoxidation using only oxygen as the oxidant, although conversions are low [66]. Furthermore, theoretical calculations and experiments have demonstrated that Cu-Ag bimetallic catalysts offer improved selectivity to ethene oxide compared with silver alone in the direct epoxidation of ethene using oxygen as the oxidant [67,68]. These initial studies suggest there is a great scope to explore the direct epoxidation of alkenes using Cu, Ag and their alloys in the absence of hydrogen.

1.8 Objectives and outline of this thesis

The work in this thesis has been performed as part of the ATHENA project, which is an EPSRC/Johnson Matthey sponsored project involving University Departments at Cambridge, Birmingham, Cardiff, Glasgow and Surrey in the UK together with the Fritz-Haber-Institute in Germany and Northwestern University in the USA. Cardiff is the lead organisation for the selective oxidation section. Traditional stoichiometric oxidation processes generate much waste and there is a significant need to develop

alternative methodologies, preferably using molecular oxygen (or air) as the oxidant, which this project seeks to do. Clearly, the use of molecular oxygen from air is highly desirable and presents the opportunity to develop green chemical processes. The objective of the work in this thesis is to find novel catalysts for selective oxidation of hydrocarbons with total (100%) selectivity using only molecular oxygen as oxidant

The summarized outline of the present work is described below:

Chapter 1: Introduction

This chapter introduces the history of catalysis, basic definitions and terms in catalysis and the role of catalysis in chemistry and our life. In particular, gold as a novel catalyst in the heterogeneous community and the characteristic reactions catalyzed by supported gold catalysts are introduced in this section. Meanwhile, copper and silver catalysts and their applications in the chemical industry are also described.

Chapter 2: Experimental Techniques

This chapter deals with the introduction of the main characterisation methods for the as-prepared catalysts in the present research work. The principles of X-ray powder diffraction (XRD), BET method, X-ray photoelectron spectroscopy (XPS), scanning electron microscope (SEM), transmission electron microscope (TEM) and atomic absorption spectrophotometer (AAS) are described and explained. The reactors used in this work are presented.

Chapter 3: Selective oxidation of alkenes using supported gold catalysts

In this chapter, it will be shown that supported gold catalysts can be very effective for the selective oxidation of alkenes under mild conditions. Selective oxidation of alkenes can be easily kick-started using oxygen from air as the oxidant over nano-crystalline gold particles together with a small amount of tert-butyl hydrogen peroxide (TBHP) as initiator. The distribution of the products, including epoxide, alcohol and ketone, can be actively tuned by choosing different solvents. For the first time, it has been found that bismuth can be used as an effective promoter for supported gold catalysts in the selective oxidation of alkenes.

Chapter 4: Selective oxidation of cyclohexane over supported gold catalysts

In this chapter, supported gold catalysts have been found to be effective for the selective oxidation of cyclohexane under mild conditions. High selectivity to target products, namely cyclohexanol and cyclohexanone, has been achieved. Selectivity depends only on conversion. That is, high selectivity can only be achieved at short reaction time.

Chapter 5: Selective epoxidation of propene over supported gold, silver, copper and their alloys

This chapter describes the gas-phase selective epoxidation of propene over supported Au, Ag, Cu and bimetallic catalysts using only molecular oxygen as the

oxidant. Copper has been found to be a potentially selective and inexpensive catalyst for propene epoxidation using oxygen as oxidant. The support plays an important role in the performance of the as-prepared catalysts. Interestingly, Cu-Au exhibits the best performance for selective epoxidation of propene to propene epoxide (PO), wherein high selectivity to PO with an improved conversion have been achieved when compared to Cu, Ag and Au catalysts. In addition, it has been found that supported Cu-Ag catalysts are more selective than supported Cu or Ag catalysts alone.

Chapter 6: Summary, conclusion and future work

Finally, the overall conclusions and future perspectives of the research work described in this thesis will be given.

1.9 References and notes

- [1] Lindström, B.; Pettersson L. J. *CATTECH* **2003**, 7, 130.
- [2] (a) Bond, G. C. *Catalysis: Principles and Applications* 2nd Ed. Clarendon Press, Oxford, 1987. (b) Thomas, J. M.; Thomas, W. J. *Principles and Practice of Heterogeneous Catalysis* Wiley, 1997.
- [3] Schwab, G. M.; Anderson in J. R.; Boudart M. (Ed.), *Catalysis Science and Technology* Vol 2, Springer, New York, 1981.
- [4] Barrault, J.; Pouilloux, Y.; Clacens, J. M.; Vanhove, C.; Bancquart, C. *Catal. Today* **2002**, 75, 177.
- [5] Hutchings, G. J.; Scurrell, M. S. *CATTECH* **2003**, 7, 90.
- [6] Hodnett, B. K. *Heterogeneous Catalytic Oxidation* Wiley&Sons, 1999.
- [7] Barteau, M. A. *Top. Catal.* **2003**, 22, 3.
- [8] Haruta, M. *Chem. Record* **2003**, 3, 75.
- [9] Sault, A. G.; Madix, R. J.; Campbell, C. T. *Surf. Sci.* **1986**, 169, 347.
- [10] Hammers, B.; Nørskov, J. K. *Nature* **1995**, 376, 238.
- [11] Sermon, P. A.; Bond, G. C.; Wells, P. B. *J. Chem. Soc.; Faraday Trans.1* **1979**, 75, 385.
- [12] (a) Hutchings, G. J. *Catal. Today* **2005**, 100, 55. (b) Hutchings, G. J. *Catal. Today* **2002**, 72, 11.
- [13] Hutchings, G. J. *J. Catal.* **1985**, 96, 292.
- [14] Haruta, M.; Kobayashi, T.; Sano, H.; Yamada, N. *Chem. Lett.* **1987**, 4, 405.
- [15] (a) Nkosi, B.; Coville, N. J.; Hutchings, G. J.; Adams, M. D.; Friedl, J.; Wagner, F.

- J. Catal.* **1991**, 128, 366. (b) Nkosi, B.; Coville, N. J.; Hutchings, G. J. *Chem. Commun.* **1988**, 71.
- [16] Hutchings, G. J. *Gold Bull.* **2004**, 37, 3.
- [17] (a) Bond, G. C.; Thompson, D. T. *Gold Bull.* **2000**, 33, 41. (b) Bond, G. C.; Thompson, D. T. *Catal. Rev. Sci. Eng.* **1999**, 41, 319.
- [18] Valden, M.; Lai, X.; Goodman, D. W. *Science* **1998**, 281, 1647.
- [19] Chen, M. S.; Goodman, D. W. *Science* **2004**, 306, 252.
- [20] Bell, A. T. *Science* **2003**, 299, 1688.
- [21] Lopez, N.; Nørskov, J. K. *J. Am. Chem. Soc.* **2002**, 124, 11262.
- [22] Boyen, H. G.; Kaestle, G.; Weigl, F.; Koslowski, B.; Dietrich, G.; Ziemann, P.; Spatz, J. P.; Rietmueller, S.; Hartmann, T.; Noeller, M.; Smid, G.; Garnier, M.; Oelhafen, P. *Science* **2002**, 297, 1533.
- [23] Liu, Z. P.; Gong, X. Q.; Kohanoff, J.; Sanchez, C.; Hu, P. *Phys. Rev. Lett.* **2003**, 91, 266102.
- [24] (a) Molina, L. M.; Hammer, B. *Phys. Rev. B* **2004**, 69, 155424. (b) Molina, L. M.; Hammer, B. *Phys. Rev. Lett.* **2003**, 90, 206102.
- [25] Haruta, M. *Gold Bull.* **2004**, 37, 27.
- [26] Yan, Z.; Chinta, S.; Mohamed, A. A.; Fackler, J. P., Jr.; Goodman, D. W. *J. Am. Chem. Soc.* **2004**, 127, 1604.
- [27] Carrettin, S.; Concepción, P.; Corma, A.; Nieto, J. M. L.; Puntes, V. F. *Angew. Chem., Int. Ed.* **2004**, 43, 2538.
- [28] Guzman, J.; Gates, B. C. *J. Am. Chem. Soc.* **2004**, 126, 2672.

- [29] Finch, R. M.; Hodge, N. A.; Hutchings, G. J.; Meagher, A.; Pankhurst, Q. A.; Siddiqui, M. R.; Wagner, F. E.; Whyman, R. *Phys. Chem. Chem. Phys.* **1999**, 1, 485.
- [30] Haruta, M. *Catal. Today* **1997**, 36, 153.
- [31] Haruta, M. *CATTECH* **2002**, 6, 102.
- [32] Mallat, T.; Baiker, A. *Chem. Rev.* **2004**, 104, 3037.
- [33] Prati, L.; Rossi, M. *J. Catal.* **1998**, 176, 552.
- [34] Porta, F.; Prati, L.; Rossi, M.; Colluccia, S.; Martra, G. *Top. Catal.* **2000**, 13, 231.
- [35] Prati, L. *Gold Bull.* **1999**, 32, 96.
- [36] Carrettin, S.; McMorn, P.; Johnston, P.; Griffin, K.; Hutchings, G. J. *Chem. Commun.* **2002**, 696.
- [37] Carretin, S.; McMorn, P.; Johnston, P.; Griffin, K.; Kiely, C. J.; Hutchings, G. J. *Phys. Chem. Chem. Phys.* **2003**, 5, 1329.
- [38] Abad, A.; Concepción, P.; Corma, A.; Garcíá, H. *Angew. Chem., Int. Ed.* **2005**, 44, 4066.
- [39] Enache, D. T.; Edwards, J. K.; Landon, P.; Solsona, B. E.; Carley, A. F.; Herzing, A. A.; Watanabe, M.; Kiely, C. J.; Knight, D. W.; Hutchings, G. J. *Science* **2006**, 311, 362.
- [40] Andreeva, D. *Gold Bull.* **2002**, 35, 82.
- [41] Landon, P.; Ferguson, J.; Solsona, B. E.; Garcia, T.; Carley, A. F.; Herzing, A. A.; Kiely, C. J.; Golunski, S. E.; Hutchings, G. J. *Chem. Commun.* **2005**, 27, 3385.
- [42] Landon, P.; Ferguson, J.; Solsona, B. E.; Garcia, T.; Al-Sayari, S.; Carley, A. F.; Herzing, A. A.; Kiely, C. J.; Makkee, M.; Moulijn, J. A.; Overweg, A.; Golunski, S. E.; Hutchings, G. J. *J. Mater. Chem.* **2006**, 2, 199.

- [43] Hayashi, T.; Tanaka, K.; Haruta, M. *J. Catal.* **1998**, 178, 566.
- [44] Sinha, A. K.; Seelan, S.; Tsubota, S.; Haruta, M. *Top. Catal.* **2004**, 29, 95.
- [45] Sinha, A. K.; Seelan, S.; Tsubota, S.; Haruta, M. *Angew. Chem., Int. Ed.* **2004**, 43, 1546.
- [46] Clerici, M. G.; Bellussi, G.; Romano, U. *J. Catal.* **1991**, 129, 159.
- [47] Landon, P.; Collier, P. J.; Papworth, A. J.; Kiely, C. J.; Hutchings, G. J. *Chem. Commun.* **2002**, 2058.
- [48] Nijhuis, T. A.; Visser, T.; Weckhuysen, B. M. *Angew. Chem., Int. Ed.* **2005**, 44, 1115.
- [49] Nijhuis, T. A.; Weckhuysen, B. M. *Chem. Commun.* **2005**, 48, 6002.
- [50] Daté, M.; Okumuta, M.; Tsubota, S.; Haruta, M. *Angew. Chem., Int. Ed.* **2004**, 43, 2129.
- [51] Landon, P.; Collier, P. J.; Carley, A. F.; Chadwick, D.; Papworth, A. J.; Burrows, A.; Kiely, C. J.; Hutchings, G. J. *Phys. Chem. Chem. Phys.* **2003**, 5, 1917.
- [52] Wanngard, J. *Eur. Pat.* 0816286 A1, 1998.
- [53] Edwards, J. K.; Solsona, B.; Landon, P.; Carley, A. F.; Herzing, A.; Kiely, C. J.; Hutchings, G. J. *J. Catal.* **2005**, 236, 69.
- [54] Edwards, J. K.; Solsona, B.; Landon, P.; Carley, A. F.; Herzing, A.; Watanabe, M.; Kiely, C. J.; Hutchings, G. J. *J. Mater. Chem.* **2005**, 15, 4595.
- [55] Bailie, J. J.; Hutchings, G. J. *Chem. Commun.* **1999**, 2151.
- [56] Claus, P. *Appl. Catal. A* **2005**, 291, 222.
- [57] Bailie, J. J.; Hutchings, G. J. *Catal. Commun.* **2001**, 2, 291.

- [58] Yan, L.; Zhang, X.; Ren, T.; Zhang, H.; Wang, X.; Suo, J. *Chem. Commun.* **2002**, 860.
- [59] Okumura, M.; Akita, T.; Haruta, M.; Wang, X.; Kajikawa, O.; Okada, O. *Appl. Catal. B* **2003**, 41, 43.
- [60] Veriykios, X. E.; Stein, F. P.; Coughlin, R. W. *Catal. Rev. Sci. Eng.* **1980**, 22, 197.
- [61] Nijhuis, T. A.; Makkee, M.; Moulijn, J. A.; Weckhuysen, B. M. *Ind. Eng. Chem. Res.* **2006**, 45, 3447.
- [62] Carter, E. A.; Goddard, W. A. *J. Catal.* **1988**, 112, 80.
- [63] Grant, R. B.; Lambert, R. M. *J. Catal.* **1985**, 93, 92.
- [64] Ponec, V.; Bond, G. C. *in: Catalysis by Metals and Alloys, Studies in Surface Science and Catalysis Vol 95*, Elsevier, Amsterdam, New York, 1995.
- [65] Chinchin, G. C.; Waugh, K. C. *J. Catal.* **1986**, 97, 280.
- [66] Vaughan, O. P. H.; Kyriakou, G.; Macleod, N.; Tikhov, M.; Lambert, R. M. *J. Catal.* **2005**, 236, 401.
- [67] Linic, S.; Jankowiak, J. T.; Barteau, M. A. *J. Catal.* **2004**, 224, 489.
- [68] Jankowiak, J. T.; Barteau, M. A. *J. Catal.* **2005**, 236, 366.

Chapter Two

Experimental Techniques

2.1. Introduction

Catalysis is a multidisciplinary area of science and is a combination of fundamental and applied science with contributions from chemistry, physics and material science [1,2]. Many characterisation techniques have been used in catalysis research, aiming to analyze the catalyst composition and unveil the microscopic mechanism behind reactions catalyzed by various materials. In this chapter, the basic principles of some characterisation techniques relating to the research work in this thesis are introduced. Also, a concise description of the reactors used in the present research work is given.

2.2. X-ray powder diffraction (XRD)

2.2.1 Introduction to XRD

Röntgen discovered X-rays in 1895 [3]. Since then, X-rays have found significant application in three main areas with respect to materials [3,4]. Here, crystallographic aspects of X-ray powder diffraction (XRD) are introduced since it is a common technique used in the study of heterogeneous catalysts.

XRD is a non-destructive technique and its most widespread use is for the identification of crystalline compounds by their diffraction pattern. This method was

traditionally used for phase identification, quantitative analysis and the determination of structure imperfections [3,4]. Later, applications of XRD have been significantly extended to new areas, such as the determination of crystal structures and the extraction of three-dimensional microstructural properties.

In nature, about 95% of all solid materials can be described as crystalline [4]. When X-rays interact with a crystalline substance, a diffraction pattern will be obtained. Therefore, the X-ray diffraction pattern of a pure substance is like a fingerprint of the substance. The XRD method is thus ideally suitable for characterization and identification of polycrystalline phases. Today, diffraction patterns of about 50,000 inorganic and 25,000 organic single components, crystalline phases have been collected and stored as standards. XRD can be used to identify components in a sample by a search/match procedure. Furthermore, the areas under the peaks are related to the quantity of each phase present in the sample. For pure amorphous solid materials, no phase diffraction patterns appear by XRD analysis.

2.2.2 Theoretical principles

The three-dimensional structure of crystalline materials can be defined as regular repeating planes of atoms that form a crystal lattice. When a focused X-ray beam interacts with these planes of atoms, part of it will be diffracted. X-rays are diffracted by each material differently, which depends on what atoms make up the crystal lattice and how these atoms arrange [3,4].

In X-ray powder diffractometry, X-rays are generated within a sealed tube under vacuum. A current is used that heats the filament in the tube; the higher current the greater number of electrons emitted from the filament. A high voltage, typically 15-60 kilovolts, is applied in the tube. This high voltage is used to accelerate electrons, which then hit a target, commonly made of copper. The X-rays will be produced when these electrons hit the target. A detector detects the X-rays signal and the signal is processed electronically and converted to a count rate. As a result, the well-known XRD pattern picture is obtained. **Figure 2.1** depicts a simplified schematic of the X-ray tube, the X-ray detector and the sample during the X-ray scan.

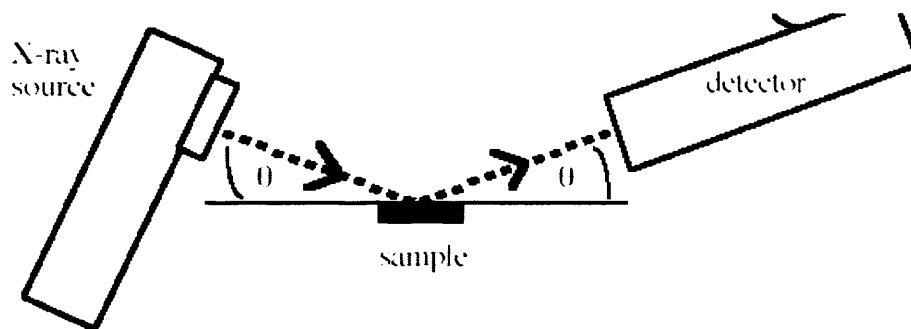


**Fig.2.1 Schematic of the X-ray tube, the X-ray detector and the sample
(θ : diffraction angle)**

When X-rays hit a crystalline sample and are diffracted, the distances between the planes of atoms that constitute the sample can be measured according to a mathematical formula called **Bragg's Law** [3,4]. Bragg's Law is shown below and in **Figure 2.2**:

$$n \lambda = 2d \sin\theta$$

Where n is an integer that represents the order of the X-ray beam, λ is the

wavelength, d is the interplanar spacing generating the diffraction and θ is the diffraction angle. Since we know λ and θ , the d -spacings can be calculated.

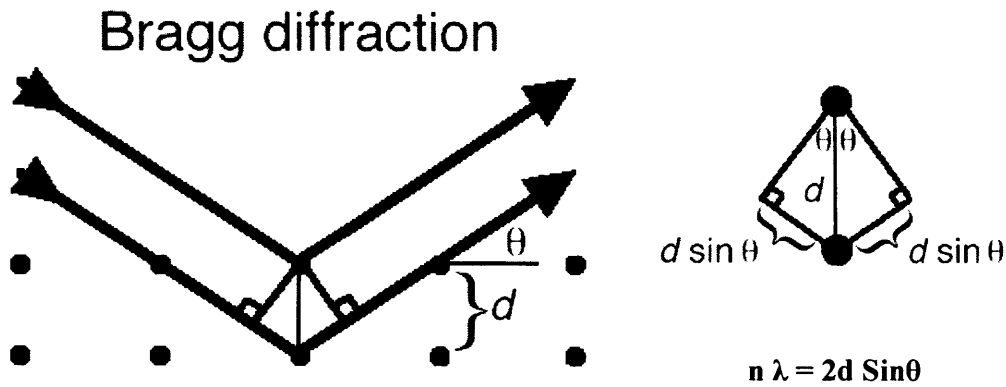


Fig.2.2 Bragg's Law of diffraction

Because each crystalline substance has a unique X-ray diffraction pattern, the characteristic sets of d -spacings generated in a typical X-ray can be used as a fingerprint of the sample. When properly and reasonably interpreted, by comparison with standard reference patterns and measurements, this fingerprint of XRD pattern allows for identification of the material. For example, the characteristic XRD patterns of crystalline NaCl and KCl are depicted in **Figure 2.3**.

The number of observed peaks in an XRD pattern is related to the symmetry of the unit cell in the crystalline structure. The d -spacings of the observed peaks are related to the repeating distances between planes of atoms in the structure. The intensities of the peaks are related to the atoms that are in the repeating planes.

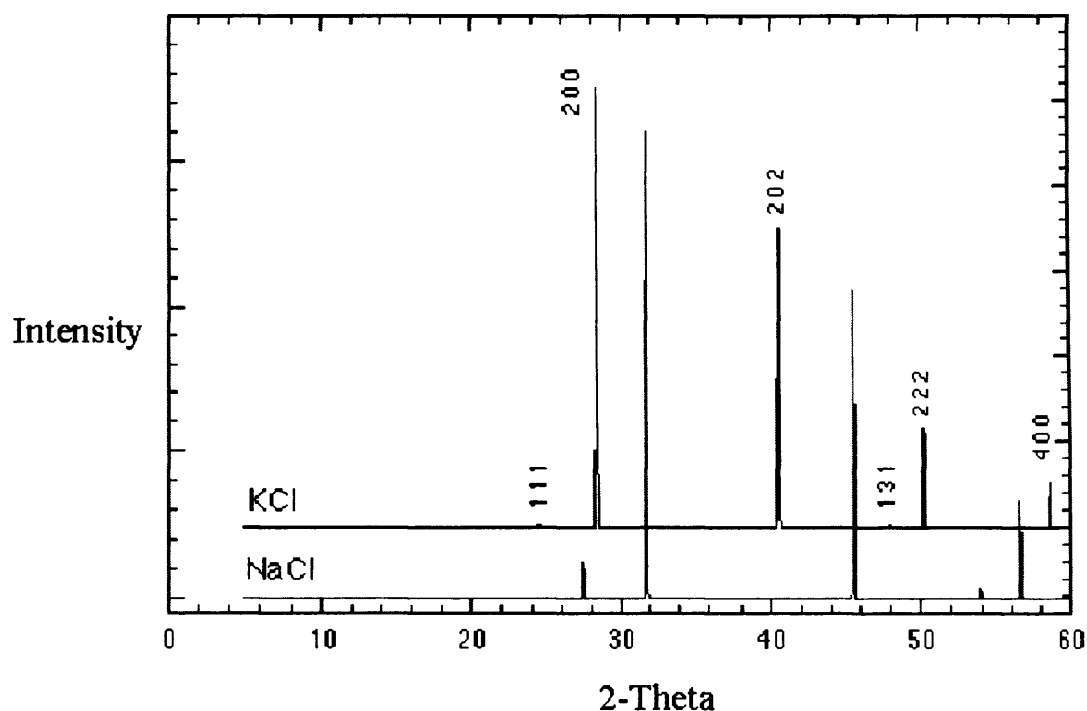


Fig.2.3 XRD patterns of NaCl and KCl

In the current work, the XRD analysis was performed using an Eraf Nonius PSD120 diffractometer with a monochromatic Cu $K_{\alpha 1}$ source operated at 40 keV and 30 mA.

2.3. BET method

Surface area is an important and intrinsic physical property of materials that can reveal crucial information concerning the usefulness of a material for a given purpose. Surface area frequently plays a significant role in the reactivity of catalysts, sintering behaviour of powdered metals and durability of rubber compounds, and so forth [5]. For example, in many cases, for a given catalyst, the greater the amount of surface available to the reacting gas the better is the conversion to products.

The most widely used technique (also the one used in this thesis) for determining the surface area is the so-called BET method (Brunauer, Emmet and Teller, proposed in 1938) [6]. The basis principle of this method is to estimate the surface area by measuring the amount of gas adsorbed (typically nitrogen) at cryogenic temperatures (liquid nitrogen). Based on the amount of gas adsorbed at a given pressure, the BET equation is employed to calculate the number of adsorbed gas molecules that would be required to form a monolayer on the surface. In combination with the knowledge of the cross-sectional area of the gas molecule adsorbed, the surface area can be easily calculated.

In the current research work, powder samples were firstly degassed for approximately 30 minutes. Then, the sample was placed in a sample vessel connected to a gas inlet (liquid N₂ at 77K used to cool the vessel), a vacuum pump and an electronic barometer. The initial step of the analysis involved evacuation of the chamber in order to remove adsorbed molecules from the surface. Then follows the deposition step where N₂ is allowed into the chamber and the pressure is measured. Based on the BET method, the specific surface area of a solid was calculated electronically.

2.4. Scanning Electron Microscopy (SEM)

Scanning electron microscopy (SEM) involves a microscope that uses electrons rather than light to form an image [7]. SEM allows a greater depth of focus than optical microscopy. For this reason, SEM is able produce an image that is a good illustration of

a three-dimensional sample. In the present work, SEM images provide the following information: surface topography (namely what the surface looks like) and surface morphology (the shape and size of particles making up the sample).

A schematic of a SEM is shown in **Figure 2.4**. Heating a metallic filament in a vacuum generates a beam of electrons. The electron beam follows a vertical path through the column of the microscope. It makes its way through electromagnetic lenses that are able to focus and direct the beam toward the sample. When it hits the sample, two sorts of electrons are produced, namely secondary electrons and backscattered electrons. Secondary electrons are the result of the high-energy electron beam displacing loosely held surface electrons that are recorded using a secondary electron detector to produce an image of the surface. Secondary electrons are more dependent upon the surface area within a given area of intersection of the beam and therefore relate to topographic features. Backscattered electrons are high-energy electrons from the primary beam that are scattered back out of the sample by the atomic nuclei. The intensity of the signal is dependent upon the mean atomic number of the area of interaction. The backscattered image mainly shows the contrast in chemical composition. The primary image is formed by collecting secondary electrons that are released by the samples. Secondary and backscattered electrons are collected by the detector and then converted to a signal that is sent to a viewing screen like a TV screen. The image given by the SEM is strikingly similar to what would be seen by an optical scope. The illumination and shadowing in the SEM image will display a quite natural looking surface topography. Some examples of SEM images are shown in **Figure 2.5**.

Current SEM analysis was performed using a Hitachi S-2460N instrument operating at 25KV on gold coated powder samples.

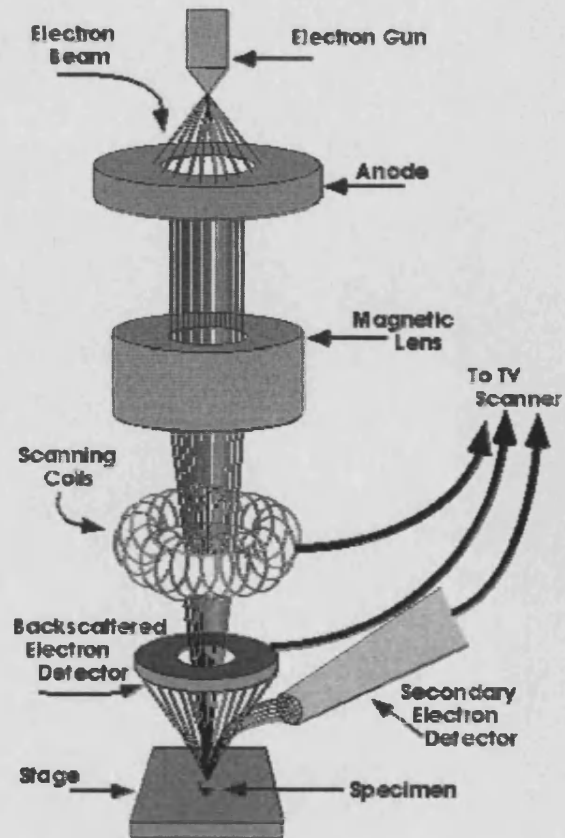
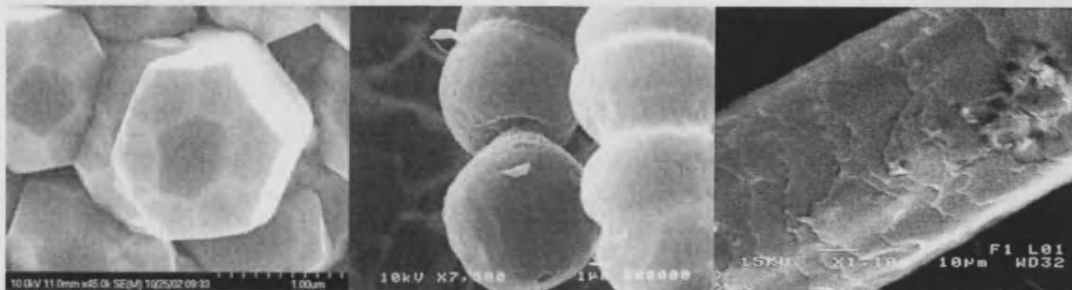


Fig.2.4 Schematic of scanning electron microscope (SEM)



ZnO crystal

Algae

Human hair

Fig.2.5 Examples of SEM images

2.5. Transmission Electron Microscopy (TEM)

Similar to scanning electron microscopy (SEM) mentioned above, transmission electron microscopy (TEM) is another kind of electron microscopy using electrons instead of light as source to image the target [8]. The main difference between the SEM and TEM lies in the resolution power.

The spatial resolution of SEM depends on the size of the electron spot, which in turn depends on the magnetic electron-optical system that generates the scanning beam. In addition, the resolution of SEM is limited by the size of the interaction volume, or the extent of material which interacts with the electron beam. The spot size and the interaction volume are both very large compared to the distances between atoms. As a consequence, the resolution of SEM is not high enough to image down to the atomic scale, as is possible in TEM. However, it should be noted that SEM has compensating advantages. For example, SEM has the ability to image a comparatively large area of the specimen and the ability to image bulk materials. Generally speaking, SEM images are much easier to interpret than TEM images.

SEM generates the image of the three-dimensional surface structure by detecting the secondary and backscattered electrons reflected by the sample whereas TEM works much like a slide projector, as shown in **Figure 2.6**. TEM uses electromagnetic lenses to focus the electrons into a very thin beam. Then, the electron beam travels through the specimen. Depending on the density of the material present, some of the electrons are scattered and disappear from the beam. At the bottom of the microscope, the unscattered

(transmitted) electrons hit a fluorescent screen, which gives rise to a "shadow image" of the specimen with its different parts displayed in varied darkness according to their density. The as-formed TEM image can be photographed with a camera.

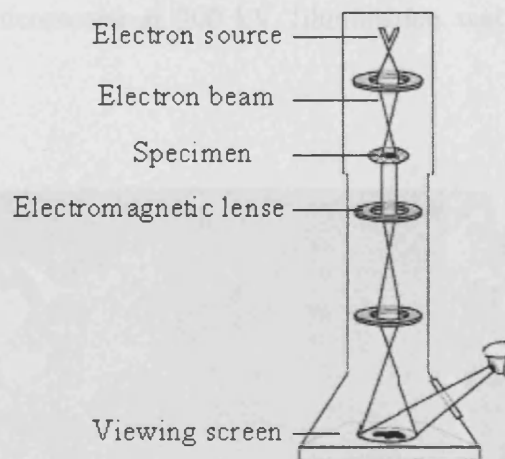


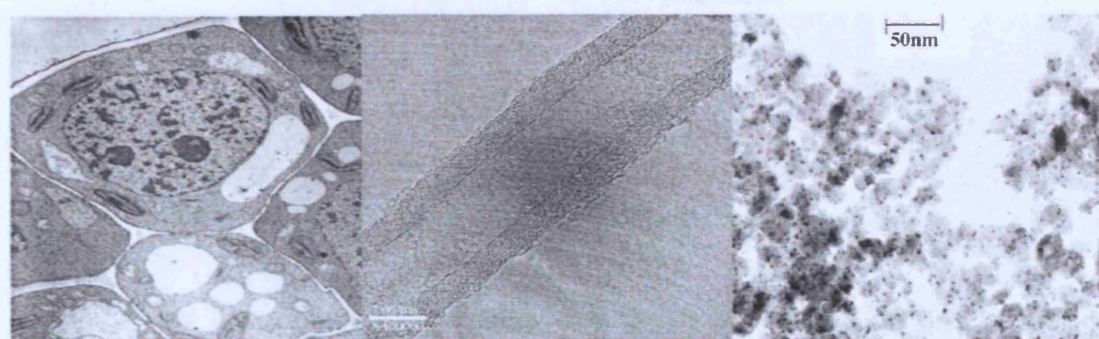
Fig.2.6 Schematic of transmission scanning microscope (TEM)

Although TEM has higher resolution than SEM, there are some drawbacks. Many materials require extensive sample preparation to produce a sample thin enough to be electron transparent, which makes TEM analysis relatively time consuming. Also, the structure of the sample may be changed during the preparation process. The field of view is relatively small, raising the possibility that the region analysed may not be characteristic of the whole sample. In a few cases, it is possible that the sample may be damaged by the electron beam, particularly for biological materials. Some examples of TEM images are showed in **Figure 2.7**.

The joint-use of SEM and TEM is regarded as a valuable tool in both medical, biological, materials and heterogeneous catalysis [8]. They can provide complementary

information at a microscopic level and hence generate an image of the composition, shape and size of a given catalyst.

In the current work, TEM studies were performed using a Jeol 2000EX high resolution electron microscope at 200 kV. Illumination was achieved using a LaB6 filament.



Sunflower cell

Multi-walled carbon nanotube

Gold supported on Fe₂O₃

Fig.2.7 Examples of TEM images

2.6. X-ray photoelectron spectroscopy (XPS)

X-ray photoelectron spectroscopy (XPS) is also known as electron spectroscopy for chemical analysis (ESCA) [9]. This technique usually consists of a fixed X-ray energy source and an electron energy analyzer, as shown in **Figure 2.8**. Al K_α (1486.6eV) or Mg K_α (1253.6eV) is often the most commonly employed X-ray source, XPS is a useful technique used to determine the electronic state, elemental composition and chemical species that exist on the surface of samples [9].

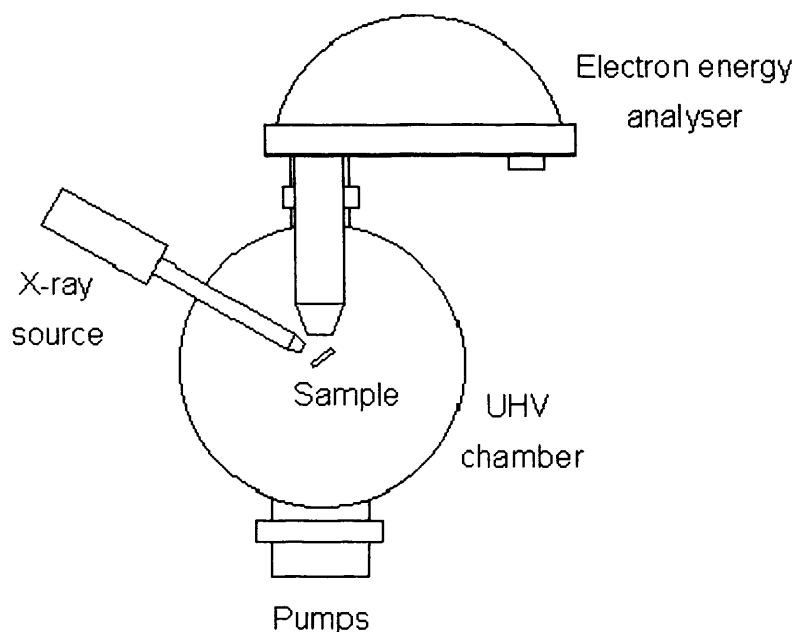


Fig.2.8 Schematic of X-ray photoelectron spectrometer

XPS uses X-ray radiation to examine core-levels of the elements on the surface. XPS must be carried out under a ultra high vacuum (UHV) environment, which enables the photoelectrons to be analyzed without interference from gas phase collisions. For each and every element, there will be a characteristic binding energy associated with each core atomic orbital i.e. each element will give rise to a characteristic set of peaks in the photoelectron spectrum at kinetic energies determined by the photon energy and the respective binding energies. The shape of each peak and the binding energy can be slightly altered by the chemical state of the emitting atom. Therefore, XPS can also offer us chemical bonding information. XPS is not sensitive to hydrogen or helium, but can detect all other elements.

The principle of XPS is based on the photoelectric effect outlined by Einstein in 1905 where the concept of the photon was used to describe the ejection of electrons

from a surface when photons impinge upon it. An X-ray photon ionizes an atom, producing an ejected free electron from the core shell of atom, as shown in **Figure 2.9**.

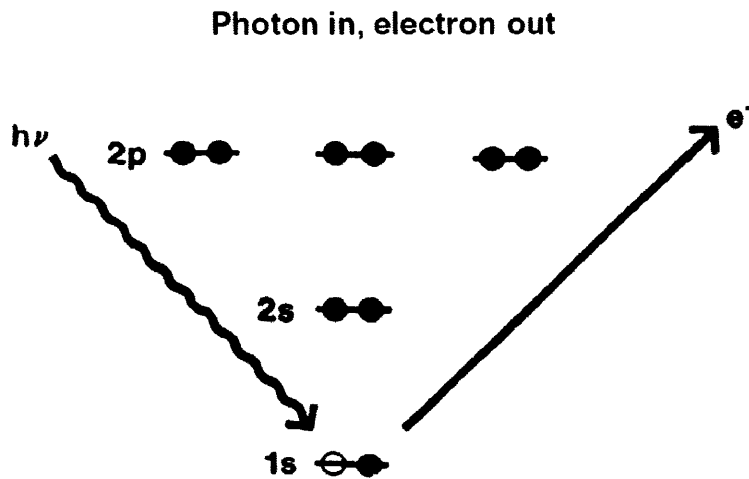


Fig.2.9 Ejection of electrons excited by X-rays

The kinetic energy of the ejected photoelectron is dependent on the energy of the impinging photon expressed as:

$$E_k = h\nu - E_b - \Phi$$

Where E_k is the kinetic energy of the photon ejected, $h\nu$ is the x-ray energy, E_b is the binding energy of the parent atom relative to the ejected electron and Φ is the work function, typically < 2 eV and often ignored. Measuring the E_k and calculating the E_b will produce the 'fingerprint' of the parent atom. Namely, the emitted electron signal excited by X-rays can be plotted as a spectrum of binding energies. Because the energy of core electrons is very specific for the element that the atom belongs to, the spectrum is able to provide information on the electronic state, elemental composition and chemical species that exist on the surface of samples. Figure 10 shows the XPS of

palladium (Pd) metal, where the most intense peak at ca. 335 eV is ascribed to emission from the 3*d* levels of the Pd atoms, while the 3*p* and 3*s* levels give rise to the peaks at ca. 534/561 eV and 673 eV respectively.

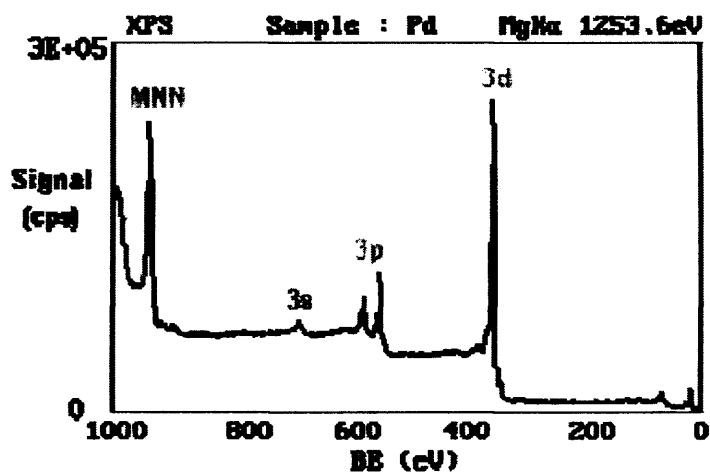


Fig.2.10 The XPS spectrum of a Pd metal sample

In the current work, XPS analysis was carried out with an ESCALAB 220 spectrometer using an achromatic AlK α source and an analyser pass energy of 100eV.

2.7. Atomic Absorption Spectrophotometry (AAS)

Atomic absorption spectrophotometry (AAS) is an analytic technique for determining the concentration of a particular metal element within a sample. AAS involved the measurement of an absorption of optical radiation by atoms in the gaseous state and can be used to analyse the concentration of over 62 different metals in a solution [10]. AAS primarily consists of the following sections: light source, sample cell, monochromator and detector, as shown in **Figure 2.11**.

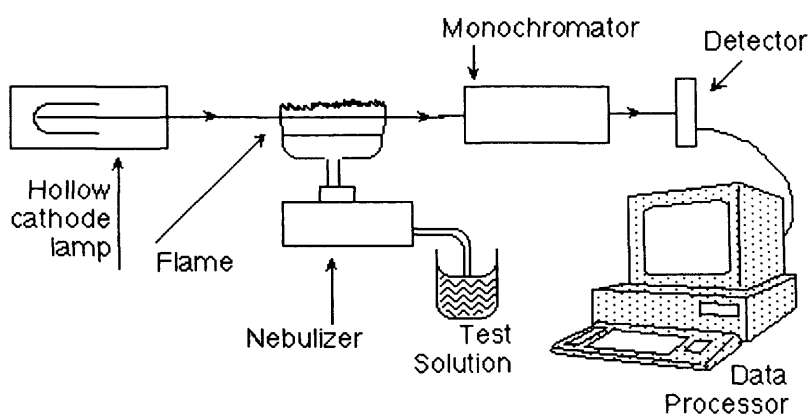


Fig.2.11 Schematic of atomic absorption spectrophotometer

A light source is used to emit the atomic spectrum of a particular element. According to the element to be determined, specific lamps generally hollow cathode lamps (HCL), are utilized. A hollow cathode lamp contains a tungsten anode and a cylindrical hollow cathode made of the element to be determined. These are sealed in a glass tube filled with an inert gas, for example, argon or neon. The sample cell is a section where an atomic sample vapor is produced in the light beam from the source. In general, this is accomplished by introducing the sample into a burner system or electrically heated furnace, aligned in the optical path of the spectrophotometer.

A monochromator is used to select the specific wavelength of light, namely spectral line, which is absorbed by the sample and to exclude other wavelengths. The selection of the specific light allows the determination of the selected element in the presence of others. The detector is typically a photomultiplier tube that magnifies and converts the light intensity selected by the monochromator. Thus, an electrical signal proportional to the light intensity will be produced. This electrical signal is a measure of

the light attenuation occurring in the sample cell and is further processed to generate instrument readout in concentration units.

The concentration measurement is usually determined from a working curve (or calibration curve) after calibrating the instrument with standards of known concentration. A calibration curve is produced using a series of known standard solutions. The calibration curve shows the concentration against the amount of radiation absorbed, as shown in **Figure 2.12**.

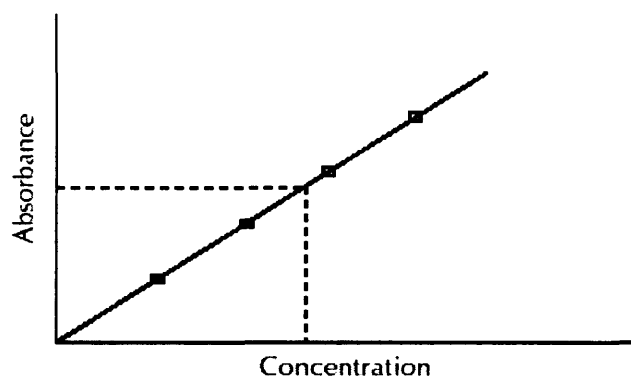


Fig.2.12 Example of calibration curve in AAS

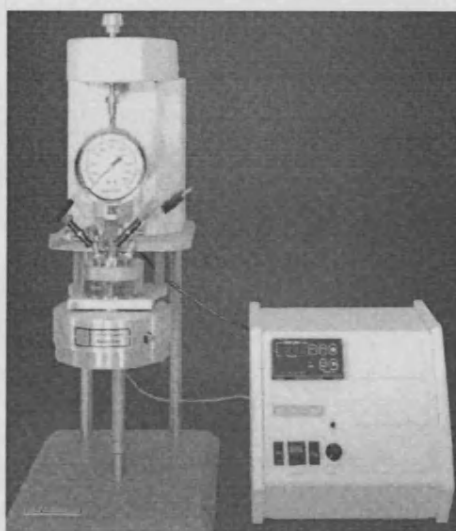
The concentration of the element to be determined can be readily derived from this calibration curve. Successful operation of AAS often depends on the correct choice of flame, suitable preparation of samples and standards, careful optical alignment of the lamp with the monochromator and careful alignment of the burner with the light path. In the present work, AAS is used to determine the loading of metal on a support, and in some cases to analyze for leaching of metal from the catalyst during liquid phase experiments. AAS was performed with a Perkin-Elmer 2100 Atomic Absorption spectrometer using an air-acetylene flame.

2.8. Reactors used in the present work

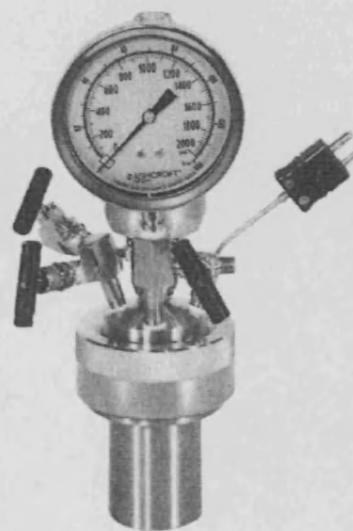
Three different kinds of reactors have been used in the present research work.

(a) For liquid phase oxidation reactions at atmospheric pressure, a round-bottomed glass reactor equipped with a cooling condenser has been used.

(b) For liquid phase oxidation reactions under pressure, an autoclave with associated control equipment (**Figure 2.13**) has been used.



(a) autoclave and controller



(b) autoclave assembly

Fig.2.13 Photographs of autoclave and controller

(c) Gas phase oxidation reactions were performed in a single stage fixed bed reactor.

2.9. References and notes

- [1] Brückner, A. *Catal. Rev.* **2003**, 45, 97.
- [2] Gai-Boyes, P. L. *Catal. Rev. Sci. Eng.* **1992**, 34, 1.
- [3] Cullity, B. D.; Stock, S. R. *Elements of X-ray Diffraction* 3rd Ed. Addison-Wesley, 2001.
- [4] Jenkins, R.; Snyder, R. L. *Introduction to X-ray Powder Diffraction* John Wiley, 1996.
- [5] Thomas, J. M.; Thomas, W. J. *Principles and Practice of Heterogeneous Catalysis* Wiley, 1997.
- [6] Brunauer, S.; Emmett, P. H.; Teller, E. *J. Am. Chem. Soc.* **1938**, 60, 309.
- [7] Staniforth, M.; Goldstein, J.; Newbury, D. E.; Lyman, C. E.; Echlin, P.; Lifshin, E.; Sawyer, L. C.; Michael, J. R.; Joy, D. C. *Scanning Electron Microscopy and X-ray Microanalysis* Springer 2002.
- [8] Flegler, S. L.; Heckman, J. W.; Klomparens, K. L. *Scanning and Transmission Electron Microscope* Oxford University Press 1993.
- [9] Watts, J. F.; Wolstenholme, J. *An Introduction to Surface Analysis by XPS and AES* John Wiley & Sons 2003.
- [10] Robinson, J. W.; Robinson, R. *Atomic Spectroscopy* Marcel Dekker 1996.

Chapter Three

Heterogeneous Selective Oxidation of Alkenes over Supported Gold Catalysts

3.1. Introduction

Selective oxidation of hydrocarbons to produce oxygen-containing organic compounds is of key importance in modern industrial chemistry process [1-4]. For example, selective epoxidation of alkenes represents a very intriguing topic in heterogeneous catalysis and the as-formed epoxides are of great commercial and synthetic significance. However, most industrial oxidation processes involve using chlorine or organic peroxides, which in the case of the former produce huge amounts of chloride salts as well as lesser amounts of toxic chlorinated organic by-products, whereas for the latter the cost is high [5,6]. The introduction of catalytic systems using oxygen from air is attractive and presents immense scope for minimising waste and generating green chemical processes [7]. Gold, previously regarded as an inert metal, now appears to have significant potential for selective oxidation processes based on heterogeneous catalysis [8-13].

In this chapter, it will be shown that nano-crystalline supported gold catalyst can provide tuneable activity for effectively oxidizing alkenes, including cyclohexene and cis-cyclooctene, using molecular oxygen from air under mild conditions.

3.2. Experimental

3.2.1 Preparation of gold and Bi, Sn, Sb or Pb-doped gold catalysts

Graphite (as-received from Johnson Matthey) is used as the support for preparing nano-crystalline gold catalyst. Gold supported on graphite (Au/G) is used in the present study. Our research group has previously shown that this Au/G catalyst can be used for selective oxidation of glycerol to glyceric acid with 100% selectivity, hence providing a sound starting point. 1 wt % Au/G catalyst is prepared as the following: The carbon support (graphite, Johnson Matthey, 113.2 g) was stirred in deionised water (1 l) for 15 min. An aqueous solution of HAuCl_4 (49.94% Au, Johnson Matthey, 2.38 g) in water (70 ml) was slowly added dropwise over a period of 30 min. The slurry was then refluxed for 30 min, cooled and reduced with formaldehyde over a period of 30 min. The slurry was then refluxed for 30 min and, following cooling, the catalyst was recovered by filtration and washed with water until the washings contained no chloride. The catalyst was dried for 16 h at 105 °C. This method was also used to prepare 0.25 wt% Au/G and 0.5 wt% Au/G catalyst samples using smaller amounts of chloroauric acid.

For Bismuth-doped catalyst, it is prepared as follows: $\text{Bi}(\text{NO}_3)_3$ (0.0359g) was dissolved in ultrapure water (50ml) and stirred for 2h. The required amount to obtain a particular surface concentration was transferred to an evaporating basin containing Au/G (1g), and stirred for 3h, after which the stirring was then stopped and the solution was allowed to evaporate overnight. This catalyst was washed and filtered off under

vacuum. The catalyst was finally washed with 60ml ultrapure water and dried at 100⁰C for 1h. In a similar way, Sn, Sb or Pb doped Au catalysts were also prepared.

3.2.2 Characterisation of supports and catalysts

The techniques of XRD, BET, SEM and TEM have been used to characterize the support and supported gold catalyst. In selected cases, X-ray photoelectron spectra (XPS) of the catalyst were performed, which were recorded with an ESCALAB 220 spectrometer using an achromatic AlK α source and an analyser pass energy of 100eV. In addition, AAS is used to detect if there is gold leaching after the reaction.

3.2.3 Catalyst testing

In general, reactions were performed in a glass reactor consisting of a 50ml round-bottomed flask with reflux cooling condenser connected. A supported gold catalyst (0.22g) in a solution of alkene (0.012mol) in 20ml solvent with a small amount of radical initiator tert-butyl hydrogen peroxide (TBHP) (0.077g, *ca.* 5mol% of alkene) was used. Experiments were generally performed using an oil bath at 80⁰C for 24h. In selected cases where initial results showed that expected products of selective oxidation of alkenes were observed, time on-line studies were performed to explore the profile of the reaction vs. time. In addition, some reactions were carried out in a high-pressure autoclave by suspending a gold catalyst (0.22g) in a solution of alkene (0.012mol) in 20ml solvent in a Parr autoclave (50ml). The autoclave was pressurized to the required pressure with oxygen (43 psi) and stirred for the desired time at 80⁰C.

The products for the oxidation of alkenes, such as cyclohexene and cis-cyclooctene, were analyzed using a gas chromatograph (Varian Star 3400 CX) fitted with a DB-5 column and a flame ionization detector (FID). Samples were taken at the end of reactions for quantification; 200 μ l of sample was added to 20 μ l of internal standard (3-pentanone, 98%, Aldrich) and 0.5 μ l of this sample was injected into the GC.

3.3. Results and discussions

3.3.1 Characterisation of supports and catalysts

For the graphite support, BET analysis show that this graphite has low surface area of 10m²/g. The surface morphology can be clearly seen in the SEM images as shown in **Figure 3.1**. For supported 1%Au/G catalyst, BET analysis shows it has the surface area of 11m²/g, similar to the support. **Figure 3.2** shows the SEM images of as-prepared 1%Au/G catalyst. Compared to that of graphite support in **Figure 3.1**, no significant change of surface morphology has been observed.

Figure 3.3 shows the XRD pattern of graphite and 1%Au/G catalyst. There is no discernable gold peak in the XRD pattern of 1%Au/G catalyst. However, analysis by TEM of the catalyst shows that it comprises nano-crystalline Au particles with a broad size range from 5nm to 50nm, with a mean particle diameter of *ca.* 25nm of multiply twinned character, as displayed in **Figure 3.4**. For lower loading Au on graphite catalysts, the particle density varies with gold loading in the expected manner.

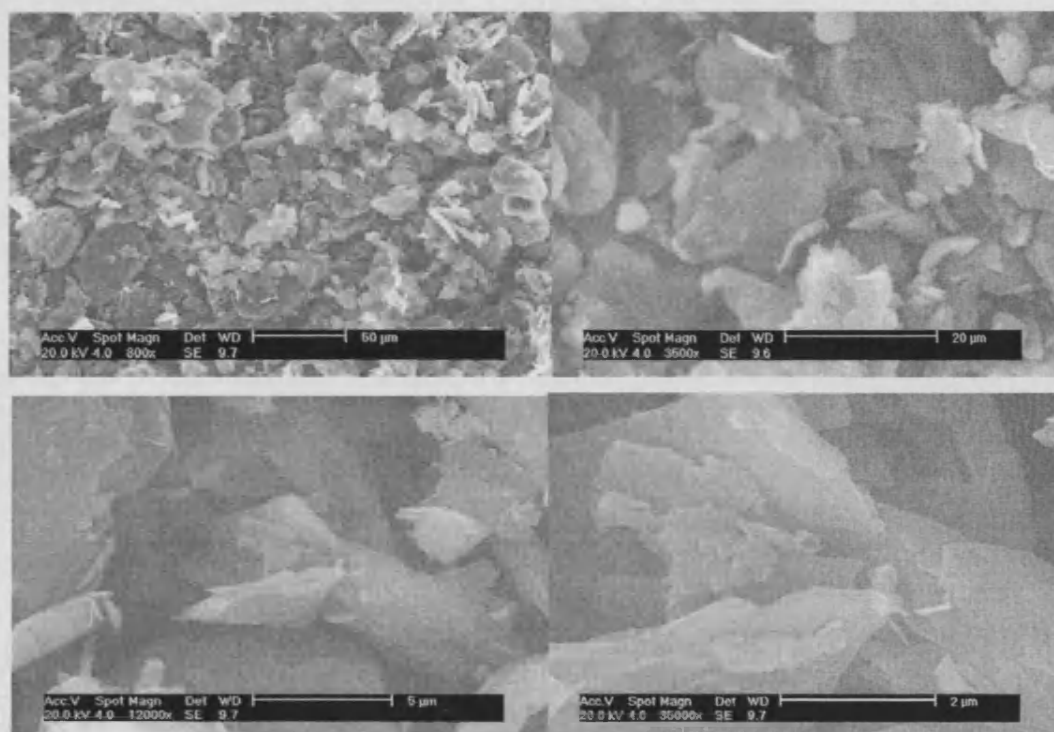


Fig.3.1. SEM images of graphite

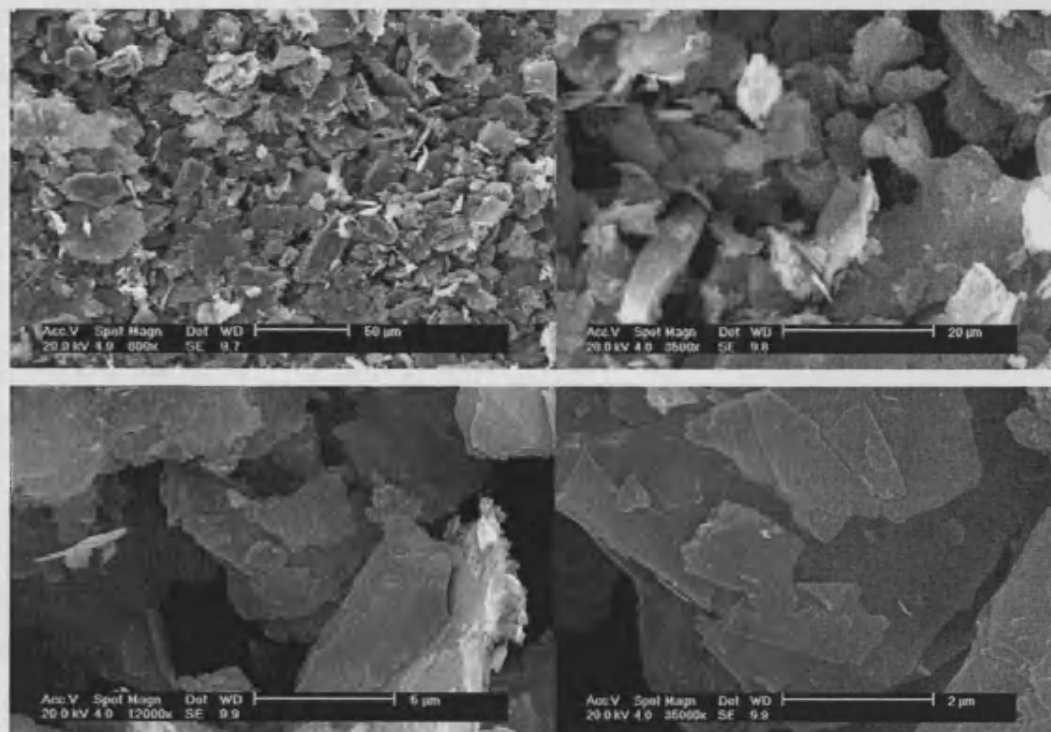


Fig.3.2. SEM images of 1% Au/G catalyst

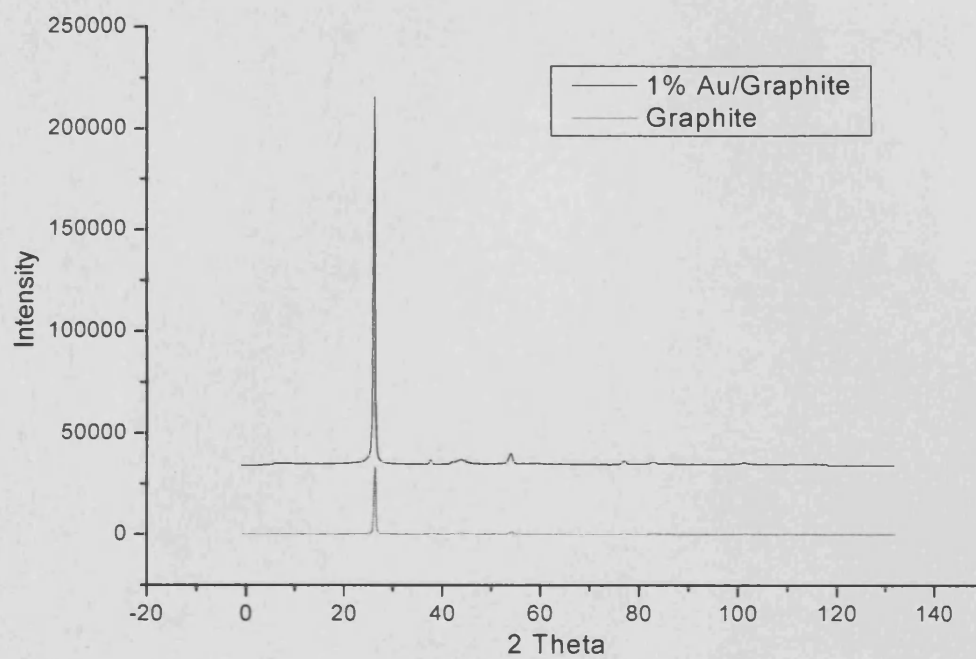
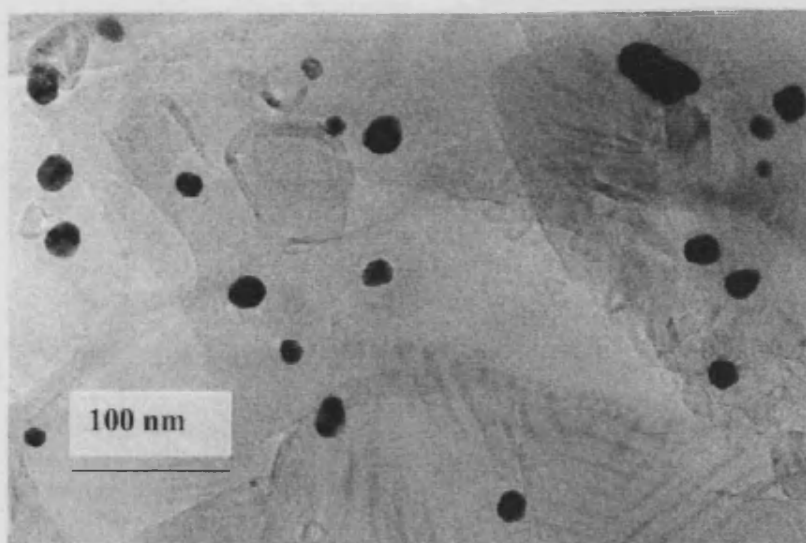


Fig.3.3. XPD pattern of graphite and 1%Au/G catalyst



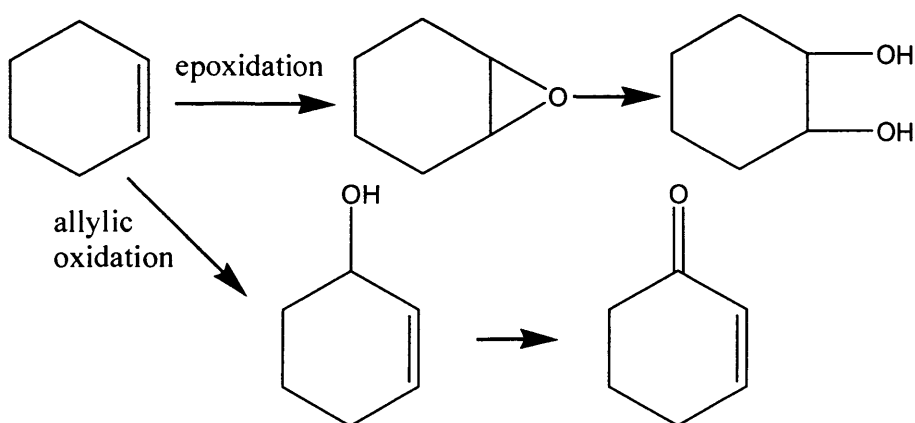
**Fig.3.4. Bright field transmission electron microscopy
(TEM) of 1%Au/G catalyst**

3.3.2 Selective oxidation of cyclohexene

3.3.2.1 Initial experiments for cyclohexene oxidation

In the initial stages of the project, the cyclohexene oxidation over 1%Au/G catalyst was investigated. Mathew Hughes primarily finished this pioneering work on cyclohexene oxidation and showed that supported Au/G catalyst can be used effectively for the selective oxidation of cyclohexene under mild conditions.

Cyclohexene can be oxidised to form several possible products, including direct epoxidation to cyclohexene epoxide, followed by ring-opening to cyclohexane-1,2-diol or allylic oxidation to 2-cyclohexen-1-ol plus possible further oxidation to 2-cyclohexen-1-one (Scheme 3.1). In general, epoxidation involves a single-step concerted mechanism and allylic oxidation involves a radical mechanism.



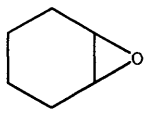
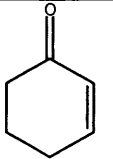
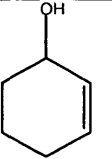
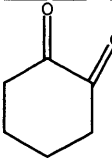
Scheme 3.1 Cyclohexene selective oxidation pathways

Table 3.1 shows the data for initial experiments for oxidation of cyclohexene using several polar solvents, including water, methanol and acetonitrile over 1%Au/G

catalyst in a stirred glass reactor. Obviously, using these solvents, no expected target C₆ oxidation products were observed, although significant conversions were obtained when using water and methanol as solvents. Meanwhile, the results for cyclohexene oxidation in an autoclave using molecular oxygen (3bar) as oxidant, as shown in **Table 3.2**, also demonstrate that the desired C₆ oxidation products were not observed. Under these conditions, only CO₂, formic acid, and oxalic acid are formed when using water and methanol as solvents.

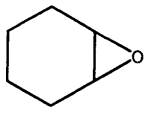
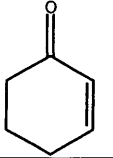
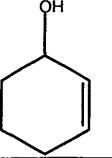
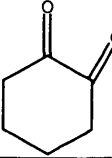
The stability of the potential reaction of expected target C₆ products has been tested using water and acetonitrile as solvents under identical conditions. The results are shown in **Table 3.3**. It can be seen that the expected C₆ products have relatively good stability under such reaction conditions. For example, when reacted in water for 24h in a glass reactor, conversions of only 5.3%, 7.7%, 1.1% and 0% were observed, for cyclohexene oxide, 2-cyclohexen-1-one, 2-cyclohexen-1-ol and cyclohexane-1, 2-dione, respectively. This suggests that, if these expected C₆ products had been formed, they would have been observed. In addition, it is clear that in these solvents the oxidation of cyclohexene does not proceed via the epoxide. However, it should be noted that, although the expected C₆ products are not observed under these conditions, these initial results indicate that supported gold on graphite catalyst is very active for oxidation. If appropriate reaction conditions could be found, it should be possible to form the target C₆ products.

Table 3.1. Cyclohexene oxidation in polar solvents over 1%Au/G catalyst operated in a stirred glass reactor

Solvent	Conv (%)	Selectivity (%)				Total sel of C ₆ (%)
						
Water	100	0	0	0	0	0
Methanol	27.1	0	0	0	0	0
Acetonitrile	0	0	0	0	0	0

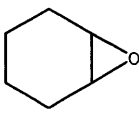
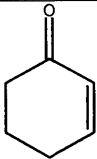
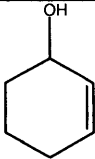
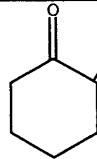
Reaction conditions: 0.22g catalyst, 20ml solvent, 0.012mol substrate, 0.077g TBHP, 80°C reaction for 24h.

Table 3.2. Cyclohexene oxidation in polar solvents over 1%Au/G catalyst operated in an autoclave using oxygen as oxidant

Solvent	Conv (%)	Selectivity (%)				Total sel of C ₆ (%)
						
Water	100	0	0	0	0	0
Methanol	37.2	0	0	0	0	0
Acetonitrile	0	0	0	0	0	0

Reaction conditions: 0.22g catalyst, 20ml solvent, 0.012mol substrate, 43psi oxygen, 80°C reaction for 4h.

Table 3.3. Reaction of potential oxidation products over 1%Au/G catalyst

Solvent	Conversion (%)			
				
Water ^a	5.3	7.7	1.1	0
Acetonitrile ^a	4.2	2.4	0.5	0
Water ^b	6.7	7.5	0.9	0
Acetonitrile ^b	2.1	1.4	0.2	0

a: reactions in a stirred glass reactor; b: reactions in an autoclave

Reaction conditions in a glass reactor: 0.22g catalyst, 20ml solvent, 0.012mol substrate, 0.077g TBHP, 80°C reaction for 24h.

Reaction conditions in an autoclave: 0.22g catalyst, 20ml solvent, 0.012mol substrate, 43psi oxygen, 80°C reaction for 4h.

3.3.2.2 Solvent effect on cyclohexene oxidation over Au/G catalyst

Following the initial experiments, cyclohexene oxidation was investigated using a series of different solvents. The data are summarized in **Table 3.4**. It was found that with these media some partial oxidation C₆ products were observed. In particular, the results show that selective oxidation of cyclohexene to the desired C₆ products is favourable in aromatic solvents. Using selected aromatic solvents, the selectivity to C₆ products is in the range 60~80%. What is more, the distribution of C₆ products obtained is clearly dependent on the solvent. For example, the highest selectivity to cyclohexene epoxide, *ca.* 50%, has been obtained using 1,2,3,5-TMB(tetramethylbenzene) as solvent; meanwhile, 26.3% selectivity to 2-cyclohexen-1-one is obtained. When using

1,4-dimethylbenzene as solvent, no cyclohexene epoxide is obtained and only 12.0% and 43.5% selectivities to 2-cyclohexen-1-one and cyclohexane-1, 2-dione are respectively observed. For reactions in these aromatic solvents, the total selectivity to C₆ products are also different, which can be clearly seen from **Figure 3.5**.

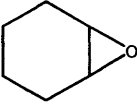
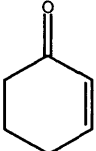
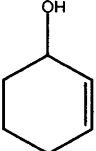
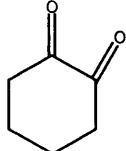
The results mentioned above strongly illustrate that the C₆ products are solvent dependent and hence the product selectivity can be tailored by choosing the appropriate solvent. Blank experiments (**Table 3.5**) show that, in the absence of an initiator, TBHP, no cyclohexene conversion is observed. However, it should be noted that only a catalytic amount of initiator is required. In the absence of 1%Au/G catalyst, but in the presence of catalytic amount of TBHP, again no conversion of cyclohexene is observed. For an experiment of cyclohexene oxidation using only graphite support, no conversion is achieved. Thus, these control experiments confirm that the supported gold catalyst is necessary and is intimately involved in selective oxidation of cyclohexene to desired C₆ products. It is the nano-crystalline gold particles along with a small amount of catalytic TBHP that readily kick-start the selective oxidation reaction of cyclohexene.

To understand if aromatic solvents are involved in the reaction mechanism, an experiment using d₈-deuterotoluene as solvent was performed. No discernable change for the selectivity to C₆ products and the rate of the reaction to 2-cyclohexen-1-ol and 2-cyclohexen-1-one was observed compared to that using deuterated toluene as solvent. In addition, no incorporation of deuterium into the products was observed. This indicates that the aromatic solvent is not intimately involved with the reaction and the

absence of a kinetic isotope effect suggests that the solvent is not acting as a sacrificial source of hydrogen in the rate-determining step, in contrast to the epoxidation of propene in which sacrificial H₂ is required to activate molecular oxygen.

In addition, for reactant mixtures with 1,2,3,5-TMB and 1,4-dimethylbenzene as solvent, atomic absorption spectroscopy (AAS) showed that no gold leaching occurred, suggesting that supported gold particles act as a purely heterogeneous catalyst.

Table 3.4. Solvents effects on cyclohexene oxidation over 1%Au/G catalyst operated in a stirred glass reactor

Solvent	Conv (%)	Selectivity (%)				Total sel of C ₆ (%)
						
Water	100	0	0	0	0	0
Methanol	27.1	0	0	0	0	0
Acetonitrile	0	0	0	0	0	0
THF	5.8	0	0	0	0	0
Hexane	26.1	Trace	Trace	Trace	0	0
Toluene	29.1	Trace	35.1	25.1	0	60.2
1,4-Dimethylbenzene	53.5	0	12.0	0	43.5	55.5
1,3,5-Trimethylbenzene	8.0	Trace	78.1	Trace	0	78.1
1,2,3,5-TMB	29.7	50.2	26.3	0	0	76.5
1,2,4,5-TMB ^a	23.1	26.0	42.0	9.1	0	77.1
Quinoline	33.2	0	10.5	0	0	10.5
1,4-Difluorobenzene	29.1	0	47.1	26.8	0	73.9
Hexafluorobenzene	15.8	8.9	36.1	2.5	0	47.5
Tert-butylbenzene	16.5	9.1	25.5	10.9	0	45.5
Isopropylbenzene	19.9	12.1	39.2	16.6	0	67.9
Triisopropylbenzene	27.8	6.1	20.1	15.1	0	41.3

Reaction conditions: 0.22g catalyst, 20ml solvent, 0.012mol substrate, 0.077g TBHP, 80⁰C reaction for 24h. a: 1,2,4,5-TMB is dissolved in 1,4-dimethylbenzene; TMB: tetramethylbenzene.

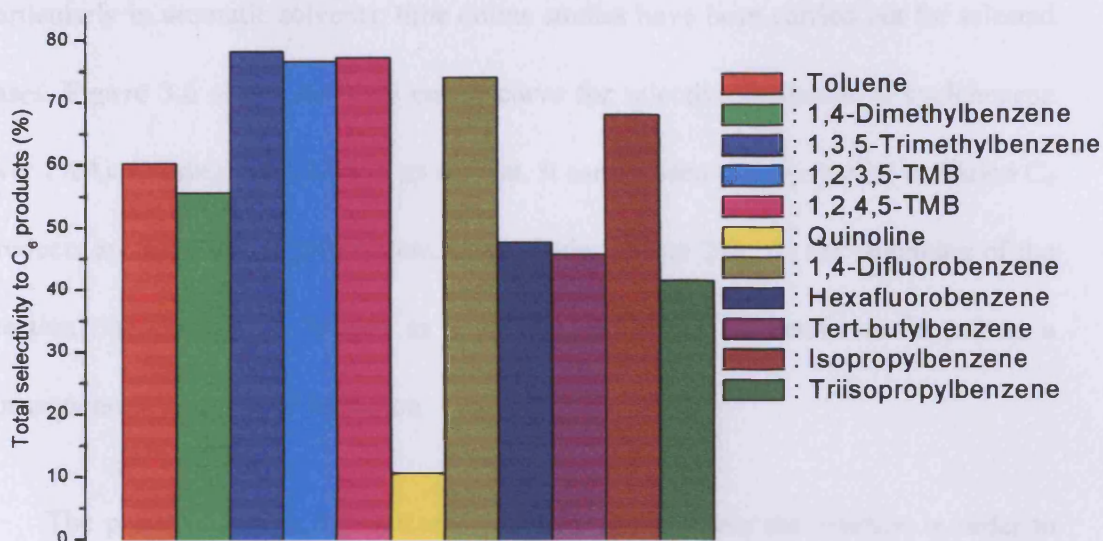


Figure 3.5. Total selectivity to C₆ products using aromatic solvents

Table 3.5. Blank experiments for cyclohexene oxidation in a glass reactor

Entry ^a	Conversion (%)
1%Au/G + Solvent without TBHP	0
Graphite + Solvent with TBHP	0
Solvent and TBHP without 1%Au/G	0

a: blank experiments carried out using 1,2,3,5-TMB and toluene as solvent.

TBHP (0.077g, 5%mol cyclohexene), reaction at 80⁰C for 24h.

3.3.2.3 Time online studies for cyclohexene oxidation over Au/G catalyst

In order to understand the detailed reaction profile of selective oxidation of cyclohexene over supported Au/G catalyst in the presence of solvents with reaction time,

particularly in aromatic solvents, time online studies have been carried out for selected cases. **Figure 3.6** shows the time online curve for selective oxidation of cyclohexene over 1%Au/G using 1,2,3,5-TMB as solvent. It can be seen that the partial oxidation C₆ products are favoured in this system, in particular before 24h. At the beginning of the reaction, the epoxide is formed as a primary product. The ketone is formed as a consequence of sequential oxidation.

The profile suggests it is necessary to carefully monitor the reaction in order to ensure the highest selectivity to C₆ products is obtained. Fortunately, these C₆ products are relatively stable under these reaction conditions and therefore the results for reaction for 24h can roughly reflect the point where the highest selectivity to C₆ products is obtained, although it is possible to observe higher selectivity to C₆ products before 24h in other solvents. This is also in agreement with the stability of potential C₆ products in the present catalyst system, as shown in **Table 3.6**.

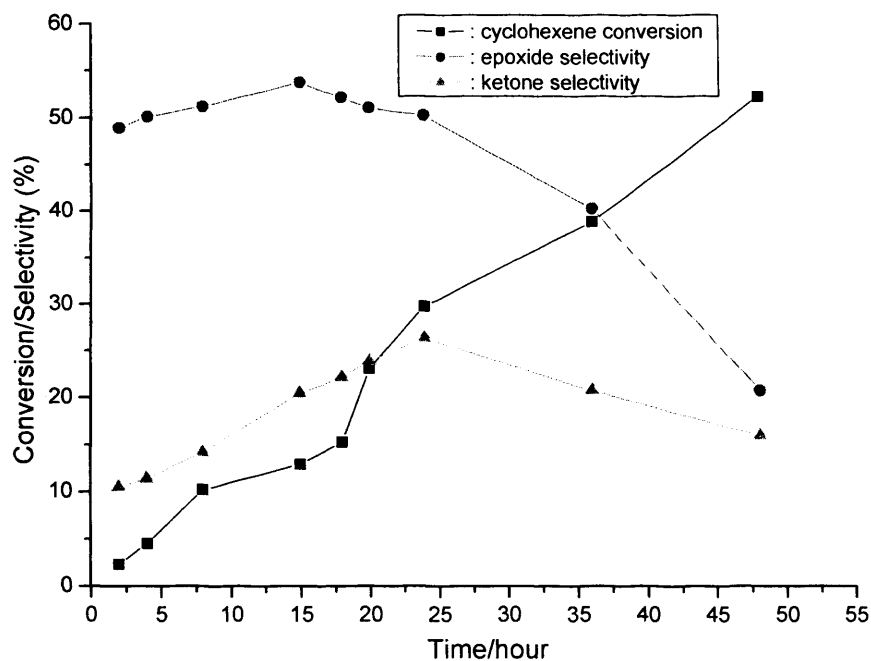
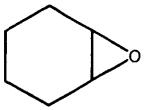
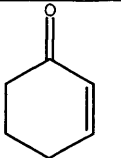
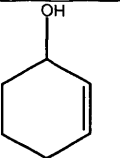
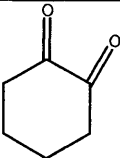


Fig.3.6 Time online curve for cyclohexene oxidation over 1%Au/G catalyst

Table 3.6. Reaction of potential oxidation products over 1%Au/G catalyst in the presence of solvents at 80⁰C for 24h in a stirred glass reactor

Solvent	Conversion (%)			
				
1,2,3,5-TMB	4.8	8.2	--	--
Toluene	--	8.4	3.3	--
1,4-Dimethylbenzene	--	9.5	--	1.7

3.3.2.4 Cyclohexene oxidation over Bi-doped Au/G catalyst

To identify and add appropriate promoters to supported catalysts represents an important strategy to improve the activity of the catalyst in the heterogeneous domain. For example, Bi is well known to be a promoter, which can affect the selectivity of supported Pt catalysts [14]. However, so far, there is no report on the discovery of promoters for supported gold catalysts for liquid phase reactions, although Hutchings' research group recently demonstrated that traces of nitrate can be used as a beneficial promoter to enhance the activity of supported gold catalyst for CO oxidation.

The modification of the Au/G catalyst has been investigated using bismuth (Bi) at first. It was found that Bi can be used as a promoter for our gold catalyst; using Bi-doped Au/G catalyst the selectivity to C₆ products can be significantly enhanced. The following experiments were performed using 1,2,3,5-TMB or 1,4-dimethylbenzene as solvent, over different Bi-doped Au/G catalysts. The data are reported in **Tables 3.7** and **3.8**.

The results over Bi-modified Au/G catalysts show that the selectivity to C₆ products was significantly enhanced, particularly for the case using the solvent 1,2,3,5-TMB. The highest selectivity of *ca.* 98% for total C₆ products was obtained using a 0.5%Au/G (10ml Bi modification) catalyst in the solvent 1,2,3,5-TMB. Similar enhancement of selectivity has also been observed in the experiment carried out using 1,4-dimethylbenzene as solvent, although the improvement in total selectivity to C₆ products was less than for 1,2,3,5-TMB. On the other hand, it should be noted that the

conversion of cyclohexene was decreased while the total selectivity to C₆ products was improved. Therefore, Bi-modification of the catalyst seems to help maintain high selectivity. The catalytic results over Bi-doped Au/G catalyst suggest that Bi can be used as a promoter to enhance the selectivity of the supported gold catalysts. There is a potential scope to optimise Bi-modified Au catalysts.

XPS analysis of the catalyst before and after the reaction revealed a loss of Bi from the catalyst surface, as can be clearly seen in **Figure 3.7**. The molar ratio of Au:Bi for the fresh catalyst was 0.40, which decreased to 0.25 after the first reaction. In order to rule out the possibility of the leached Bi promoting a homogeneous reaction, the used catalyst has been re-tested with a new reactant mixture (see **Table 3.9**) and it was found that the conversion and selectivity observed are similar to those obtained during the initial experiment with the fresh Bi-modified Au/G catalysts although the Bi:Au molar ratio decreased further to 0.13. Furthermore, the solution recovered from the glass reactor exhibited no catalytic activity. Thus, these results confirm that the Bi-modification is due to a heterogeneously catalysed reaction. Clearly, only a small amount of Bi is required for such a promotional effect in catalytic selectivity of Au/G catalysts.

In addition to the effect of enhancement of selectivity by adding Bi to Au/G catalysts, it should be noted that, for the case in solvent 1,4-dimethylbenzene, the products observed over Bi-doped Au/G catalyst are different from those over unmodified Au/G catalyst. Using Au/G catalyst, no cyclohexene epoxide was observed. However,

cyclohexene epoxide was observed during the reaction over Bi-doped Au/G catalyst. This suggests that Bi promoter is able to play an important role and alter the reaction pathway when different solvents are used.

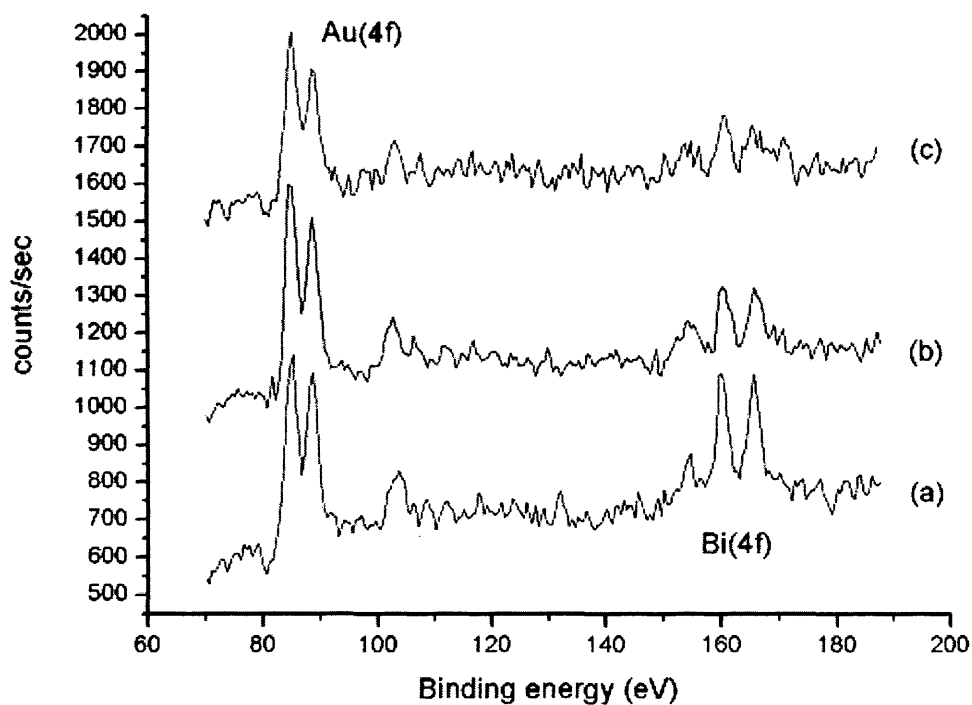
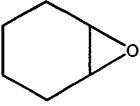
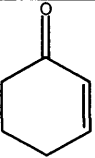
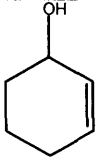


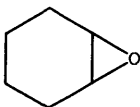
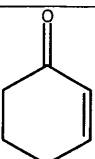
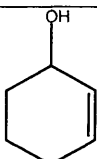
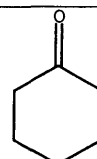
Fig.3.7. Au (4f) and Bi (4f) photoemission spectra obtained for (a) as-prepared fresh Bi-modified 1%Au/G catalyst, (b) after reaction (c) after further reaction with a fresh reactant mixture.

Table 3.7. Cyclohexene oxidation using Bi-doped Au/G catalysts in 1,2,3,5-TMB

Catalyst	Conv (%)	Selectivity (%)			Total sel of C ₆ (%)
					
1%Au/G (10ml Bi)	23.2	42.4	50.0	1.0	93.4
1%Au/G (5ml Bi)	22.5	40.8	41.8	3.2	85.8
1%Au/G ^a	29.7	50.2	26.3	Trace	76.5
0.5%Au/G (10ml Bi)	24.2	49.6	44.2	4.1	97.9
0.5%Au/G (5ml Bi)	19.5	48.6	41.7	3.7	94.0
0.5%Au/G ^a	36.4	28.6	26.1	3.0	57.7
0.25%Au/G (10ml Bi)	20.1	42.8	45.7	5.3	93.8
0.25%Au/G (5ml Bi)	18.2	44.5	40.9	3.8	89.2
0.25%Au/G ^a	32.3	28.1	25.6	3.9	57.6

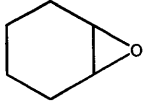
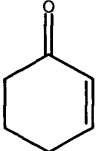
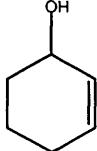
a: unmodified Au/G catalysts.

Table 3.8. Cyclohexene oxidation over Bi-doped Au/G catalysts in 1,4-dimethylbenzene

Catalyst	Conv (%)	Selectivity (%)				Total sel of C ₆ (%)
						
1%Au/G (10ml Bi)	13.9	26.6	30.9	8.6	0	66.1
1%Au/G (5ml Bi)	14.2	24.5	28.3	7.9	0	60.7
1%Au/G ^a	53.5	0	12.0	0	43.5	55.5
0.5%Au/G (10ml Bi)	14.6	24.7	25.7	5.9	0	56.3
0.5%Au/G (5ml Bi)	12.1	23.5	26.8	6.2	0	56.5
0.5%Au/G ^a	46.7	0	10.8	0	38.9	49.7

a: unmodified Au/G catalysts.

Table 3.9. Cyclohexene oxidation over fresh and re-used Bi-doped Au/G catalysts

Catalyst	Conv (%)	Selectivity (%)			Total sel of C ₆ (%)
					
1%Au/G (10ml Bi) first use ^a	13.9	26.6	30.9	8.6	66.1
1%Au/G (10ml Bi) re-used ^a	18.7	21.4	34.2	7.0	62.6
1%Au/G (10ml Bi) ^b first use ^b	23.2	42.4	50.0	1.0	93.4
1%Au/G (10ml Bi) ^b re-used ^b	21.0	39.7	48.6	1.9	90.2

a: in solvent 1,4-dimethylbenzene; b: in solvent 1,2,3,5-TMB

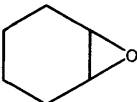
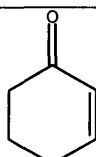
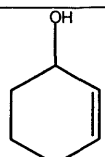
3.3.2.5 Cyclohexene oxidation over Sn, Sb or Pb-doped Au/G catalyst

In view of the promising effect of enhanced selectivity for Bi-modified Au catalysts, the reaction using Sn, Sb and Pb as promoters was further explored. The solvent 1,2,3,5-TMB was selected for this study considering that the highest selectivity to desired C₆ products had been observed when using this solvent to tune the reaction over an Au catalyst. The results over Sn, Sb and Pb doped-Au catalysts are listed in **Table 3.10**. As can be seen, an analogous promotional trend is observed for cyclohexene oxidation over Sn, Sb and Pb-doped Au catalysts, although it seems that the enhancement of total selectivity is a little higher using Bi-doped Au catalyst. Using these promoters, the conversion decreased to some degree as compared to the

unmodified Au/G catalyst, but the total selectivity to potential C₆ products, namely epoxide, alcohol and ketone, was improved.

These results indicate that there is a great potential for the design of improved gold oxidation catalysts using promoters. Furthermore, there is scope to optimize the composition function of as-prepared gold catalysts with these dopants and explore other preparation methods.

Table 3.10. Cyclohexene oxidation over Sn, Sb and Pb doped Au/G catalysts in the solvent 1,2,3,5-TMB

Catalyst	Conv (%)	Selectivity (%)			Total sel of C ₆ (%)
					
1%Au/G (Sn) ^a	24.6	46.1	38.7	2.8	87.6
1%Au/G (Sb) ^a	20.4	45.0	39.6	2.3	86.9
1%Au/G (Pb) ^a	22.7	41.6	36.2	3.9	81.7
1%Au/G (unmodified)	29.7	50.2	26.3	0	76.5
1%Au/G (10ml Bi)	23.2	42.4	50.0	1.0	93.4

a: Sn, Sb and Pb doped-Au catalysts contain the same mass (0.007g) of modifier as in the 1%Au/G (10ml Bi) as stated in Table 6.

3.3.3 Selective oxidation of cis-cyclooctene

3.3.3.1 Three purposes of study of cis-cyclooctene oxidation

The results shown above strongly suggest that, using Au supported on graphite, appropriate solvent and a small amount of TBHP as initiator, selective oxidation of cyclohexene can be finely tuned. In a subsequent study, the selective oxidation of cis-cyclooctene has been studied. This opens the possibility of a gold catalyst providing tuneable activity for the selective oxidation of other alkenes. In addition, using cis-cyclooctene as substrate, selective oxidation in the absence of solvents has been performed since effective selective oxidation without solvent represents a major tenet of green chemistry. The third reason for studying the oxidation of cis-cyclooctene over Au/G catalyst is to determine if the amount of radical initiator could be markedly reduced for the selective oxidation of cis-cyclooctene in the absence of solvents while still catalyst activity and selectivity can be achieved.

3.3.3.2 Selective oxidation of cis-cyclooctene with solvents




The data for selective oxidation of cis-cyclooctene over 1%Au/G catalyst in the presence of different solvents, similar to that of cyclohexene oxidation, are listed in **Table 3.11**. Clearly, the distribution of C₈ products is strongly dependent on the solvent used for the reaction, which is analogous to cyclohexene oxidation. The very high selectivity to epoxide suggests that direct oxidation of the C=C double bond occurs in the present system. For example, using the best solvent 1,2,3,5-tetramethylbenzene, the



selectivity to epoxide of *ca.* 94% has been observed. Selective oxidation to expected C₈ products seems to be more favourable in aromatic solvents than that in non-aromatic solvents. Blank experiments show that potential C₈ products are relatively stable in this catalyst system as shown in **Table 3.12**.

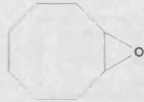


The results for selective oxidation of *cis*-cyclooctene demonstrate that gold supported on graphite catalyst has significant potential for the selective oxidation of alkenes to oxygenated products, particularly for epoxide formation rather than the competitive allylic oxidation.

Table 3.11 Cis-cyclooctene oxidation over 1%Au/G catalyst in the presence of different solvents operated in a stirred glass reactor

Solvent	Conv (%)	Selectivity (%)			Total C ₈ sel (%)
					
1,2,3,5-TMB	27.8	94.0	3.7	0.0	97.7
Toluene	7.8	77.9	13.3	2.0	93.2
Chlorobenzene	10.1	77.0	15.8	0.0	92.8
1,4-dimethylbenzene	11.2	75.4	6.9	6.2	88.5
THF	2.9	70.6	3.9	3.8	78.3
Quinoline	0.0	0.0	0.0	0.0	0.0
Methanol	0.0	0.0	0.0	0.0	0.0
DMF	9.6	58.9	4.1	2.9	65.9
DMSO	14.7	5.7	0.9	0.0	6.6
1,4-dioxane	5.6	58.8	20.0	2.8	81.6
Hexafluorobenzene	7.2	41.9	14.6	1.6	58.1
1,4-difluorobenzene	10.3	73.8	10.3	2.1	86.2
1-chloro-4-fluorobenzene	10.1	18.0	5.6	0.6	24.2
1-bromo-4-fluorobenzene	8.4	60.2	9.3	2.6	72.1
Benzonitrile	10.1	18.0	5.6	0.6	24.2
Acetonitrile	1.6	61.5	20.9	0	82.4
Chloroform	4.5	41.8	3.8	2.0	47.6

Reaction conditions: 0.12g catalyst, 10ml solvent, 0.006mol substrate, 0.077g TBHP, 80°C reaction for 24h.

Table 3.12 Reaction of potential C₈ products over 1%Au/G catalyst reaction for 24h at 80°C in a stirred glass reactor

Solvent	Conversion (%)		
			
1,2,3,5-TMB	3.1	6.2	0
Toluene	3.9	8.5	0.7
1,4-dimethylbenzene	3.4	7.3	0.4

Reaction conditions: 0.12g catalyst, 10ml solvent, 0.006mol substrate, 0.077g TBHP, 80°C reaction for 24h.

3.3.3.3 Time online studies for selective oxidation of cis-cyclooctene using solvents

Figures 3.8 and 3.9 show the time online curve for selective oxidation of cis-cyclooctene over 1%Au/G catalyst in the solvents toluene and 1,2,3,5-TMB. It can be seen that the high selectivity to the epoxide was maintained in these systems. The results at low conversion indicate that the cis-cyclooctene epoxide is formed initially and the other reaction products observed, such as alcohol or ketone, are the consequence of a sequential oxidation process.

The time online curves demonstrate that the partial oxidation C₈ products are relatively stable in the present catalyst system, similar to the case for selective oxidation of cyclohexene in the presence of solvents over Au/G catalyst. This is also consistent with the observation for the reaction of these potential C₈ products under identical reaction conditions as shown in **Table 3.12**.

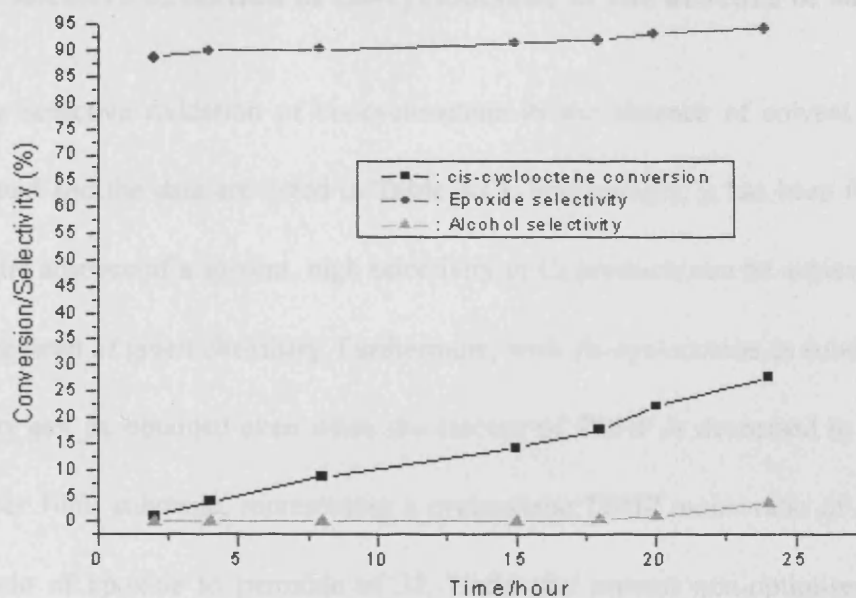


Fig.3.8 Time online curve in the solvent 1,2,3,5-TMB over 1%Au/G

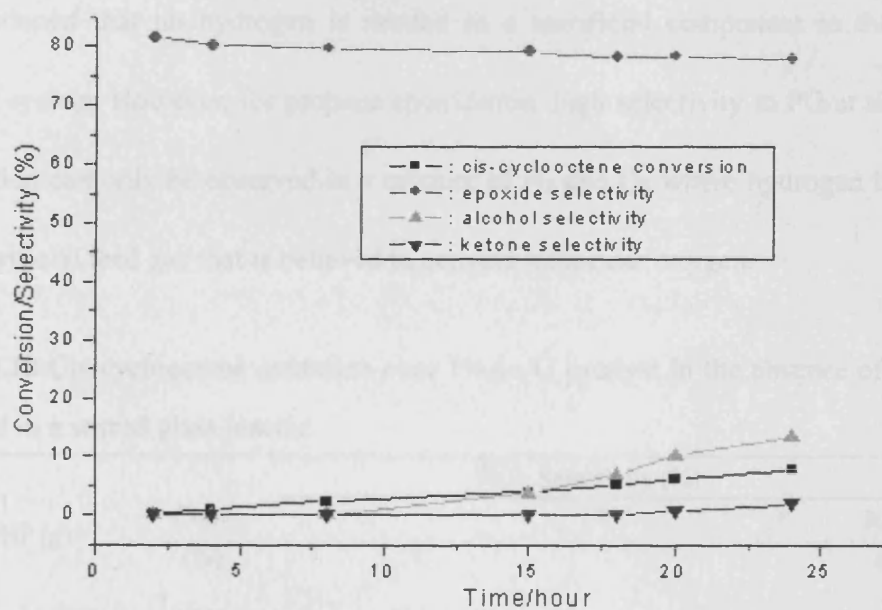





Fig.3.9 Time online curve in the solvent toluene over 1%Au/G

3.3.3.4 Selective oxidation of cis-cyclooctene in the absence of solvent

The selective oxidation of cis-cyclooctene in the absence of solvent has been investigated and the data are listed in **Table 3.13**. Interestingly, it has been found that, even in the absence of a solvent, high selectivity to C₈ products can be achieved, which is a major tenet of green chemistry. Furthermore, with cis-cyclooctene as substrate, high selectivity can be obtained even when the amount of TBHP is decreased to as low as 0.002g per 10ml substrate, representing a cyclooctene:TBHP molar ratio of 300 and a molar ratio of epoxide to peroxide of 32. Under the present non-optimised reaction system, yields of 35mol product per mol Au per h can be obtained, which is higher than previous reports for propene epoxidation by Haruta *et al.* [15,16]. Importantly, it should be mentioned that no hydrogen is needed as a sacrificial component in the present catalyst system. However, for propene epoxidation, high selectivity to PO at significant conversion can only be observed in a mixture of H₂ and O₂ where hydrogen is utilized as a sacrificial feed gas that is believed to activate molecular oxygen.

Table 3.12 Cis-cyclooctene oxidation over 1%Au/G catalyst in the absence of solvents operated in a stirred glass reactor

TBHP (g)	Conv (%)	Selectivity (%)			Total sel of C ₈ (%)
					
0.12	7.9	81.2	9.3	4.1	95.1
0.02	7.1	79.2	6.8	3.0	89.5
0.002	1.3	82.6	7.4	2.1	92.7

Reaction conditions: 0.12g catalyst, 10ml (0.066mol) cis-cyclooctene, 80°C for 24h.

3.3.4 Reaction mechanism

Commenting on the reaction mechanism in the present catalyst system, it is considered that a small amount of TBHP acts radical initiator for a chain reaction, which is sustained by molecular oxygen. The use of a radical scavenger, 2,6-ditertbutyl-4-methylphenol (BHT) demonstrates that radical chemistry is probably involved in the present reaction system over Au/G catalyst, as shown in **Tables 3.13** and **3.14**. For cyclohexene in a solvent over 1%Au/G catalyst, no conversion was obtained with radical scavenger BHT present. In a similar way, regarding the oxidation of cis-cyclooctene in the presence of solvents, no conversion has been achieved when radical scavenger is added to the reaction system. In addition, experiments were performed under a N₂ atmosphere in an autoclave in which no conversion was obtained (**Table 3.15**), suggesting that molecular oxygen from air is the active oxidant in the selective oxidation of alkenes in the presence of solvents over Au/G catalyst.

At the same time, it should be noted that, for the oxidation of cis-cyclooctene oxidation without solvent (**Table 3.14**), low conversion and low selectivity to epoxide and alcohol have been obtained when a radical scavenger is used. This indicates that, apart from radical chemistry mechanism, other possible mechanism may also exist, for example, oxygen transfer by peroxometal species formed on the gold nanoparticles surface. Furthermore, the observed distribution of products is intimately dependent on the solvent. The results strongly illustrate that the solvent does influence the selectivity observed, possibly by controlling the rates of the consecutive oxidation steps as well as

the formation of the active intermediates. The mediation of the solvent in the oxidation process could be via a weak interaction with the gold surface, particularly influencing the ease of electron transfer to, or from, the gold nanoparticles to establish the active chain carrier. Such a weak interaction has been observed with the C₆₀-mediated aggregation of gold nanoparticles [17]. The active species and intermediates leading to the target products, namely epoxide, alcohol and ketone, are likely to be closely associated with the gold surface. The experiment using d₈-deuterotoluene shown above suggests that the benzylic C-H bonds of the solvent are not attacked and consequently it is considered that very reactive O-centred radicals should not be involved in the selective oxidation reaction of alkenes in the presence of solvents.

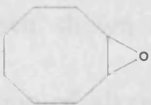


Table 3.13 Cyclohexene oxidation in the presence of radical scavenger *

Solvent	Conversion (%)
Toluene	0
1,4-Dimethylbenzene	0
1,2,3,5-TMB	0
Hexafluorobenzene	0

*: Radical scavenger is 2,6-ditertbutyl-4-methylphenol (BHT).

Reaction conditions: 0.12g 1%Au/G catalyst, 10ml solvent, 0.006mol cyclohexene, 0.077g TBHP, BHT (0.04g or 0.1g), 80°C for 24h in a stirred glass reactor.

Table 3.14 Cis-cyclooctene oxidation in the presence of radical scavenger *

Solvent	Conv (%)	Selectivity (%)			Total Sel (%)
					
--	0.5	7.5	0.5	0	8
Toluene	0	0	0	0	0
1,2,3,5-TMB	0	0	0	0	0
Hexafluorobenzene	0	0	0	0	0

*: Radical scavenger is 2,6-ditertbutyl-4-methylphenol (BHT).

Reaction conditions for experiments with solvent: 0.12g 1%Au/G catalyst, 10ml solvent, 0.006mol cis-cyclooctene, 0.077g TBHP, BHT (0.04g or 0.1g), 80°C for 24h in a stirred glass reactor.

Reaction conditions for experiments without solvent: 0.12g 1%Au/G catalyst, 10ml cis-cyclooctene, 0.077g TBHP, BHT (0.04g or 0.1g), 80°C for 24h in a stirred glass reactor.

Table 3.15 Reactions under the N₂ atmosphere

Solvent	Conversion (%)	
	Cyclohexene	Cis-cyclooctene
Toluene	0	0
1,4-Dimethylbenzene	0	0
1,2,3,5-TMB	0	0

Reaction conditions are the same as that shown in Table 3.14.

3.4. Conclusions

In summary, it has been shown that a supported Au catalyst has significant potential for selective oxidation of alkenes including cyclohexene and cis-cyclooctene using oxygen from air under mild conditions. By carefully choosing the reaction conditions, supported Au nanoparticles can provide tuneable activity for selective oxidation of alkenes. It has been found that the selective oxidation of alkenes is strongly dependent on the solvent that is used in the system; solvents do have an important influence on the distribution of target products in selective oxidation.

Bismuth has been found to be a promoter for selective oxidation of alkenes over Au/G catalysts. Using Bi-modified Au catalysts, the selectivity to target oxidation products has been significantly enhanced. For example, the highest selectivity, *ca.*98%, for selective oxidation C₆ products has been achieved for selective oxidation of cyclohexene in the presence of 1,2,3,5-tetramethylbenzene over a Bi-modified Au catalyst. Interestingly, Sn, Sb and Pb were also found to be effective promoters for enhancing the total selectivity to the target partial oxidation products, hence suggesting that there is a great scope to design supported Au catalysts with appropriate promoters. For cis-cyclooctene oxidation, it has been found that even in the absence of solvents, high selectivity to C₈ products can be obtained and the main product is the epoxide. This illustrates that supported Au catalysts have significant potential for selective epoxide formation, rather than for the competing allylic oxidation.

3.5. References and notes

- [1] Suresh, A. K.; Sharma, M. M.; Sridhar, T. *Ind. Eng. Chem. Res.* **2000**, 39, 3958.
- [2] Clark, J. H.; Macquarrie, D. J. *Org. Process Res. Dev.* **1997**, 1, 149.
- [3] Sheldon, R. A. *Stud. Surf. Sci. Catal.* **1991**, 66, 33.
- [4] Pagliaro, M.; Campestrini, S.; Ciriminna, R. *Chem. Soc. Rev.* **2005**, 34, 837.
- [5] Haruta, M. *Nature* **2005**, 437, 1098.
- [6] Pillai, U. R.; Sahle-Demessie, E. *Appl. Catal. A* **2003**, 245, 103.
- [7] Gallezot, P. *Catal. Today* **1997**, 37, 405.
- [8] Bond, G. C.; Thompson, D. T. *Catal. Rev. Eng. Sci.* **1999**, 41, 319.
- [9] Bond, G. C.; Thompson, D. T. *Gold Bull.* **2000**, 33, 41.
- [10] Hutchings, G. J.; Haruta, M. *Appl. Catal. A* **2005**, 291, 2.
- [11] Hutchings, G. J. *Catal. Today* **2005**, 100, 55.
- [12] Haruta, M. *Gold Bull.* **2004**, 37, 27.
- [13] Chen, M. S.; Goodman, D. W. *Catal. Today* **2006**, 111, 22.
- [14] Clavilier, J.; Feliu, J. M.; Aldaz, A. *J. Electroanal. Chem.* **1988**, 243, 419.
- [15] Sinha, A. K.; Seelan, S.; Tsubota, S.; Haruta, M. *Angew. Chem. Int. Ed. Engl.* **2004**, 43, 1546.
- [16] Sinha, A. K.; Seelan, S.; Tsubota, S.; Haruta, M. *Top. Catal.* **2004**, 29, 95.
- [17] Brust, M.; Kiely, J. K.; Bethell, D.; Schiffrin, D. J. *J. Am. Chem. Soc.* **1998**, 120, 12367.

Chapter Four

Selective Oxidation of Cyclohexane over Supported Gold Catalysts

4.1. Introduction

In the previous chapter, it has been shown that nano-crystalline gold catalysts supported on graphite can provide tunable catalytic activity for selective oxidation of alkenes, in particular cyclohexene and cis-cyclooctene. Selective oxidation reactions of alkenes to target products, namely epoxide, alcohol and ketone, can be readily kick-started using oxygen from air as oxidant over Au/G catalyst along with a small amount of TBHP as radical initiator. Strongly motivated by this preliminary study, in this chapter, it is demonstrated that such a Au/G catalyst can also be effective for the selective oxidation of cyclohexane to cyclohexanol and cyclohexanone under mild conditions.

The aerobic oxidation of cyclohexane to cyclohexanol and cyclohexanone is of key importance to the production of nylon-6 and nylon-6,6 and the worldwide production exceeds 10^6 tonnes per annum [1]. Commercially, this process is operated at 150-160°C with cobalt naphthenate as an initiator for the radical oxidation process that gives 70-85% selectivity at 4% conversion [1,2]. Operation at higher conversions leads to total oxidation and consequently this large-scale commercial process has been

designed to operate at low conversion. Clearly, there is a broad scope to produce a more efficient process but given the current focus on green chemistry the main aim is to design a system that gives 100% specificity. In fact, in a recent review, the selective oxidation of cyclohexane to cyclohexanol and cyclohexanone has been acknowledged as a reaction that continues to present a significant challenge [1].

On the other hand, it should be noted that activation of C-H bonds in saturated alkanes is well known to be very difficult to achieve selectively at temperatures below 100⁰C [3,4]. To date, the lowest temperature for selective oxidation of the alkane C-H bond has been reported by Thomas *et al.* using transitional metal ions substituted molecular sieve catalysts at 100⁰C [3-6]. In addition, it should be mentioned that air or molecular oxygen oxidations are intrinsically non-selective and difficult to control [4,7]. A recent study reported by Zhao *et al.* has shown that Au can be active for cyclohexane oxidation at 150⁰C and selectivities >90% can be achieved for the Au/ZSM-5 catalyst [8,9]; this study shows that supported Au catalysts are active for the activation of C-H bonds but the temperature used is 140-160⁰C, much higher than the temperature intended for the work in this thesis.

In this chapter, the activation of C-H bonds in cyclohexane at temperature below 100⁰C has been investigated. In particular, the use of Au/G catalyst has been examined and found that nano-crystalline gold particles are able to be effective at temperature as low as 70⁰C. High selectivity to cyclohexane and cyclohexanone, >90%, has been achieved using such a Au/G catalyst.

4.2. Experimental

4.2.1 Catalyst preparation

The same Au/G catalyst as used for selective oxidation of alkenes was chosen for this work. In addition, other series of Au/G catalysts were tried; these catalysts were prepared as the following: Firstly, the graphite support was pretreated by 2% or 5% (volume ratio) HNO₃, H₃PO₄, H₂SO₄ and NH₄OH, respectively. Namely, graphite support (2g) was immersed into the acid or base (20ml) stirring for 2h. The pretreated support was dried at 80⁰C. This pretreated support was then used to prepare Au catalysts supported on pretreated graphite. The procedures for preparation of supported 1wt %Au catalysts are as follows: the graphite support was stirred in deionised water (10ml) for 15min. An aqueous solution of HAuCl₄ (49.94% Au, Johnson Matthey, 0.04g) in water (5ml) was slowly added dropwise over a period of 10min. The slurry was refluxed for 15min, cooled and reduced with formaldehyde over a period of 15min and, following cooling, the catalyst was recovered by filtration and washed with water until the washings contained no chloride. The catalyst was dried for 16h at 105⁰C.

In addition, for comparison, cyclohexane oxidation over supported Pd or Pt catalyst was studied. 5 wt% Pt or Pd catalyst supported on graphite were prepared as follows. An aqueous solution of a platinum or palladium chloride salt (5% Pt or Pd metal by weight of support) was added to the stirred graphite slurry and reduced with formaldehyde. The slurry was allowed to settle and was filtered, washed free of chloride. After that, the catalyst was dried at 105 °C for 16h. This method was also used to

prepare a 1 wt% Pt or Pd/graphite catalysts using smaller amounts of metal chloride.

4.2.2 Catalyst testing

Reactions in the presence of solvent were carried out in a glass reactor consisting of a 50ml round-bottomed flask with a reflux-cooling condenser. Supported gold catalyst (0.22g) in a solution of cyclohexane (0.012mol) in solvent (20ml) along with a small amount of radical initiator TBHP (0.08g, *ca.* 5mol% of cyclohexane) was generally used. Experiments were performed using an oil bath at 70⁰C for 17h unless otherwise stated.

In addition, an autoclave was used to study reactions under high pressure. Supported gold catalyst (0.22g) in a solution of cyclohexane (0.012mol) in solvent (20ml) in a Parr autoclave (50ml) was used. Reactions using a small amount of TBHP (0.08g) were also carried out under high-pressure conditions. The autoclave was pressurized to the required pressure with oxygen or air and stirred for the required time at 70⁰C.

For experiments in the absence of solvent, reactions in a stirred glass reactor were carried out as follows: supported gold catalyst (0.12g) in a solution of cyclohexane (10ml) and radical initiator TBHP (0.08g) in a 50ml round-bottomed flask connected with a cooling condenser was used. Experiments were done in an oil bath heated to 70⁰C, with reaction mixtures stirred for 17h. Time-online studies were also performed in order to plot the profile on the reaction against time.

Analysis of reaction products for cyclohexane oxidation was carried out using a gas chromatograph (Varian Star 3400 CX) fitted with a DB-5 column and a flame ionization detector (FID). Samples were taken at the end of reactions; 200 μ l of sample was added to 20 μ l of internal standard (3-pentanone, 98%, Aldrich) and 0.5 μ l of this sample was analysed [10].

4.3. Results and discussions

4.3.1 Cyclohexane oxidation in the presence of solvents

Initial experiments were performed using a range of solvents that had been used for selective oxidation of cyclohexane to see if in these media target products, namely cyclohexanol and cyclohexanone, could be obtained. Reactions were performed either using a glass reactor at atmosphere pressure or using an autoclave at 3bar, both using air as oxidant and with a small amount of TBHP as initiator over a 1%Au/G catalyst. **Table 4.1** lists the data for these experiments.

Although cyclohexane conversion was observed, particularly with water and methanol as solvents, no partial selective oxidation products were detected. This is remarkably different from the previous observations for the selective oxidation of alkenes and reported studies of the oxidation of glycerol. Attempted oxidation of cyclohexanol and cyclohexanone under identical conditions (**Table 4.2**) demonstrated that they are relatively stable, strongly indicating that, if cyclohexanol and cyclohexanone are formed, they should be observed. However, when no solvent was

used at 70°C, the target products of cyclohexanol and cyclohexanone were observed.

Table 4.1. Cyclohexane oxidation over 1%Au/G catalyst in the presence of solvent

Solvent	Conversion ^a (%)	Conversion ^b (%)
Methanol	65.3	82.6
Water	100	100
Acetonitrile	8.9	0.0
Toluene	0.0	0.0
1,4-Dimethylbenzene	0.0	0.0
Chlorobenzene	0.0	0.0
1,2,4,5-TMB/Toluene	0.0	0.0
1,2,3,5-TMB	0.0	0.0
1,4-Difluorobenzene	0.0	0.0
Hexafluorobenzene	0.0	0.0
Cumene	15.5	0.0
Mesitylene	0.0	0.0
Quinoline	0.0	0.0
Acetic acid	6.5	16.5
Benzonitrile	12.5	0.0
Benzoy alcohol	0.0	0.0
Dioxane	0.0	0.0
DMF	0.0	0.0
DMSO	0.0	0.0
THF	0.0	0.0
Chloroform	0.0	0.0

^a Reaction conditions: 0.22g catalyst, 20ml solvent, 0.012mol cyclohexane, 0.08g TBHP, 70°C, 24h, using a glass reactor.

^b Reaction conditions: 0.22g catalyst, 20ml solvent, 0.012mol cyclohexane, 0.08g TBHP, 70°C, 3h, 3bar oxygen, 1500rpm, using an autoclave.

Table 4.2. Reaction of target partial oxidation products over 1%Au/G catalyst

Solvent	Conversion (%)	
	Cyclohexanol	Cyclohexanone
Water ^a	4.2	0.6
Methanol ^a	2.4	0.4
Acetonitrile ^a	0.4	0.0
Water ^b	2.5	0.3
Methanol ^b	0.9	0.0
Acetonitrile ^b	0.2	0.0

a: Reaction carried out in a glass reactor: 0.22g catalyst, 20ml solvent, 0.012mol substrate, 0.08g TBHP, 70°C, 24h, using a glass reactor.

b: Reactions carried out in an autoclave: 0.22g catalyst, 20ml solvent, 0.012mol substrate, 0.08g TBHP, 70°C, 3h, 3bar oxygen, 1500rpm

4.3.2 Cyclohexane oxidation without solvents

4.3.2.1 Glass reactor reactions

Table 4.3 lists the data for cyclohexane oxidation in the absence of solvents. In this case, the selective oxidation products, cyclohexanol and cyclohexanone, were observed. For example, over a 1%Au/G catalyst without solvent, a combined selectivity of 23.1% for cyclohexanol and cyclohexanone has been obtained at 3.7% cyclohexane conversion after reaction for 17h. Blank experiments with graphite or without catalyst showed that no conversion was obtained. Controlled experiments with graphite or without catalyst showed that no conversion was obtained.

These experiments suggest that, without solvents, nanocrystalline gold particles

can be effective for selective oxidation of cyclohexane to cyclohexanol and cyclohexanone. More interestingly, it has been found that the addition of a small amount of substituted aromatic substrate can act as an effective inhibitor, and the conversion of cyclohexane is apparently decreased and high selectivity to target selective oxidation products can be achieved, as shown in **Table 4.4** and **Figure 4.1**.

Table 4.3. Cyclohexane oxidation in the absence of solvent in glass reactor

Catalyst	Conv. (%)	Selectivity (%)		
		Cyclohexanol	Cyclohexanone	Total
0.25%Au/G	4.7	9.5	5.8	15.3
0.5%Au/G	6.0	11.0	6.2	17.2
1%Au/G	3.7	14.4	8.7	23.1
2%Au/G	7.3	5.9	4.0	9.9

Reaction conditions: 10ml cyclohexane, 0.12g Au/G catalyst, 0.08g TBHP, 70°C for 17h.

In particular, it has been found that high selectivity, *ca.* 92%, for cyclohexanol and cyclohexanone can be achieved at 1.0% conversion using a 0.5%Au/G catalyst when a small amount of 1,4-difluorobenzene is added. Thus, it seems that 1,4-difluorobenzene can be potentially used as an effective inhibitor that decreases the conversion of cyclohexane and increases the selectivity to target products of selective oxidation.

However, it should be noted that, under these conditions, the conversion is relatively low, typically around 1%. Detailed time online study showed that such a high selectivity can only be obtained at low conversion, and a longer reaction time will lead

to the loss of selectivity, as shown in **Figure 4.2**. In addition, for experiments using an increased amount of TBHP, it was found that the conversion increased but with a loss of selectivity.

Table 4.4. Cyclohexane oxidation with inhibitor, no solvent in a glass reactor

Additive	Conv. (%)	Selectivity (%)		
		Cyclohexanol	Cyclohexanone	Total
1,4-Difluorobenzene	1.0	48.1	43.5	91.6
1,4-Dichlorobenzene	1.4	32.2	20.1	52.3
Fluorobenzene	1.1	35.7	29.0	64.7
Chlorobenzene	1.1	32.4	21.1	53.5
Hexafluorobenzene	1.3	25.4	15.2	40.6
1-Chloro-4-Fluorobenzene	0.9	36.5	23.4	59.9
Toluene	1.2	12.1	7.2	19.3
1,4-Dimethylbenzene	1.1	10.6	6.4	17.0

Reaction conditions: 10ml cyclohexane, 0.05g additive, 0.12g 0.5%Au/G catalyst, 0.08g TBHP, 70°C for 17h.

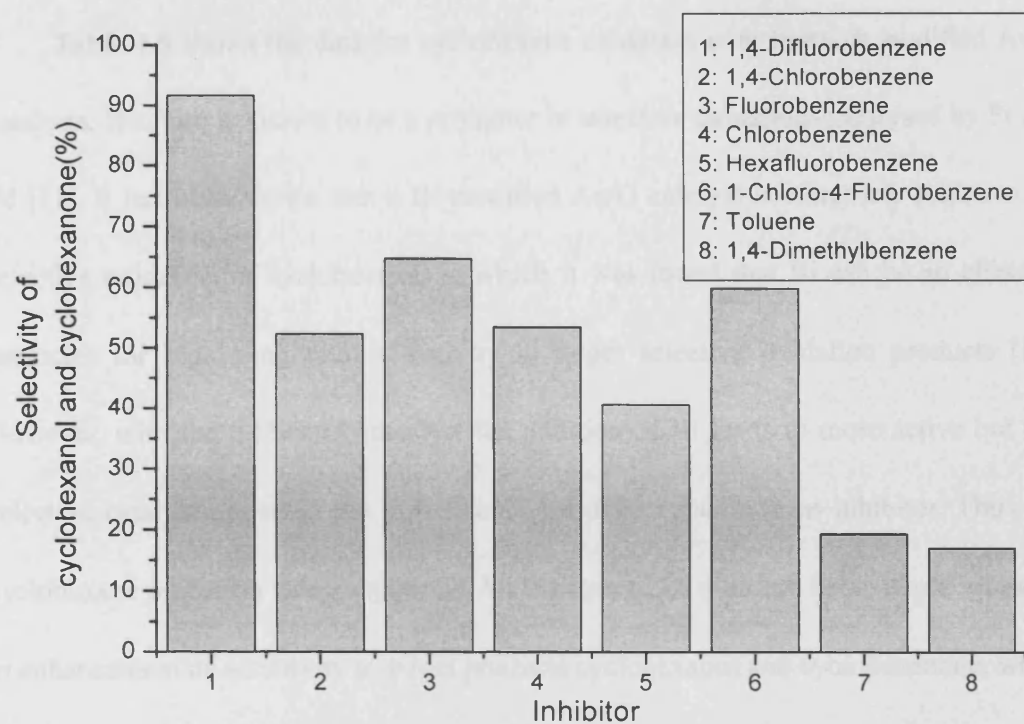


Fig. 4.1 The effect of inhibitor on the total selectivity of cyclohexanol and cyclohexanone

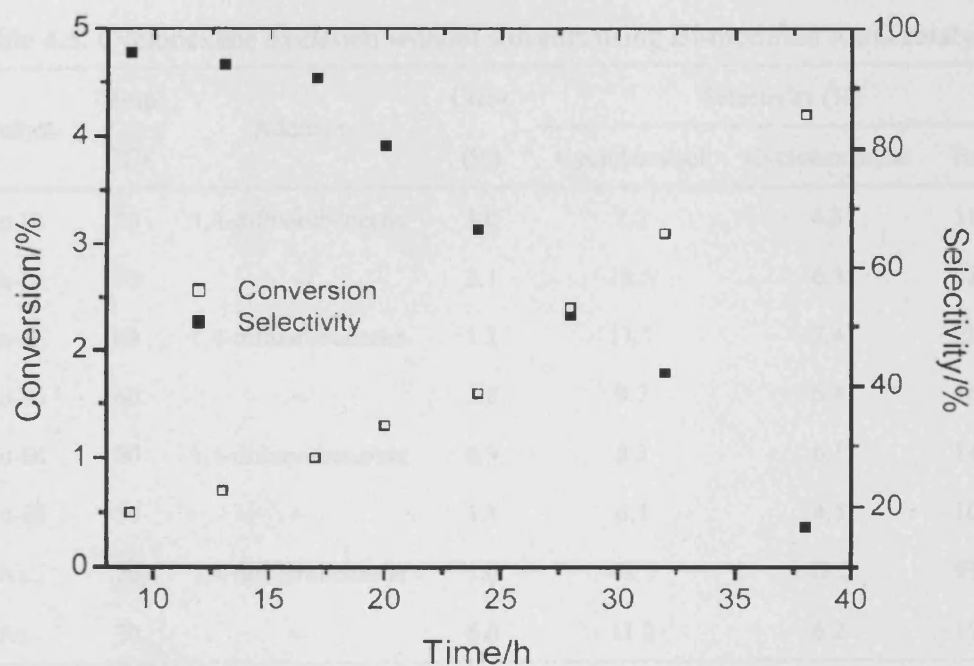


Fig. 4.2 Time dependence of the conversion of cyclohexane and the selectivity for cyclohexanol and cyclohexanone over 0.5%Au/G catalyst with 1,4-difluorobenzene as inhibitor at 70°C

Table 4.5 shows the data for cyclohexane oxidation over bismuth modified Au/G catalysts. Bismuth is known to be a promoter in selective oxidations catalysed by Pt and Pd [11]. It has been shown that a Bi-modified Au/G catalyst is extremely selective for selective oxidation of cyclohexene, in which it was found that Bi can be an effective promoter for improving total selectivity to target selective oxidation products [12]. However, with the 0.5%Au/G catalyst the addition of Bi leads to more active but less selective catalysts, even in the presence of 1,4-difluorobenzene as inhibitor. Thus, for cyclohexane oxidation using supported Au/G catalyst, Bi does not behave as a promoter in enhancement of selectivity to target products cyclohexanol and cyclohexanone, which is different from alkenes oxidation as demonstrated in the previous chapter.

Table 4.5. Cyclohexane oxidation without solvents using Bi-modified Au/G catalysts

Catalyst	Temp (°C)	Additive	Conv. (%)	Selectivity (%)		
				Cyclohexanol	Cyclohexanone	Total
Au-Bi	70	1,4-difluorobenzene	5.0	7.2	4.3	11.5
Au-Bi	70	--	2.1	12.5	6.3	18.8
Au-Bi	60	1,4-difluorobenzene	1.2	11.1	7.4	18.5
Au-Bi	60	--	1.8	9.7	6.4	16.1
Au-Bi	50	1,4-difluorobenzene	0.9	8.3	6.1	14.4
Au-Bi	50	--	1.1	6.1	4.5	10.6
Au	70	1,4-difluorobenzene	1.0	48.1	43.5	91.6
Au	70	--	6.0	11.0	6.2	17.2

Reaction conditions: 10ml cyclohexane, 0.05g additive, 0.12g Au/G catalyst, 0.08g TBHP, 70°C, 17h; catalyst Au-Bi: 0.5%Au/G modified with Bi, Au: non-modified 0.5%Au/G catalyst.

4.3.2.2 Autoclave reactions

Cyclohexane oxidation has been performed in a high-pressure autoclave using oxygen or air as oxidant and the data are summarized in **Tables 4.6** and **4.7**. Obviously, when using high-pressure molecular oxygen or air as oxidant, conversion can be improved to some extent with respect to reaction for 2h. At higher pressure, cyclohexane conversion has been observed to increase correspondingly. However, high selectivity to cyclohexanol and cyclohexanone can only be achieved at low conversion.

Under high-pressure conditions, 1,4-difluorobenzene also behaves as an inhibitor, which leads to the improved selectivity and decreased conversion. This is similar to those experiments carried out in a stirred glass reactor at atmospheric pressure.

Table 4.6. Cyclohexane oxidation over 0.5%Au/G without solvent using high-pressure air in an autoclave

Air (bar)	Additive	Conv. (%)	Selectivity (%)		
			Cyclohexanol	Cyclohexanone	Total
2	1,4-difluorobenzene	0.6	39.8	20.2	60.0
3	1,4-difluorobenzene	0.8	28.4	15.8	44.2
5	1,4-difluorobenzene	0.9	26.8	14.7	41.5
8	1,4-difluorobenzene	1.1	25.6	14.0	39.6
2	--	1.7	18.3	14.5	32.8
3	--	2.1	14.2	10.1	24.3
5	--	3.0	11.1	8.4	19.5
8	--	4.2	7.4	6.2	13.6

Reaction conditions: 10ml cyclohexane, 0.05g additive, 0.12g 0.5%Au/G, 0.08g TBHP, 70⁰C, 1500rpm, reaction for 2h.

Table 4.7. Cyclohexane oxidation over 0.5%Au/G without solvent using high-pressure O₂ in an autoclave

O ₂ (bar)	Additive	Conv. (%)	Selectivity (%)		
			Cyclohexanol	Cyclohexanone	Total
2	1,4-difluorobenzene	1.2	25.0	12.4	37.4
3	1,4-difluorobenzene	1.3	22.4	10.3	32.7
5	1,4-difluorobenzene	1.8	17.8	9.7	27.5
8	1,4-difluorobenzene	2.4	14.2	7.2	21.4
2	--	1.9	17.2	11.3	28.5
3	--	2.7	12.5	10.0	22.5
5	--	3.3	9.4	7.5	16.9
8	--	4.9	7.2	5.1	12.3

Reaction conditions: 10ml cyclohexane, 0.05g additive, 0.12g 0.5%Au/G, 0.08g TBHP, 70°C, 1500rpm, reaction for 2h.

4.3.2.3 Reactions over Au/pretreated-graphite catalysts

Pretreatment of graphite using different acids or bases can be used to introduce oxygen-containing functional groups onto the graphite support. Typical functional groups that can be attached to the carbon surface are depicted in **Figure 4.3** [13]. As a consequence, if different functional groups exist on the surface of graphite support, there will be different surface chemistry. In turn, these functional groups attached to the surface will play an effect on the nucleation of gold particles. Generally, it can be expected that the nucleation process leads to small-sized gold particles if a number of functional groups are present on the surface. Otherwise, if only a few functional groups reside on the surface, it can be expected that have relatively large-sized gold particles

will be formed. Furthermore, the surface functional groups will make the support active and will interact strongly with the gold particles. Without any pretreatment, the graphite can be regarded as an inert support and the peripheral interaction between nanocrystalline gold particles and the support will be minimal.

For example, Bulushev and co-workers reported a gold catalyst supported on pretreated carbon for low-temperature CO oxidation [14]. They used HNO₃ to pretreat the support followed by calcination in helium. They found that the phenolic groups on the surface were able to attach Au³⁺ ions, leading to the formation of small Au nanoparticles. However, the surface carboxylic groups will result in the formation of bigger gold particles and this catalyst exhibits lower catalytic activity as compared to the ones containing small gold particles.

Recently, Hutchings' group found that Au catalysts supported on carbon pretreated with acids can provide enhanced activity for hydrogen peroxide synthesis. Thus, in the following experiments, such pretreated-carbon supported gold catalysts have been studied for cyclohexane oxidation without solvents.

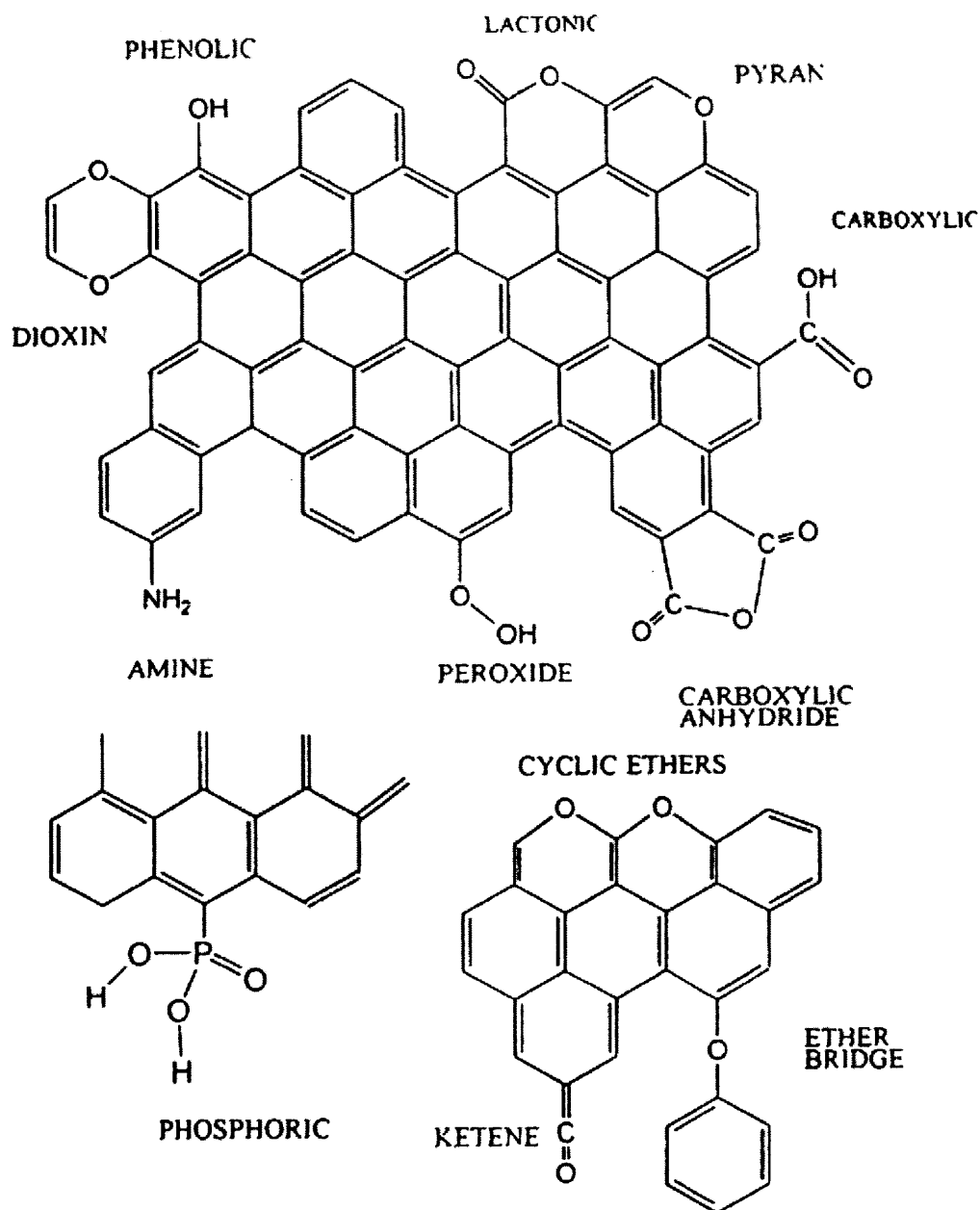


Fig. 4.3 Heteroatoms and functional groups commonly on carbon surfaces [13]

HNO₃, H₂SO₄, H₃PO₄ and NH₄OH have been used to pretreat the graphite support. After that, the same deposition-precipitation method described previously was used to prepare supported gold catalysts. The data for selective oxidation of cyclohexane without solvent using Au/pretreated-graphite catalysts are listed in **Table 4.8**. Obviously,

using these Au/pretreated-graphite catalysts, the selectivity to cyclohexanol and cyclohexanone has not been significantly improved. This suggests that, for the carbon support, pretreatments may be not an effective strategy for preparation of gold catalyst for selective oxidation of cyclohexane under mild conditions.

Table 4.8. Cyclohexane oxidation without solvent in glass reactor over Au/pretreated graphite support in a glass reactor

Pretreatment	Inhibitor	Conv. (%)	Selectivity (%)		
			Cyclohexanol	Cyclohexanone	Total
2%HNO ₃	No	1.8	24.1	12.4	36.5
2%H ₃ PO ₄	No	2.2	22.5	13.5	36.0
2%H ₂ SO ₄	No	2.5	19.8	17.3	37.1
2%NH ₄ OH	No	2.9	17.2	13.2	30.4
5%HNO ₃	Yes	0.8	40.1	25.2	65.3
5%H ₃ PO ₄	Yes	1.1	38.8	27.3	66.1
5%H ₂ SO ₄	Yes	1.0	35.4	21.6	67.0
5%NH ₄ OH	Yes	1.4	30.2	18.4	48.6

Reaction conditions: 10ml cyclohexane, 0.05g additive, 0.12g 1%Au/pretreated-graphite catalyst, 0.08g TBHP, 70°C, reaction for 17h.

4.3.2.4 Comparison with supported Pd or Pt catalysts

The results shown above suggest that the selectivity observed at longer reaction time is much lower than that at shorter reaction time, but both shown the same trends, i.e. that the selectivity is dependent on conversion and seems to be independent of the nature of the gold catalyst. In view of this, supported Pt and Pd catalysts have been further tested. The data for these catalysts are shown in **Figures 4.4** and **4.5**. Interestingly, the data for Pd or Pt catalyst fall on the same curves showing that gold is not particularly different from supported Pd or Pt for this reaction.

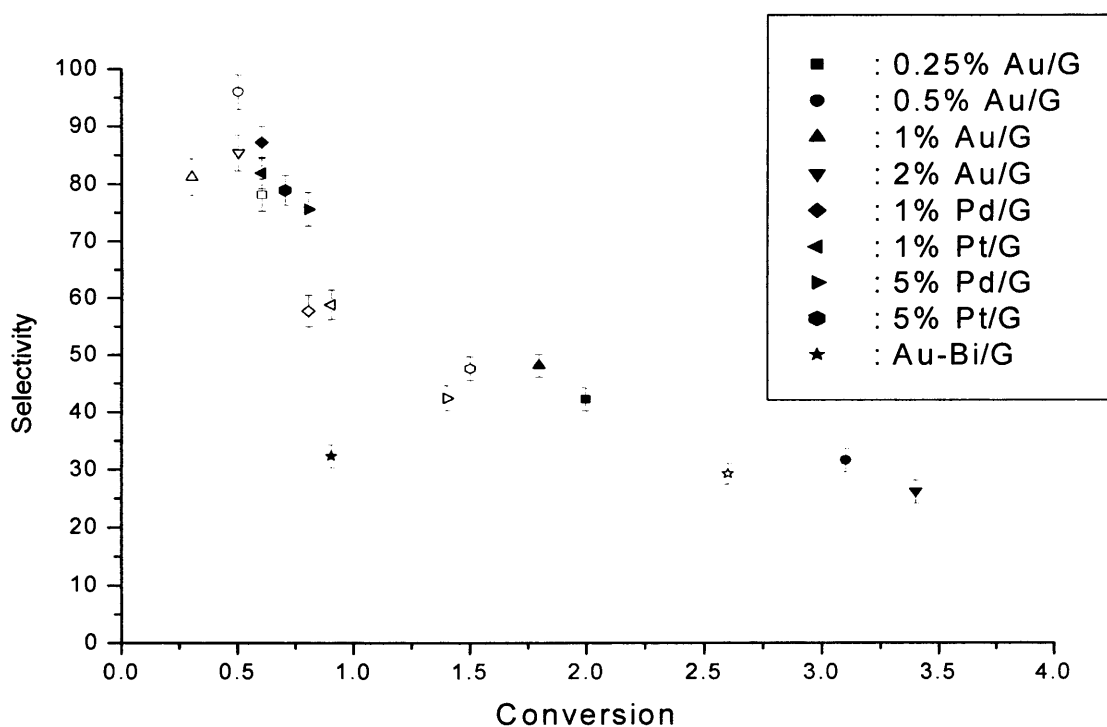


Fig.4.4 Relationship between cyclohexane conversion and the total selectivity to cyclohexanol and cyclohexanone, data collected at 9 h reaction time. Solid symbols represent the reaction without inhibitor 1,4-difluorobenzene. Open symbols represent the reaction with inhibitor 1,4-difluorobenzene present.

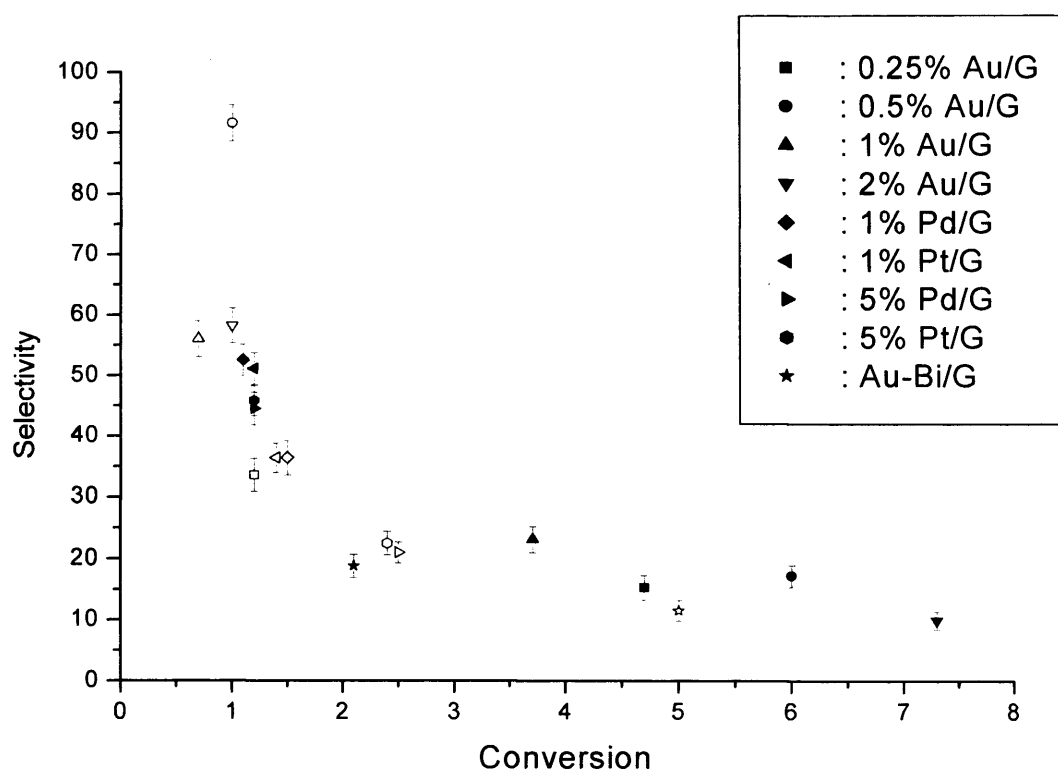


Fig.4.5 Relationship between cyclohexane conversion and the total selectivity to cyclohexanol and cyclohexanone, data collected at 17 h reaction time. Solid symbols represent the reaction without inhibitor 1,4-difluorobenzene. Open symbols represent the reaction with inhibitor 1,4-difluorobenzene present.

4.4. Conclusions

Based on the results described above, the following main conclusions can be drawn. Graphite-supported Au catalysts can be active and selective in the selective oxidation of cyclohexane to cyclohexanol and cyclohexanone when operated under mild conditions of temperature and pressure. However, the selectivity is solely a function of conversion, which in turn is a function of reaction time. Thus, it is clear that at very low conversions very high selectivities can be observed in the absence of solvent.

Bi-modified Au catalyst can provide a more active catalyst for cyclohexane oxidation but with a loss of selectivity. Similarly, Au supported on acid or base-pretreated graphite is not highly selective for cyclohexane oxidation. Furthermore, it has been found that supported Au catalysts do not exhibit significantly different behaviour from supported Pt or Pd catalyst.

4.5. References and notes

- [1] Schuchardt, U.; Cardoso, D.; Sercheli, R.; Pereira, R.; da Cruz, R. S.; Guerreiro, M. C.; Mandelli, D.; Spinace, E. V.; Pires, E. L. *Appl. Catal. A* **2001**, 211, 1.
- [2] Sawatari, N.; Yokota, T.; Sakaguchi, S.; Ishii, Y. *J. Org. Chem.* **2001**, 66, 7889.
- [3] Thomas, J. M.; Raja, R.; Sankar, G.; Bell, R. G. *Acc. Chem. Res.* **2001**, 34, 191.
- [4] Labinger, J. A.; Bercaw, J. E. *Nature* **2002**, 417, 507.
- [5] Dugal, M.; Sankar, G.; Raja, R.; Thomas, J. M. *Angew. Chem. Int. Ed.* **2000**, 39, 2310.
- [6] Thomas, J. M.; Raja, R.; Sankar, G.; Bell, R. G. *Nature* **1999**, 398, 227.
- [7] Hill, C. L.; Weinstock, I. A. *Nature* **1997**, 388, 332.
- [8] Zhao, R.; Ji, D.; Lu, G.; Qian, G.; Yan, L.; Wang, X.; Suo, J. *Chem. Commun.* **2004**, 904.
- [9] Lu, G.; Zhao, R.; Qian, G.; Qi, Y.; Wang, X.; Suo, J. *Catal. Lett.* **2004**, 97, 115.
- [10] Carretin, S.; McMorn, P.; Johnston, P.; Griffin, K.; Kiely, C. J.; Hutchings, G. J. *Phys. Chem. Chem. Phys.* **2003**, 5, 1329.

- [11] Clavilier, J.; Feliu, J. M.; Aldaz, A. *J. Electroanal. Chem.* **1988**, 243, 419.
- [12] Hughes, M.; Xu, Y. J.; Jenkin, P.; McMorn, P.; Landon, P.; Enache, D. I.; Carley, A. F.; Attard, G. A.; Hutchings, G. J.; King, F.; Stitt, E. H.; Johnston, P.; Griffin, K.; Kiely, C. J. *Nature* **2005**, 437, 1132.
- [13] Brennan, J. K.; Bandosz, T. J.; Thomson, K. T.; Gubbins, K. E. *Colloids. Surf. A: Physicochemical and Engineering Aspects* **2001**, 187-188, 539.
- [14] Bulushev, D. A.; Yuranov, I.; Suvorova, E. I.; Buffat, P. A.; Kiwi-Minsker, L. *J. Catal.* **2004**, 224, 8.

Chapter Five

Heterogeneous Gas-phase Selective Epoxidation of Propene to Propene Oxide

5.1. Introduction

The heterogeneous epoxidation of alkenes, especially ethene and propene, has been a hot topic of enduring interest because epoxides are of great commercial and synthetic importance [1]. Although the epoxidation of ethene to form ethene oxide (EO) over a $\text{Ag}/\alpha\text{-Al}_2\text{O}_3$ catalyst has been practised for decades, and catalyst activities and selectivities as well as understanding of the reaction mechanism have progressed steadily for this commercial process, the heterogeneous epoxidation of higher alkenes is more challenging [2]. Many attempts on the epoxidation of propene to propene epoxide (PO) over the same silver catalyst commercially used for ethene oxidation have failed due to very low activity and selectivity.

The difficulty in the epoxidation of higher alkenes is mainly ascribed to the presence of labile allylic atoms, whose facile abstraction results in combustion rather than selective epoxidation [1,2]. Selective epoxidation of propene to propene epoxide (PO) represents a typical case [1-3]. PO is one of the most important starting materials in the chemical industry, which can be used for making polyurethane, unsaturated resins, surfactants and other products [3-5]. The production of PO consumes over 10% of all

propene produced. In 1999, the total production of PO was *ca.* 5.8 million tons per year [5]. The market demand for PO has been increasing over the years. Due to the poor activity and selectivity of Ag catalyst for propene epoxidation to PO, current commercial production of PO involves two-stage liquid phase processes: the chlorohydrin method and the Halcon method [6,7]. In the chlorohydrin method, large amounts of Cl₂ are consumed, giving rise to serious problems of equipment corrosion and environmental pollution. In the Halcon method, autoxidation of ethylbenzene or isobutene is applied to make alkylhydroperoxide, which acts as an oxidant for catalytic epoxidation of propene to PO, along with a large amount of by-products. Clearly, the Halcon method is complicated and needs heavy capital investment. However, because of the environmental impacts of the chlorohydrin process, the most recently built plants all use the Halcon process technology.

Currently, major research effort has been applied to the development of alternative direct epoxidation processes for the production of PO. It has been reported that, when TS-1 (titanium silicalite-1) is used as a catalyst, hydrogen peroxide can be efficiently used for the selective epoxidation of propene to PO (*ca.* 95% selectivity) [8]. The major problem of this process is that PO and hydrogen peroxide have comparable market values on a molar basis, hence making it impossible to run the process profitably at this time. However, the disadvantage of the high cost of hydrogen peroxide for propene epoxidation can be resolved by using the *in situ* production of hydrogen peroxide; this process is now under construction by Dow-BASF [9]. On the other hand, Olin has developed a process for the direct propene epoxidation using molten salt

catalysis. In this process, at a pressure of 20 bar and a temperature of 473K, a PO selectivity of 65% with propene conversion of 15% has been achieved when a mixture of propene and air is flowed through a molten alkali-nitrate salt mixture [10].

Some researchers have also reported propene epoxidation using nitrous oxide (N_2O) as an alternative oxidant [11,12]. Since the pioneering work of Panov showed that Fe-ZSM-5 zeolite selective oxidations can be carried out using N_2O , this oxidant has received much attention for many different oxidation reactions, such as oxidation of benzene to phenol and oxidation of methane and ethane to the corresponding alcohols [13]. However, studies on the use of N_2O as oxidant for propene epoxidation are relatively scarce. Using a potassium-promoted iron oxide on SBA-15 (a typical mesoporous silica) catalyst, Wang's group reported that they obtained 80% PO selectivity at propene conversions up to 5% [14]. Recently, they reported a detailed study on the effect of alkali metal salts on SBA-15-supported iron catalysts for propene epoxidation by N_2O [15]. However, a major disadvantage for propene epoxidation process using N_2O as oxidant is that N_2O is not commercially available in significant quantities.

In 1998, Haruta and co-workers showed that supported gold catalysts can give very high selectivity to PO (nearly 100%), although at low conversion [16]. Recently, using a gold catalyst supported on 3D mesoporous silylated titanosilicates in the presence of $Ba(NO_3)_2$ as a promoter, Haruta's group reported that a conversion of 9.8% together with selectivity to PO, *ca.* 90%, were achieved using a mixture of hydrogen

and oxygen [17]. However, it should be noted that, in this catalyst system, hydrogen is always needed as a sacrificial feed gas for propene epoxidation and the hydrogen efficiency is insufficient, typically <30%. The mode of operation of this catalyst system is unclear although it is speculated that peroxy species are involved. The catalyst deactivation, conversion and hydrogen efficiency must be further improved in order to realize a commercial process [18,19].

Recently, some research groups have worked on propene epoxidation using only molecular oxygen over supported Cu catalysts. Lambert's group reported that Cu/SiO₂ catalysts prepared by either a micro-emulsion technique or an impregnation method showed good promise for the direct gas-phase epoxidation of propene by dioxygen, without the need for H₂ addition, at atmospheric pressure [20]. The highest PO selectivity was *ca.*53% at propene conversion, *ca.* 0.25%. The performance of these materials is comparable to that reported by Haruta and co-workers in their first paper on propene epoxidation catalyzed by a TiO₂-supported-Au catalyst. However, it should be noted that, over such supported Cu catalysts, high PO selectivity can only be obtained at low temperature. Increasing the temperature will improve the propene conversion, but at the same time decrease the PO selectivity. Li *et al.* have also reported the direct epoxidation of propene by molecular oxygen over a NaCl-modified VCe_{1-x}Cu_x oxide catalyst; a PO selectivity of 43% was achieved at 0.19% propene conversion [21]. These two studies using Cu-based materials as catalysts propose that metallic Cu(0) may be the main active phase for propene epoxidation.

Most recently, Wang's group reported that a halogen-free K^+ -modified $CuO_x/SBA-15$ catalyst exhibited much better catalytic performance than other Cu-based catalysts reported so far for propene epoxidation using molecular oxygen. PO selectivity, *ca.* 15-50, can be sustained as the propene conversion increased from *ca.* 1 to 12% [22]. This catalyst does not require any pre-reduction. Importantly, their results suggest that it is not the metallic $Cu(0)$, but rather the copper in an oxidized state that accounts for the propene epoxidation by molecular oxygen. Thus, it is clear that the nature and active sites for supported Cu catalysts are complicated and need further detailed investigation [20-22]. Nevertheless, these studies indicate that Cu could be potentially used as an inexpensive catalyst for propene epoxidation.

Undoubtedly, a one-step, environmentally benign, heterogeneous process for the catalytic epoxidation of propene to PO with total selectivity using oxygen or air as oxidant would be preferred. The aim of the present research has been to find novel catalysts for the selective epoxidation of propene to PO using only dioxygen as oxidant without the need of hydrogen. The goal of the present study is to try to obtain very high PO selectivity. This chapter mainly focuses on the direct gas-phase selective epoxidation of propene to PO over supported Ag, Cu and Au catalysts, and their bimetallics (Au-Cu, Cu-Ag and Au-Ag), using only molecular oxygen as oxidant.

5.2. Experimental

5.2.1 Supports used for catalyst preparation

Different supports have been used for the preparation of supported metal catalysts.

Table 5.1 summarizes these supports, which include Al₂O₃, SiO₂, ZnO, TiO₂ and CeO₂.

Among these supports, CeO₂ nanopowder-2 was prepared by a supercritical carbon dioxide process (ScCO₂), other supports were used as received.

Table 5.1. Support materials used for catalyst preparation

Support material	Supplier	Specification
Regular SiO ₂	Aldrich	99.6%
SiO ₂ nanopowder	Aldrich	99.5%, particle size 10nm
Regular α -Al ₂ O ₃	Alfa	99.9%, particle size 1 μ m
Regular γ -Al ₂ O ₃	Alfa	99.9%
Al ₂ O ₃ nanopowder-1	Aldrich	γ -phase, particle size 40-47nm
Al ₂ O ₃ nanopowder-2	Aldrich	γ -phase, particle size 2-4nm
Regular ZnO	Aldrich	99.9%
ZnO nanopowder	Aldrich	Particle size 50-70nm
TiO ₂ (P25)	Degussa	Particle size 20-50nm
Regular CeO ₂	Aldrich	99.9%, particle size < 5 μ m
CeO ₂ nanopowder-1	Aldrich	Particle size 10nm
CeO ₂ nanopowder-2	--	Prepared via ScCO ₂ process, particle size 20-30nm

5.2.2 Characterisation of supports

As shown in **Table 5.1**, a series of different catalyst supports have been used. Analysis by XRD, BET and SEM has been performed to determine the differences among these supports.

5.2.3 Catalyst preparation

5.2.3.1 Preparation of supported Ag, Cu or Au catalysts

A supported 2wt% Ag catalyst was prepared by a wet impregnation method. The procedure is as follows: silver nitrate (AgNO_3 , 0.063g) was dissolved in deionised water (10ml) and support (2g) was impregnated by this solution and then vigorously stirred for 2h. After that, the catalyst was dried at 80°C for 16h. In some cases, supported Ag catalysts prepared by Ag-colloid precursor were tested. The synthesis of Ag-colloid is based on the literature: AgNO_3 was dissolved in water and citric acid was added, and stirred at boiling point [23]. Then, a mud-red Ag-colloid was obtained.

A supported 2wt% Cu catalyst was prepared by a wet impregnation method, similar to the preparation of Ag catalyst: $\text{CuNO}_3 \cdot x\text{H}_2\text{O}$ (0.145g) was dissolved in deionised water (10ml) and support (2g) was impregnated by this solution and then vigorously stirred for 2h. After that, the catalyst was dried at 80°C for 16h.

A supported 2wt%Au catalyst was prepared by a deposition-precipitation method. The general procedure is as follows: $\text{HAuCl}_4 \cdot 3\text{H}_2\text{O}$ (0.08g) was dissolved in deionised

water (10ml). NaOH was added with stirring until pH=9.0 was obtained. This solution was added to support (2g) with stirring for 1h at 80⁰C at pH=9.0. After filtration, the catalyst was dried at 80⁰C for 16h. For Au catalyst supported on CeO₂ prepared by a ScCO₂ process, the preparation procedure is as follows: HAuCl₄.3H₂O (0.08g) was dissolved in deionised water (10ml). NaOH was added with stirring until pH=9.0 was obtained. This solution was added to support (2g), adjusting pH=9.0 and then stirring for 16h at room temperature. After that, this catalyst was dried at 80⁰C for 16h.

Dried catalysts were treated at 450⁰C in air or 5%H₂/Ar for 2h.

5.2.3.2 Preparation of supported Ag-Cu, Ag-Au or Cu-Au bimetallic catalysts

A supported Ag-Cu catalyst was prepared by a wet impregnation method. The procedure is as follows: AgNO₃ (0.063g) and CuNO₃.xH₂O (0.145g) were dissolved in deionised water (10ml) and support (2g) was impregnated by this solution, and then vigorously stirred for 2h. After that, the catalyst was dried at 80⁰C for 16h. Dried catalysts were treated at 450⁰C in air or 5%H₂/Ar for 2h.

A supported Au-Cu catalyst was prepared by two different methods. One is the wet impregnation method: CuNO₃.xH₂O (0.145g) and HAuCl₄.3H₂O (0.08g) were dissolved in deionised water (10ml) and the support was impregnated using this solution, and then vigorously stirred for 2h. After that, the catalyst was dried at 80⁰C for 16h. Dried catalysts were treated at 450⁰C in air or 5%H₂/Ar for 2h. In some selected cases, a

two-step procedure consisting of deposition-precipitation (DP) method and impregnation method was used to prepare Au-Cu catalysts. The general procedure is as follows: $\text{HAuCl}_4 \cdot 3\text{H}_2\text{O}$ (0.08g) was dissolved in deionised water (10ml). NaOH was added with stirring until $\text{pH}=9.0$ was obtained. Then, this solution was added to support (2g) with stirring for 1h at 80°C with at $\text{pH}=9.0$. After filtration, the catalyst was dried at 80°C for 16h. Secondly, an impregnation method was used to prepare Au-Cu catalysts: the as-prepared Au catalyst (0.4g) was impregnated by a solution of $\text{Cu}(\text{NO}_3)_2 \cdot x\text{H}_2\text{O}$ (0.029g copper nitrate dissolved in 10ml H_2O) with stirring at 80°C for 1h. After that, the solution was dried at 80°C for 16h. However, for the preparation of Au-Cu supported on CeO_2 prepared by a ScCO_2 process, the first step to prepare supported Au catalyst was different, as mentioned above.

A supported Au-Ag catalyst was prepared by a wet impregnation method. The procedure is as follows: AgNO_3 (0.063g) and $\text{HAuCl}_4 \cdot 3\text{H}_2\text{O}$ (0.08g) were dissolved in deionised water (10ml) and support (2g) was impregnated by this solution, and then vigorously stirred for 2h. After that, the catalyst was dried at 80°C for 16h. Dried catalysts were treated at 450°C in air or 5% H_2 /Ar for 2h.

5.2.4 Reaction conditions

Typically, oxidation reactions of propene in the gas-phase were carried out in a single-stage fixed-bed tube reactor as shown in **Figure 5.1**. Samples of each catalyst (0.1g) was used and the reaction temperatures ranged from 200°C to 350°C . The volume

ratio of propene: oxygen: helium was 22: 9: 69 and the GHSV (gas hourly space velocity) was 47760h^{-1} based on the total flow rate. In some selected cases, other reaction conditions were also tested as stated in the text. The as-prepared catalysts treated using other conditions, such as calcination in air or hydrogen/helium, were also tested in order to consider the effect of calcination on the catalyst performance.

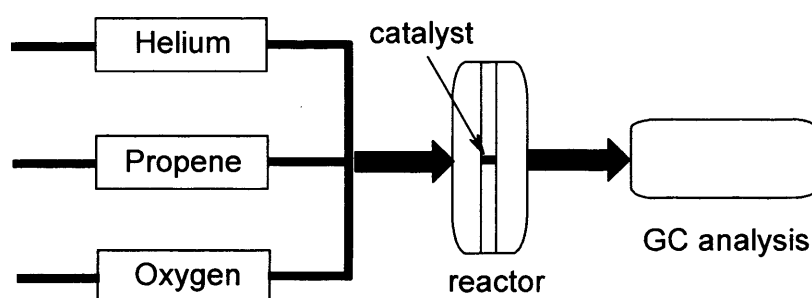


Fig.5.1 Schematic diagram of experimental apparatus

The analysis of reaction products were carried out with a Varian Star 3800 fitted with a TCD and FID detector. Standard calibration cylinders containing known concentrations of PO, CO and CO₂ were used to quantify the amount of PO, CO or CO₂ generated during the reaction. The conversion of propene was calculated as follows:

$$\text{Propene conversion (\%)} = 1 - ([\text{Propene}]_t / [\text{Propene}]_{t_0}) \times 100\%$$

Where: $[\text{Propene}]_t$ is the concentration, vol%, of propene at time t;

$[\text{Propene}]_{t_0}$ is initial concentration, vol%, of propene.

5.3 Results and discussions

5.3.1 Characterisation of supports

5.3.1.1 XRD analysis

Figures 5.2-6 display the XRD patterns of SiO_2 , ZnO , Al_2O_3 , TiO_2 and CeO_2 respectively. The difference between regular and nanopowder supports is reflected in the XRD patterns. Namely, the strong sharp reflections indicate that relatively large particles feature in the support, whereas the broad reflections mean the particle size of the support material is relatively small. The qualitative information for particle sizes of different supports is consistent with the observations shown in the SEM images below.

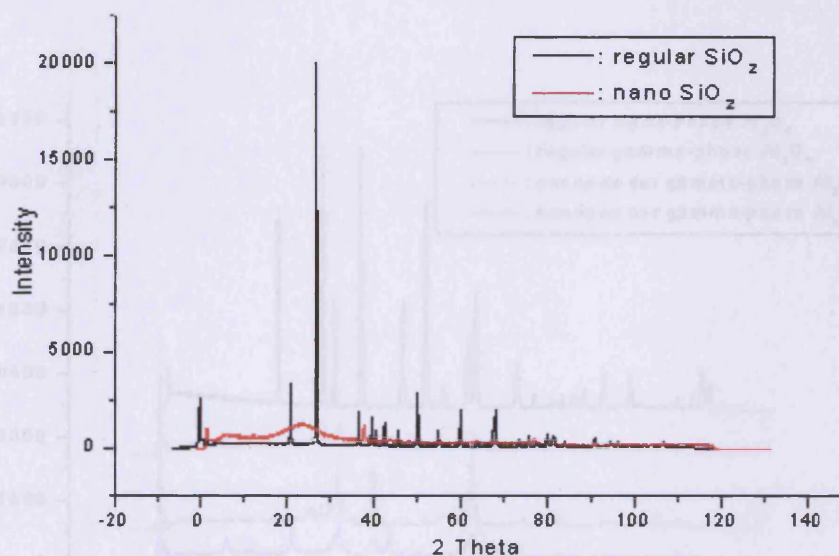


Fig.5.2 XRD pattern of regular and nanopowder SiO_2

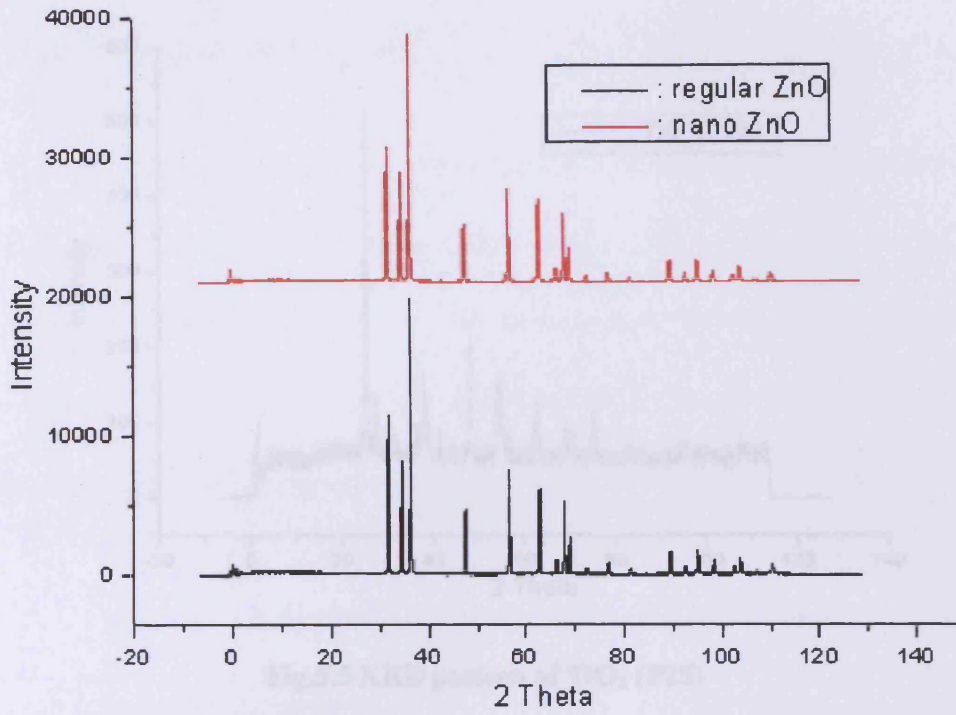


Fig.5.3 XRD pattern of regular and nanopowder ZnO

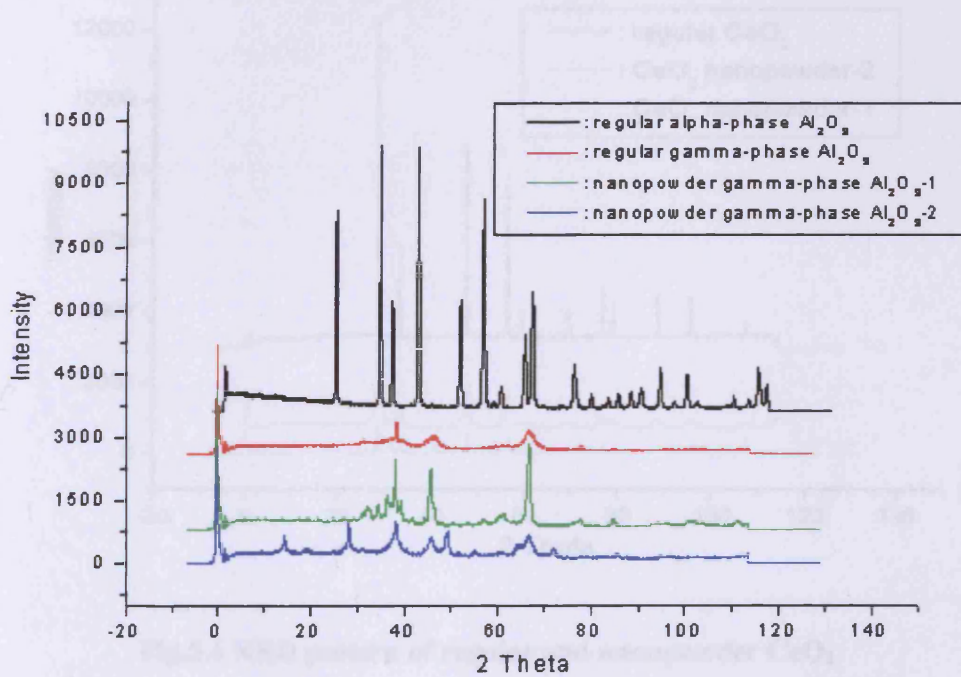


Fig.5.4 XRD pattern of regular and nanopowder Al₂O₃

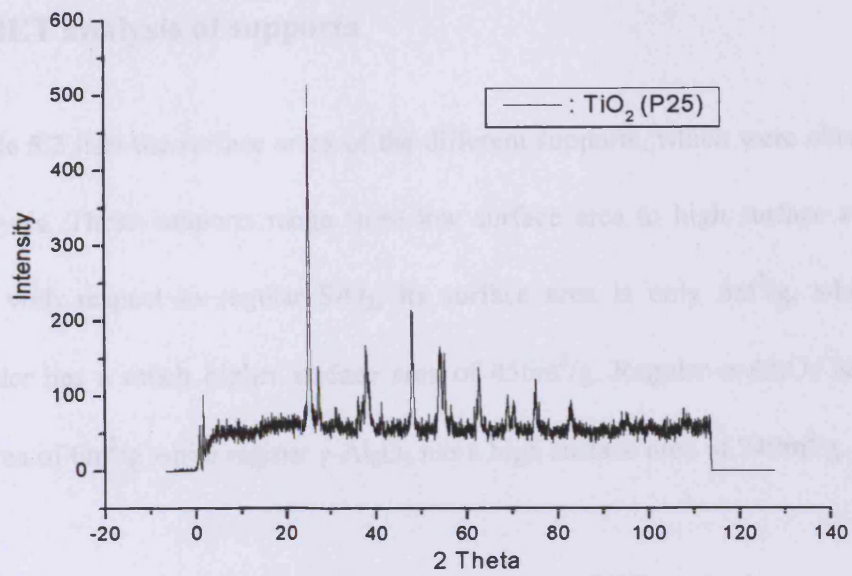


Fig.5.5 XRD pattern of TiO₂ (P25)

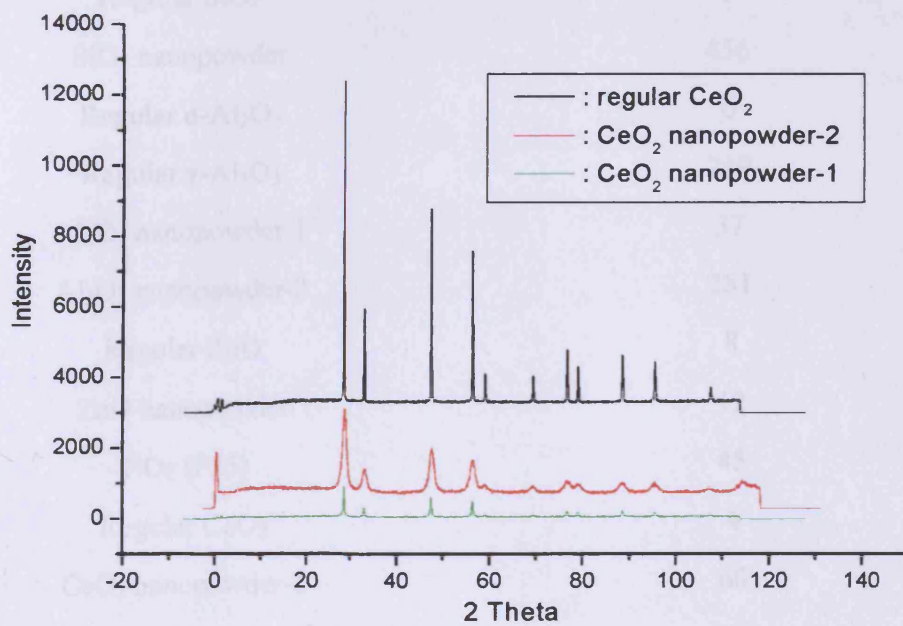


Fig.5.6 XRD pattern of regular and nanopowder CeO₂

5.3.1.2 BET analysis of supports

Table 5.2 lists the surface areas of the different supports, which were obtained by BET analysis. These supports range from low surface area to high surface area. For example, with respect to regular SiO₂, its surface area is only 5m²/g, while SiO₂ nanopowder has a much higher surface area of 456m²/g. Regular α-Al₂O₃ has a low surface area of 6m²/g while regular γ-Al₂O₃ has a high surface area of 249m²/g.

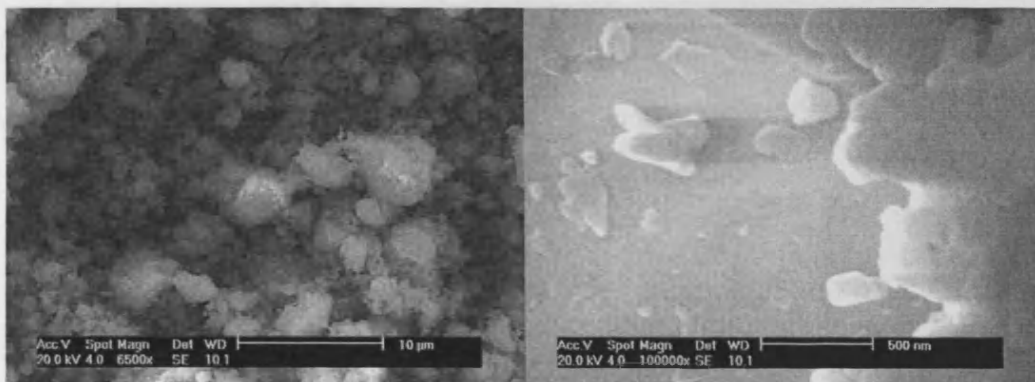
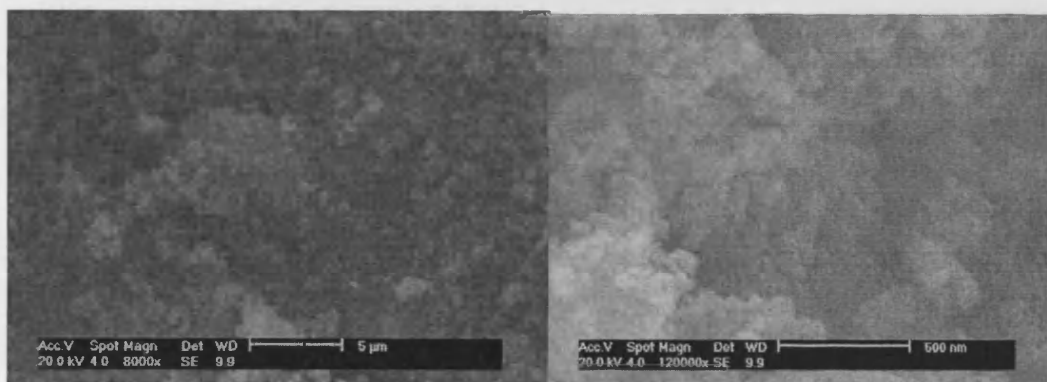
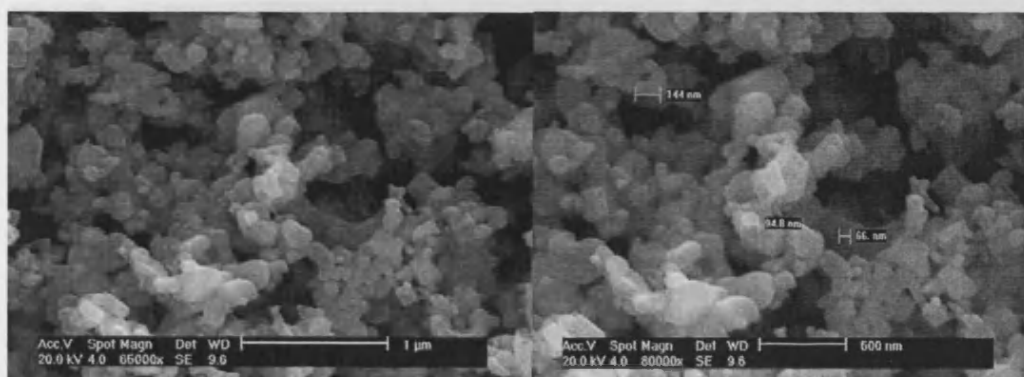
Table 5.2. Surface area of supports by BET method

Support materials	Surface area (m ² /g)
Regular SiO ₂	5
SiO ₂ nanopowder	456
Regular α-Al ₂ O ₃	6
Regular γ-Al ₂ O ₃	249
Al ₂ O ₃ nanopowder-1	37
Al ₂ O ₃ nanopowder-2	281
Regular ZnO	8
ZnO nanopowder	12
TiO ₂ (P25)	45
Regular CeO ₂	4
CeO ₂ nanopowder-1	66
CeO ₂ nanopowder-2	25

5.3.1.3 SEM images of supports

The detailed information on surface morphology of these supports can be clearly seen from their SEM images as shown in **Figures 5.7-18**. In addition, according to the SEM images, we can approximately determine the particle size of the different supports. For instance, the SEM image of regular SiO₂ (**Figure 5.7**) shows that the particle size is relatively large with an uneven distribution on the surface. However, for SiO₂ nanopowder (**Figure 5.8**), the SEM image illustrates that very small particles are evenly distributed on the surface. The observed particles sizes in the SEM images for regular SiO₂ and nanopowder SiO₂ are fully consistent with their XRD patterns. That is, the sharper the reflections in the XRD pattern, the larger is the particle size of the support.

Interestingly, it should be noted that, for regular ZnO and nanopowder ZnO supports (**Figures 5.9 and 5.10**), the SEM images show relatively small differences between them. The surface morphology is rather similar between regular ZnO and nanopowder ZnO. Further inspection of the SEM images indicates that the particle size of the nanopowder ZnO is only a little smaller than that of regular ZnO, which is in good agreement with their XRD patterns. For the other supports, the observed particle sizes in the SEM images are broadly in accordance with their XRD patterns.

Fig.5.7 SEM image of regular SiO_2 Fig.5.8 SEM image of SiO_2 nanopowderFig.5.9 SEM image of regular ZnO

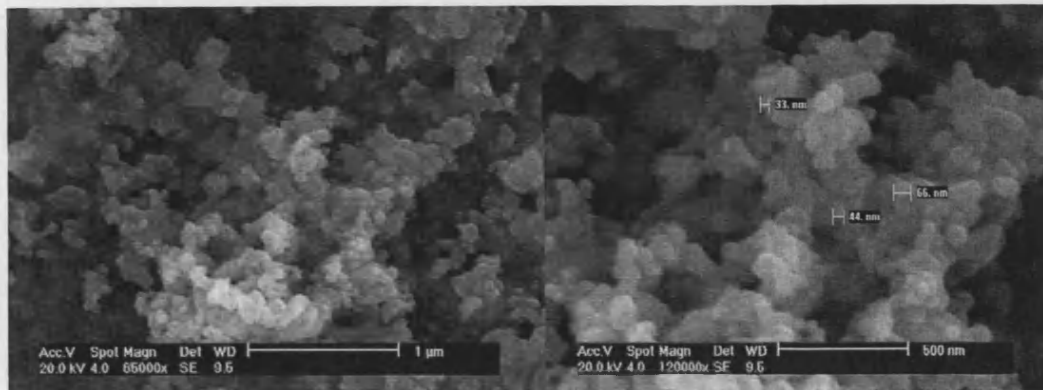


Fig.5.10 SEM image of ZnO nanopowder

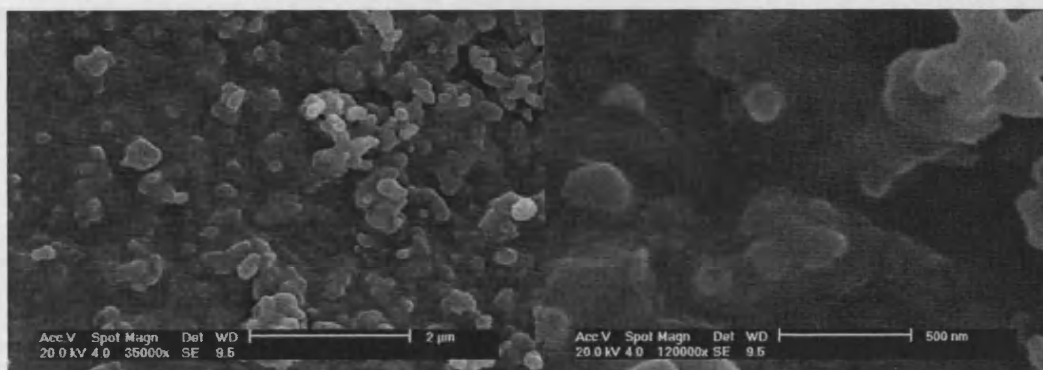


Fig.5.11 SEM image of regular α -Al₂O₃

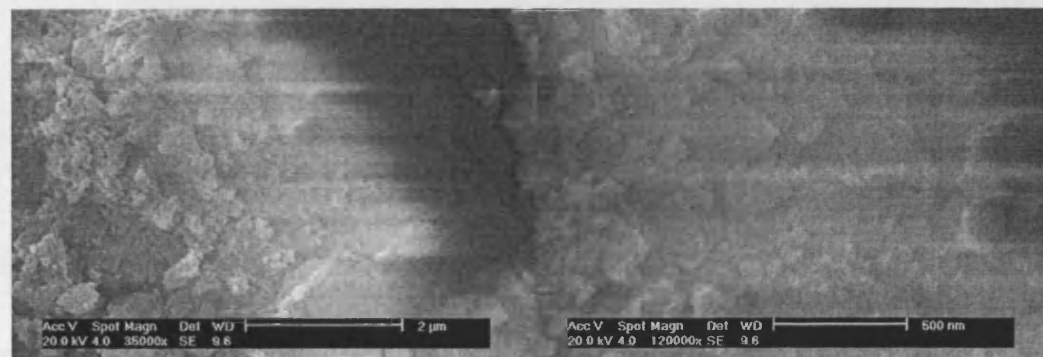


Fig.5.12 SEM image of regular γ -Al₂O₃

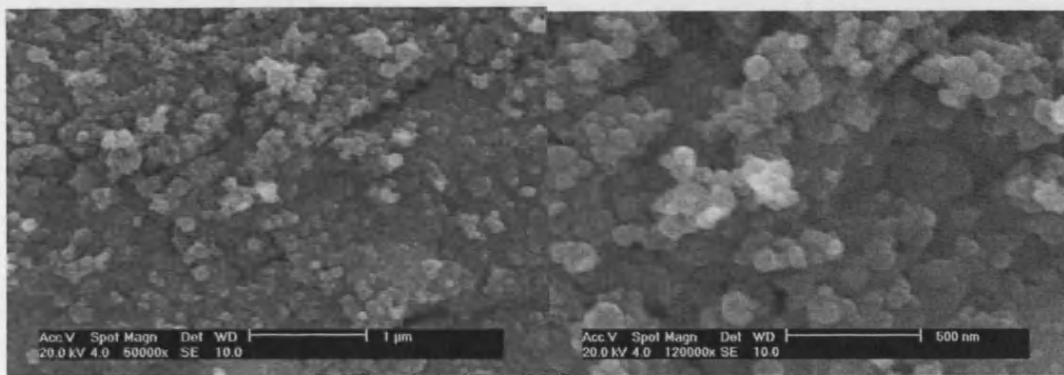


Fig.5.13 SEM image of Al₂O₃ nanopowder-1

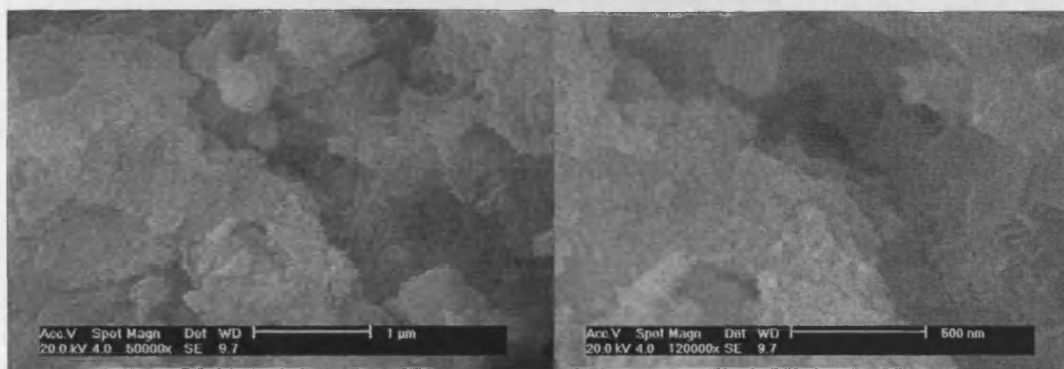


Fig.5.14 SEM image of Al₂O₃ nanopowder-2



Fig.5.15 SEM image of TiO₂ (P25)

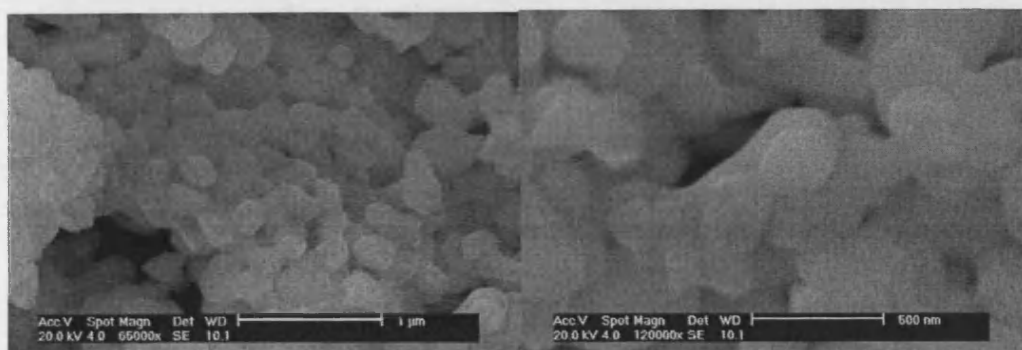


Fig.5.16 SEM image of regular CeO_2

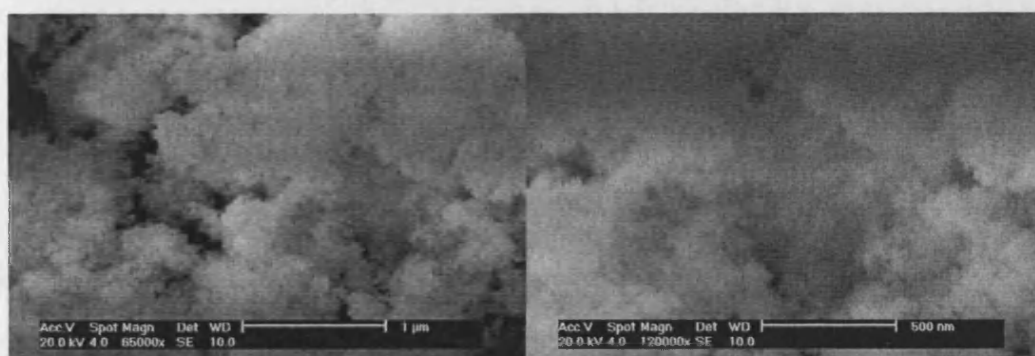


Fig.5.17 SEM image of CeO_2 nanopowder-1

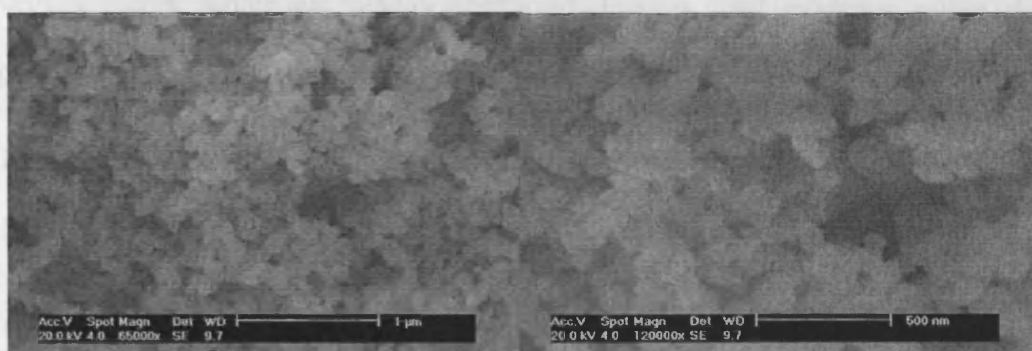
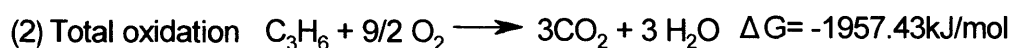
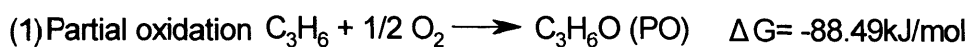


Fig.5.18 SEM image of CeO_2 nanopowder-2

5.3.2 Propene oxidation over supported Ag catalysts

As for propene oxidation, there are two main competitive reaction pathways in the oxidation of propene to propene epoxide (PO), as shown in **Scheme 5.1**.



Scheme 5.1 Two main reaction pathways in the oxidation of propene to PO

It is well known that total oxidation of propene to carbon dioxide and water is much more energetically favoured compared to selective oxidation of propene to PO from the thermodynamic point of view [24]. Furthermore, the presence of allylic hydrogen atoms, which are readily abstracted, favours total oxidation rather than selective oxidation of propene to PO [1,2]. This is the main reason why high selectivity to PO has not been achieved with Ag-based catalysts so far.

However, the success of Ag catalysts for ethene epoxidation to ethene oxide (EO) has encouraged researchers to continue studying epoxidation of propene to PO over supported Ag catalysts [2]. Moderate selectivity to PO has been obtained using modified supported Ag catalysts containing chloride or other additives as promoters.

Initial studies in the present work have involved supported Ag catalysts. In particular, the primary interest herein has been to look at the effect of the support on catalytic performance for selective oxidation of propene. It has been found that the

support has a major influence on the catalytic activity of supported Ag catalysts. The data for propene epoxidation using supported Ag catalyst are listed from **Table 5.3** to **Table 5.9**.

According to the data from **Table 5.3** to **Table 5.5**, it can be found that, among these supported Ag catalysts, SiO₂ nanopowder seems to be the best support because a much higher selectivity to PO, *ca.* 57-74%, has been observed although the conversion is low, *ca.* 0.1-0.5%. For Ag catalysts supported on Al₂O₃, TiO₂ and CeO₂, the selectivity to PO is typically lower than 30%. With respect to ZnO-supported Ag catalysts, PO selectivity is typically lower than 40%. Furthermore, it should be mentioned that the relatively high selectivity to PO has only been achieved at low conversions, typically <0.5%. This is particularly true because at higher temperature total oxidation of propene will be much more favourable than selective oxidation of propene to PO.

Table 5.6 lists the results for propene epoxidation over supported Ag-colloid catalysts. It is interesting to find that supported Ag-colloid catalysts are completely non-selective for propene epoxidation to PO; over these Ag-colloid catalysts, only CO and CO₂ are observed as the primary reaction products. The literature shows that such Ag-colloid catalysts generally contain small particles sized Ag particles, *ca.* 20nm [23]. Therefore, small-sized Ag particles do not favour the selective epoxidation of propene, which is in good agreement with observations in the literature [25].

Table 5.3. Results for propene epoxidation over uncalcined Ag catalysts supported on SiO₂

Catalyst	Temp (°C)	Conversion (%)	Sel of PO (%)
2%Ag/regular SiO ₂	200	0	0
	220	0	0
	250	0	0
	270	0	0
	290	0	0
	300	0.82	21.1
	350	2.3	8.9
2%Ag/SiO ₂ nanopowder	200	0	0
	220	0	0
	250	0.09	73.6
	270	0.30	60.0
	290	0.47	57.4
	300	3.4	26.8
	350	9.1	0.6

Table 5.4. Results for propene epoxidation over uncalcined Ag catalysts supported on Al₂O₃

Catalyst	Temp (°C)	Conversion (%)	Sel of PO (%)
2%Ag/regular α -Al ₂ O ₃	200	0	0
	220	0	0
	250	0.32	28.8
	270	0.51	21.3
	290	2.9	15.7
	300	3.7	11.2
	350	7.9	1.9
2%Ag/regular γ -Al ₂ O ₃	200	0	0
	220	0	0
	250	0.41	24.1
	270	0.62	19.8
	290	2.2	11.4
	300	3.6	8.8
	350	8.4	2.4
2%Ag/Al ₂ O ₃ nanopowder-1	200	0	0
	220	0	0
	250	0.50	26.3
	270	1.13	17.7
	290	3.2	10.6
	300	5.1	4.2
	350	8.5	0.9
2%Ag/Al ₂ O ₃ nanopowder-2	200	0	0
	220	0	0
	250	0.66	15.6
	270	1.45	14.7
	290	3.8	9.6
	300	5.9	3.0
	350	8.0	0.6

Table 5.5. Results for propene epoxidation over uncalcined Ag catalysts supported on ZnO, TiO₂ and CeO₂

Catalyst	Temp (°C)	Conversion (%)	Sel of PO (%)
2%Ag/regular ZnO	220	0	0
	250	Trace	0
	270	0.13	38.4
	290	0.21	32.9
	300	0.42	22.0
	350	2.8	12.7
2%Ag/ZnO nanopowder	220	0	0
	250	Trace	0
	270	0.19	37.2
	290	0.26	31.9
	300	0.58	19.8
	350	2.9	10.7
2%Ag/TiO ₂ (P25)	220	0	0
	250	0.05	0
	270	0.10	0
	290	0.34	0
	300	0.84	0
	350	5.7	Trace
2%Ag/regular CeO ₂	220	1.7	19.8
	250	2.8	12.7
	270	3.5	9.7
	290	4.2	7.4
	300	4.9	5.6
	350	8.6	0.8
2%Ag/CeO ₂ nanopowder-1	220	2.8	10.2
	250	3.7	8.4
	270	4.4	4.8
	290	5.6	2.4
	300	7.1	0.8
	350	9.2	Trace

Table 5.6. Results for propene epoxidation over uncalcined supported Ag-colloid catalysts

Catalyst	Temp ($^{\circ}$ C)	Conversion (%)	Sel of PO (%)
2%Ag-colloid/regular SiO ₂	220	0	0
	250	0.6	0
	270	2.4	0
	290	4.3	0
	300	5.9	0
	350	8.1	0
2%Ag-colloid/SiO ₂ nanopowder	220	0	0
	250	0.3	0
	270	5.2	0
	290	6.0	0
	300	7.8	0
	350	8.8	0
2%Ag-colloid/regular Al ₂ O ₃	220	0.4	0
	250	1.0	0
	270	2.9	0
	290	3.3	0
	300	4.7	0
	350	7.9	0
2%Ag-colloid/ Al ₂ O ₃ nanopowder-2	220	0.6	0
	250	2.1	0
	270	4.0	0
	290	5.7	0
	300	7.8	0
	350	9.0	0
2%Ag-colloid/TiO ₂ (P25)	220	0.4	0
	250	2.4	0
	270	3.2	0
	290	4.8	0
	300	6.3	0
	350	8.6	0

Tables 5.7, 5.8 and 5.9 show the data for propene epoxidation over supported Ag catalysts after calcination in air or hydrogen, respectively. It has been found that these calcined Ag catalysts do not exhibit enhanced selectivity for PO formation. In general, selectivity to PO was decreased compared to that using supported Ag catalysts without calcination. In particular, for Ag/SiO₂ nanopowder that is highly selective for propene epoxidation, calcination in air or hydrogen led to a very poor catalyst, which are much lower PO selectivity than that using Ag/SiO₂ nanopowder without calcination (Figure 5.19). For example, the highest selectivity to PO is only *ca.* 22% using Ag/SiO₂ nanopowder catalysts after calcination in air or hydrogen.

Because calcination in air or hydrogen will reduce Ag particles to low oxidation state Ag or metallic Ag, it can be concluded that the high oxidation state of Ag favours propene epoxidation. This can be ascribed to the fact that the high oxidation state of Ag is helpful to produce electrophilic oxygen species that play an important role in selective epoxidation of propene [26].

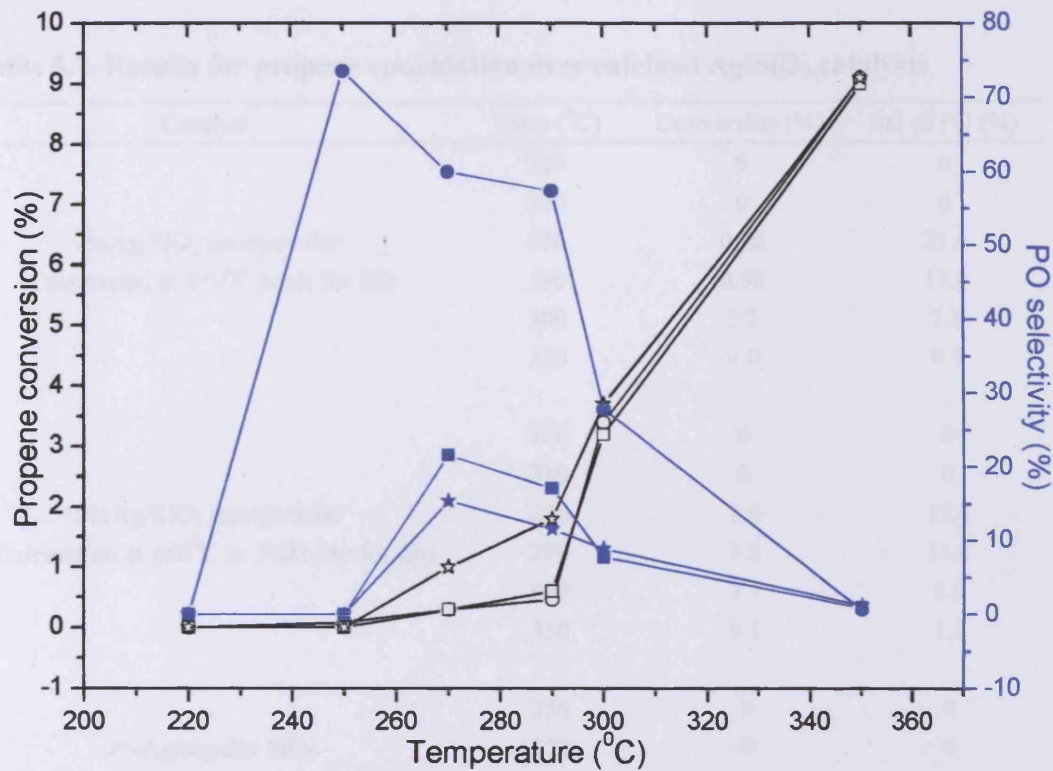


Fig.5.19 Catalytic activity for selective oxidation of propene using 2%Ag/SiO₂ nanopowder catalysts

■: catalyst after calcination in air at 450°C for 2h;

●: catalyst without calcination;

★: catalyst after calcination in 5%H₂/Ar at 450°C for 2h;

Solid symbols: PO selectivity; Open symbols: Propene conversion

Table 5.7. Results for propene epoxidation over calcined Ag/SiO₂ catalysts

Catalyst	Temp (°C)	Conversion (%)	Sel of PO (%)
2%Ag/SiO ₂ nanopowder (Calcination at 450 ⁰ C in air for 2h)	220	0	0
	250	0	0
	270	0.30	21.6
	290	0.58	17.1
	300	3.2	7.8
	350	9.0	0.9
2%Ag/SiO ₂ nanopowder (Calcination at 450 ⁰ C in 5%H ₂ /Ar for 2h)	220	0	0
	250	0	0
	270	1.0	15.4
	290	1.8	11.6
	300	3.7	8.9
	350	9.1	1.2
2%Ag/regular SiO ₂ (Calcination at 450 ⁰ C in air for 2h)	250	0	0
	270	0	0
	290	0.35	16.8
	300	0.96	11.0
	350	2.9	4.2
2%Ag/regular SiO ₂ (Calcination at 450 ⁰ C in 5%H ₂ /Ar for 2h)	250	0	0
	270	0	0
	290	0.67	15.7
	300	1.6	9.5
	350	3.8	2.1
2%Ag-colloid/SiO ₂ nanopowder (Calcination at 450 ⁰ C in air for 2h)	250	0	0
	270	0.21	0
	290	0.29	0
	300	0.38	0
	350	3.1	0
2%Ag-colloid/SiO ₂ nanopowder (Calcination at 450 ⁰ C in 5%H ₂ /Ar for 2h)	250	0	0
	270	0.36	0
	290	0.47	0
	300	1.2	0
	350	3.9	0

Table 5.8. Results over calcined Ag/ZnO, Al₂O₃ and TiO₂ catalysts

Catalyst	Temp (°C)	Conversion (%)	Sel of PO (%)
2%Ag/regular ZnO (Calcination at 450°C in air for 2h)	250	0	0
	270	0.12	25.0
	290	0.21	18.4
	300	0.36	14.6
	350	3.4	8.3
2%Ag/regular ZnO (Calcination at 450°C in 5%H ₂ /Ar for 2h)	220	0	0
	250	0.18	17.6
	270	0.29	13.2
	290	0.52	11.6
	300	1.06	9.4
2%Ag/TiO ₂ (Calcination at 450°C in air for 2h)	350	3.7	3.8
	220	0	0
	250	1.1	19.8
	270	1.9	15.2
	290	2.8	10.6
2%Ag/TiO ₂ (Calcination at 450°C in 5%H ₂ /Ar for 2h)	300	4.9	6.7
	350	8.8	2.0
	220	0	0
	250	0.15	17.5
	270	0.98	14.3
2%Ag/regular α-Al ₂ O ₃ (Calcination at 450°C in air for 2h)	290	1.6	10.5
	300	3.9	6.8
	350	7.9	1.4
	220	0	0
	250	0.26	22.1
2%Ag/regular α-Al ₂ O ₃ (Calcination at 450°C in air for 2h)	270	0.69	18.7
	290	2.7	13.2
	300	4.2	7.7
	350	8.3	0.5
	2%Ag/regular α-Al ₂ O ₃ (Calcination at 450°C in 5%H ₂ /Ar for 2h)	220	0
250		0.57	17.8
270		1.1	11.2
290		2.9	7.4
300		5.6	3.2
	350	8.7	0.2

Table 5.9. Results over calcined Ag/Al₂O₃ and CeO₂ catalysts

Catalyst	Temp (°C)	Conversion (%)	Sel of PO (%)
2%Ag/Al ₂ O ₃ nanopowder-1 (Calcination at 450 ⁰ C in air for 2h)	220	0.45	20.3
	250	0.67	18.2
	270	1.6	14.1
	290	3.8	9.7
	300	7.1	4.5
	350	9.3	0.2
2%Ag/Al ₂ O ₃ nanopowder-1 (Calcination at 450 ⁰ C in 5%H ₂ /Ar for 2h)	220	0.61	19.8
	250	1.2	14.0
	270	2.2	10.3
	290	3.8	6.4
	300	7.4	3.6
	350	8.9	0.3
2%Ag/regular CeO ₂ (Calcination at 450 ⁰ C in air for 2h)	220	2.2	13.8
	250	3.7	10.1
	290	4.6	8.0
	300	5.9	4.5
	350	8.7	0.7
2%Ag/regular CeO ₂ (Calcination at 450 ⁰ C in 5%H ₂ /Ar for 2h)	220	2.5	11.4
	250	3.9	7.9
	290	5.2	5.3
	300	7.1	2.7
	350	8.9	0.5
2%Ag/ CeO ₂ nanopowder-1 (Calcination at 450 ⁰ C in air for 2h)	220	3.8	7.1
	250	4.8	3.6
	290	6.4	Trace
	300	7.8	Trace
	350	9.2	Trace
2%Ag/ CeO ₂ nanopowder-1 (Calcination at 450 ⁰ C in 5%H ₂ /Ar for 2h)	220	4.1	5.6
	250	5.2	Trace
	290	6.6	Trace
	300	8.1	Trace
	350	9.3	Trace

In agreement with common observations, supported Ag catalysts generally give low selectivity for propene epoxidation. Also, moderate selectivity can only be obtained at low conversion. However, the present results strongly indicate that the support plays an important role in the catalytic performance of supported Ag catalysts.

Previous studies suggested that supports do not play a significant part in the commonly observed low PO selectivity; this viewpoint only pertains to supported Ag catalysts over which low PO selectivity is observed, typically <30% [27,28]. In fact, because of the low intrinsic selectivity of supported Ag catalysts for PO formation, structural effects will be dominated by the complete combustion reaction. In this case, it is difficult to identify the support effects for selective epoxidation of propene.

For the most selective catalyst, Ag/SiO₂ nanopowder, TEM analysis has been performed to characterise the composition of this catalyst. The TEM images are shown in **Figure 5.20**. It indicates that Ag₃O₄ is the main phase and only a very small amount of metallic Ag is found. Blank experiments using SiO₂ nanopowder show no activity is observed. Consequently, it confirms that the primary active phase should be Ag in an oxidised state for this catalyst.



Fig.5.20 TEM images of 2%Ag/SiO₂ nanopowder catalyst

5.3.3 Propene oxidation over supported Cu catalysts

Recently, some studies have shown that Cu-based materials could be promising catalysts for selective propene epoxidation to PO. Li and co-workers firstly reported that, using a NaCl-modified $\text{VCe}_{1-x}\text{Cu}_x$ oxide catalyst, a PO selectivity of 43% can be achieved at 0.19% propene conversion [21]. Lambert *et al.* demonstrated that Cu/SiO_2 catalyst can provide a PO selectivity of 53% at 0.25% propene conversion [20]. In these two studies, it was found that with the increase of propene conversion the PO selectivity would significantly be decreased. The moderate PO selectivity, *ca.* 40-50%, can only be obtained at very low propene conversion, typically <0.3%. Nevertheless, these initial studies strongly indicate that Cu-based material can be used as a potential and inexpensive catalyst for selective epoxidation of propene to PO.

In addition, a series of surface science studies under ultrahigh vacuum (UHV) conditions on Ag and Cu single-crystal surfaces have shown that Cu surfaces are more selective than Ag surfaces for the epoxidation of higher alkenes, such as styrene and methylstyrene [29-31]. It was reported that when allylic hydrogen atoms are present in the alkene molecules, epoxidation can still occur on a Cu(111) surface, whereas the combustion of alkenes occurs mainly on Ag surfaces [31]. Therefore, there is a great scope to design Cu-based catalysts for propene epoxidation by molecular oxygen.

Most recently, Chu and co-workers reported that a halogen-free K^+ -modified $\text{CuO}_x/\text{SBA-15}$ catalyst exhibited significantly better catalytic performance than other Cu-based catalysts so far for the epoxidation of propene by molecular oxygen [22]. The

PO selectivity, *ca.* 15-50%, can be sustained as propene conversion increases, *ca.* 1-12%. More interestingly, this study suggests that it is not the metallic Cu(0), but rather the copper in an oxidized state that accounts for the propene epoxidation by molecular oxygen. This is significantly different from previous studies over supported Cu catalysts, which suggest that metallic Cu may be the active phase for propene epoxidation. Clearly, the nature of active sites of Cu-based catalysts for propene epoxidation is not yet clear. In fact, depending on the different supports that are used for preparation of Cu catalysts, it is difficult to say if metallic Cu or oxidized Cu is the main active phase for propene epoxidation. Furthermore, it should be mentioned that under conditions of an oxygen atmosphere, metallic Cu can be oxidized during the reaction. These factors suggest the nature of the active sites on supported Cu catalysts should be complicated and need further systematic exploration.

Nevertheless, these initial studies illustrate that it is interesting to continue the experiments for propene epoxidation using different supported Cu catalysts. The data for propene epoxidation by molecular oxygen over a series of supported Cu catalysts are summarized from **Table 5.10** to **Table 5.13**. Inspection of these data can lead to the following main conclusions.

All these supported Cu catalysts are active for propene epoxidation although the PO selectivity is different from each other, suggesting that supported Cu catalysts are truly active for selective epoxidation of propene. The obtained PO selectivity over these supported Cu catalysts is comparable or much better than that over supported Ag

catalysts as discussed above. Therefore, in good agreement with previous proposals, there is a significant scope to develop inexpensive Cu-based catalysts for propene epoxidation using molecular oxygen [20-22].

Similar to supported Ag catalysts, a support effect has also been observed with respect to supported Cu catalysts. For example, when using supported Cu/SiO₂ nanopowder catalyst, the PO selectivity, *ca.* 18-61%, has been obtained along with propene conversion, *ca.* 0.3-8.9%. However, only traces of PO have been produced using supported Cu/TiO₂ catalyst. For propene epoxidation over supported Cu catalysts, the high PO selectivity has only been observed at relatively low propene conversion, which is similar to that over supported Ag catalysts. This is because of the intrinsic instability of PO and the fact that total oxidation of propene will be favoured at higher temperature.

From the standpoint of PO selectivity, nanopowder-SiO₂-supported Cu catalysts exhibit much better catalytic performance than other Cu-based catalysts reported in the literature. Over the Cu/SiO₂ nanopowder catalyst, calcined in air at 450⁰C for 2h, a selectivity of *ca.* 81%, has been achieved at a conversion of *ca.* 0.4% (**Table 5.13**). Note that the highest selectivity to PO over supported Cu catalysts in the literature is only *ca.* 50% with propene conversion <0.3%.

Regarding the supported Cu catalysts after calcination in air or hydrogen, they exhibit different reactivities as compared to uncalcined Cu catalysts, depending on the support. The results for propene epoxidation over calcined Cu catalysts are shown in

Table 5.13. In general, calcination in air led to an improved PO selectivity. Interestingly, it has been found that a nano-SiO₂-supported Cu catalyst calcined in air at 450⁰C for 2h provides significantly enhanced PO selectivity when compared to the uncalcined one. Selectivity to PO, *ca.* 47-81%, has been achieved along with a propene conversion of *ca.* 0.4-2.6% over a nanopowder-SiO₂-supported Cu catalyst after calcination in air. For nanopowder-SiO₂-supported Cu catalyst after calcination in 5%H₂/Ar at 450⁰C for 2h, the PO selectivity was moderately improved at low conversions as compared to the uncalcined one (**Figure 5.21**). Analogous catalytic performance for propene epoxidation has also been found for other supported Cu catalysts. This is probably because that, after calcination in air, the amount of Cu⁺ in the catalyst is increased to some extent, which may readily activate molecular oxygen to produce electrophilic-type oxygen species that is required for propene epoxidation [22].

Calcination in air or hydrogen for supported Cu catalysts seems to have no significant influence on the catalytic activity for Al₂O₃, TiO₂ and CeO₂-supported Cu catalysts, although the PO selectivity has been moderately improved when compared to the uncalcined one. This may be due to the low intrinsic selectivity of these supported Cu catalysts (typically PO selectivity <40%), with structural effects being dominated by the total combustion reaction. Because the main phase of copper exists in an oxidised state in the present supported Cu catalysts, it can be suggested that copper in an oxidised state should be the primary active species for propene epoxidation, which is consistent with the latest study [22].

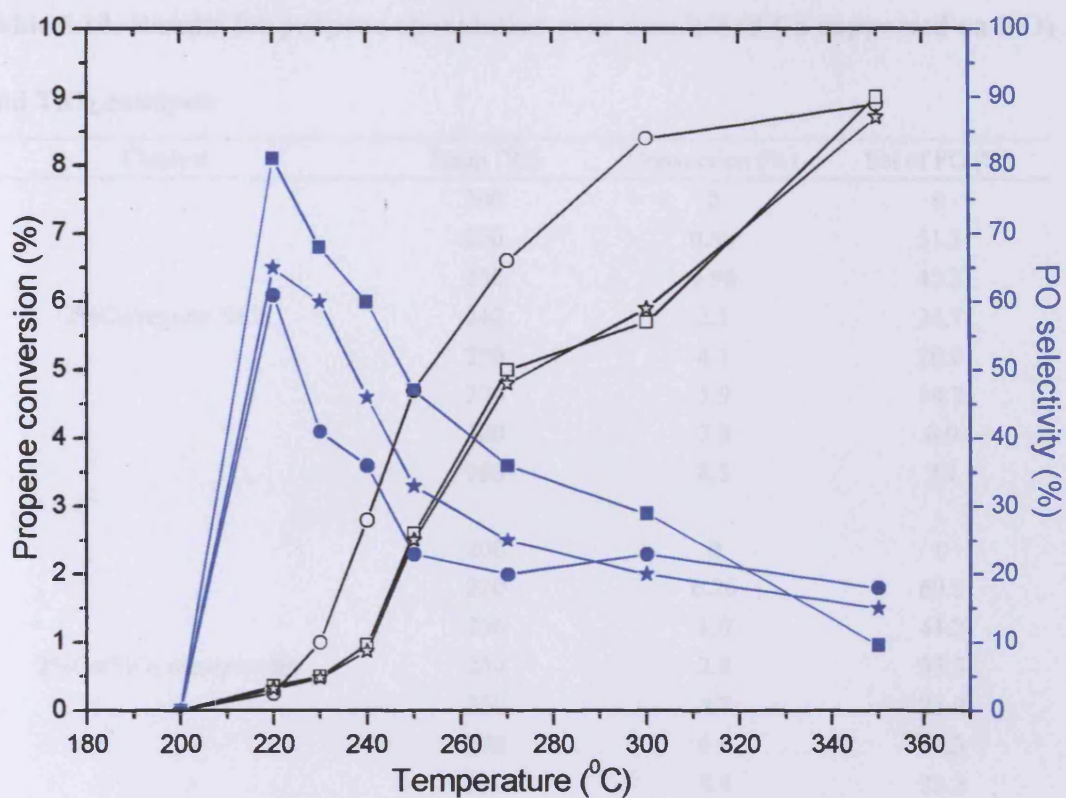


Fig.5.21 Catalytic activity for selective oxidation of propene using 2%Cu/SiO₂ nanopowder catalysts

■: catalyst after calcination in air at 450°C for 2h;

●: catalyst without calcination;

★: catalyst after calcination in 5%H₂/Ar at 450°C for 2h;

Solid symbols: PO selectivity; Open symbols: Propene conversion

Table 5.10. Results for propene epoxidation over uncalcined Cu supported on SiO₂ and TiO₂ catalysts

Catalyst	Temp (°C)	Conversion (%)	Sel of PO (%)
2%Cu/regular SiO ₂	200	0	0
	220	0.39	51.3
	230	0.96	45.2
	240	2.1	34.7
	250	4.1	20.0
	270	5.9	14.7
	300	7.8	8.9
	350	8.3	7.1
2%Cu/SiO ₂ nanopowder	200	0	0
	220	0.26	60.5
	230	1.0	41.2
	240	2.8	35.5
	250	4.7	22.9
	270	6.6	20.3
	300	8.4	23.2
	350	8.9	18.2
2%Cu/TiO ₂ (P25)	200	0	0
	220	0.09	0
	230	0.38	Trace
	240	7.8	Trace
	250	9.1	Trace
	270	9.2	Trace
	300	9.1	Trace
	350	9.3	Trace

Table 5.11. Results for propene epoxidation over uncalcined Cu supported on ZnO and CeO₂ catalysts

Catalyst	Temp (°C)	Conversion (%)	Sel of PO (%)
2%Cu/regular ZnO	200	0.10	51.9
	220	0.21	48.3
	230	0.28	45.6
	240	0.40	28.7
	250	0.52	23.2
	270	0.63	20.8
	300	1.2	11.8
	350	7.4	2.3
2%Cu/ZnO nanopowder	200	0	0
	220	0.11	54.4
	230	0.15	51.1
	240	0.2	49.2
	250	0.25	48.2
	270	0.41	29.3
	300	1.2	14.9
	350	6.8	1.2
2%Cu/regular CeO ₂	200	0	0
	230	0	0
	240	0	0
	250	0.04	30.1
	280	0.23	23.0
	300	0.73	20.2
	320	3.6	10.4
	350	8.9	2.8
2%Cu/CeO ₂ nanopowder-1	200	0.8	14.9
	220	1.9	8.2
	230	2.6	4.6
	240	3.3	0.9
	250	5.2	Trace
	280	7.8	Trace
	300	8.9	Trace
	350	9.2	Trace

Table 5.12. Results for propene epoxidation over uncalcined Cu supported on Al₂O₃ catalysts

Catalyst	Temp (°C)	Conversion (%)	Sel of PO (%)
2%Cu/regular α -Al ₂ O ₃	200	0	0
	220	0	0
	230	0.37	27.0
	240	0.51	20.2
	250	0.60	14.1
	280	4.1	6.0
	300	5.2	8.5
	350	8.8	2.0
2%Cu/regular γ -Al ₂ O ₃	200	0	0
	220	0	0
	230	0.15	33.4
	240	0.24	27.2
	250	0.61	15.4
	270	1.17	14.9
	300	4.7	4.9
	350	8.3	0.2
2%Cu/Al ₂ O ₃ nanopowder-1	200	0	0
	220	0.47	27.6
	230	0.65	26.2
	240	0.93	22.5
	250	1.5	20.6
	280	4.9	13.2
	300	7.8	0.5
	350	9.2	0
2%Cu/Al ₂ O ₃ nanopowder-2	200	0	0
	220	0.49	0
	230	1.6	12.6
	240	2.3	9.7
	250	3.8	7.7
	280	5.8	3.1
	300	8.4	0.6
	350	9.6	0

Table 5.13. Results for propene epoxidation over calcined supported Cu catalysts

Catalyst	Temp ($^{\circ}$ C)	Conversion (%)	Sel of PO (%)
2%Cu/regular SiO ₂ (Calcination at 450 $^{\circ}$ C in air for 2h)	200	0	0
	220	0.35	56.9
	230	0.89	48.8
	240	1.9	37.6
	250	3.9	21.3
	270	4.8	15.4
	300	7.5	10.2
	350	8.1	8.3
2%Cu/regular SiO ₂ (Calcination at 450 $^{\circ}$ C in 5%H ₂ /Ar for 2h)	200	0	0
	220	0.38	50.2
	230	1.2	45.6
	240	2.3	36.4
	250	4.2	22.3
	270	5.7	15.9
	300	7.9	9.3
	350	8.7	5.1
2%Cu/ SiO ₂ nanopowder (Calcination at 450 $^{\circ}$ C in air for 2h)	200	0	0
	220	0.36	80.9
	230	0.50	68.0
	240	0.96	60.1
	250	2.6	47.0
	270	5.0	36.5
	300	5.7	29.0
	350	9.0	9.6
2%Cu/ SiO ₂ nanopowder (Calcination at 450 $^{\circ}$ C in 5%H ₂ /Ar for 2h)	200	0	0
	220	0.32	65.2
	230	0.48	60.1
	240	0.87	46.2
	250	2.5	32.6
	270	4.8	25.1
	300	5.9	20.3
	350	8.7	14.5

Continued Table 5.13. Results for propene epoxidation over calcined supported Cu

catalysts

Catalyst	Temp ($^{\circ}$ C)	Conversion (%)	Sel of PO (%)
2%Cu/regular ZnO (Calcination at 450 $^{\circ}$ C in air for 2h)	200	0.13	59.8
	220	0.18	57.2
	230	0.31	49.6
	240	0.48	41.2
	250	0.56	30.1
	270	0.82	28.3
	300	1.5	20.1
	350	7.8	4.8
2%Cu/regular ZnO (Calcination at 450 $^{\circ}$ C in 5%H ₂ /Ar for 2h)	200	0.10	44.6
	220	0.23	40.1
	230	0.36	37.8
	240	0.56	32.7
	250	0.74	24.5
	270	1.1	17.3
	300	2.3	10.4
	350	8.4	3.0
2%Cu/ ZnO nanopowder (Calcination at 450 $^{\circ}$ C in air for 2h)	200	0	0
	220	0.12	58.4
	230	0.19	56.1
	240	0.47	45.7
	250	0.50	43.1
	270	0.78	26.7
	300	1.8	18.8
	350	8.7	2.9
2%Cu/ ZnO nanopowder (Calcination at 450 $^{\circ}$ C in 5%H ₂ /Ar for 2h)	200	0	0
	220	0.14	47.5
	230	0.18	39.9
	240	0.53	31.4
	250	0.69	25.6
	270	0.95	18.6
	300	1.9	11.7
	350	7.7	3.6

Continued Table 5.13. Results for propene epoxidation over calcined supported Cu catalysts

Catalyst	Temp ($^{\circ}$ C)	Conversion (%)	Sel of PO (%)
2%Cu/regular γ -Al ₂ O ₃ (Calcination at 450 $^{\circ}$ C in air for 2h)	200	0	0
	220	0.11	39.4
	230	0.15	38.1
	240	0.2	35.2
	250	0.25	32.1
	270	0.41	24.3
	300	1.15	14.9
	350	6.8	1.2
2%Cu/regular γ -Al ₂ O ₃ (Calcination at 450 $^{\circ}$ C in 5%H ₂ /Ar for 2h)	200	0	0
	220	0.12	33.9
	230	0.27	29.2
	240	0.51	18.1
	250	0.6	15.6
	270	0.88	12.0
	300	1.5	9.9
	350	7.9	0.5
2%Cu/regular α -Al ₂ O ₃ (Calcination at 450 $^{\circ}$ C in air for 2h)	200	0	0
	220	0.16	33.8
	230	0.35	24.2
	240	0.90	20.7
	250	1.4	17.8
	270	4.1	11.3
	300	7.2	0.9
	350	8.7	Trace
2%Cu/regular α -Al ₂ O ₃ (Calcination at 450 $^{\circ}$ C in 5%H ₂ /Ar for 2h)	200	0	0
	220	0.25	30.4
	230	0.48	22.3
	240	1.1	14.6
	250	1.8	11.1
	270	3.9	7.4
	300	7.5	2.1
	350	9.0	Trace

Continued Table 5.13. Results for propene epoxidation over calcined supported Cu

catalysts

Catalyst	Temp (°C)	Conversion (%)	Sel of PO (%)
2%Cu/TiO ₂ (P25) (Calcination at 450°C in air for 2h)	200	0	0
	220	0.16	8.2
	230	0.62	4.7
	240	6.3	Trace
	250	9.1	Trace
	270	8.9	Trace
	300	9.2	Trace
	350	9.2	Trace
2%Cu/TiO ₂ (P25) (Calcination at 450°C in 5%H ₂ /Ar for 2h)	200	0	0
	220	0.28	4.2
	230	1.1	0.3
	240	2.4	Trace
	250	7.6	Trace
	270	8.5	Trace
	300	8.9	Trace
	350	9.2	Trace
2%Cu/regular CeO ₂ (Calcination at 450°C in air for 2h)	200	0	0
	220	0	0
	230	0	0
	240	0.09	38.2
	250	0.28	25.6
	270	0.91	17.2
	300	3.9	8.2
	350	9.3	1.3
2%Cu/regular CeO ₂ (Calcination at 450°C in 5%H ₂ /Ar for 2h)	200	0	0
	220	0	0
	230	0.08	34.7
	240	0.20	24.1
	250	0.37	20.2
	270	1.3	11.5
	300	4.5	6.4
	350	9.1	0.4

5.3.4 Propene oxidation over supported Au catalysts

In 1998, Haruta and co-workers discovered that a TiO₂-supported Au catalyst can give propene epoxidation selectivity close to 100%, although at very low propene conversion, *ca.* 1% [16]. Since then, significant interest and effort have been devoted to the selective epoxidation of propene over supported Au catalysts. Most recently, using a gold catalyst supported on 3D mesoporous silylated titanosilicates in the presence of Ba(NO₃)₂ as a promoter, Haruta's group reported that a conversion of 9.8% together with selectivity to PO of 90.3% had been achieved [17]. However, it should be noted that, in this catalyst system, hydrogen is always needed as a sacrificial feed gas for propene epoxidation and the hydrogen efficiency is insufficient, typically <30%. In addition, the nature of the active site involved and the mechanism of Au-TiO₂-catalysed propene epoxidation still remain controversial, there being no consensus view [18,19].

In this section, the activity of supported Au catalysts for propene epoxidation has been tested using only oxygen as oxidant. In particular, the activity of supported Au catalysts for propene epoxidation by molecular oxygen is used for comparison with over supported Au-contained alloy catalysts as discussed in the next section. Based on the data in **Table 5.14** and **Table 5.17**, the following main conclusions can be obtained.

For propene epoxidation over a Au/TiO₂ catalyst using only molecular oxygen as oxidant, very low propene conversion and PO selectivity have been observed. However, as mentioned above, very high PO selectivity was obtained over a Au/TiO₂ catalyst using a mixture of O₂ and H₂. This suggests that hydrogen plays an important role in

activating molecular oxygen to produce active species that are responsible for PO formation. However, it should be emphasized that herein the main interest and aim are on propene epoxidation using only oxygen as oxidant, without the need of hydrogen as a sacrificial feedstock.

Other supported Au catalysts generally give low PO selectivity except for Au/ZnO. The selectivity of PO observed is dependent on the given support. SiO₂ and CeO₂ seem to be the very poor supports for selective epoxidation of propene. Using Au/SiO₂, very low conversion of propene is obtained even at high temperature. Whereas, using Au/CeO₂ catalysts particularly Au/CeO₂ nanopowder catalyst, the selectivity to PO is very low although high propene conversion is achieved at relatively low temperature. This is reasonable since CeO₂ support is intrinsically active for total oxidation of propene, which is confirmed by the blank experiment using only CeO₂ support. Namely, CeO₂ nanopowder support is highly active for total oxidation of propene at low temperature. Interestingly, it has been found that, for propene epoxidation by molecular oxygen, Au/ZnO can provide high PO selectivity, *ca.*50-70% although with very low conversion, *ca.*0.1-1%.

The PO selectivity observed is generally decreased to some degree for supported Au catalysts after calcination in air or hydrogen,, which may be primarily due to the formation of larger Au particles after calcination [3,32].

Table 5.14. Results for propene epoxidation over uncalcined Au supported on TiO₂ and ZnO catalysts

Catalyst	Temp (°C)	Conversion (%)	Sel of PO (%)
1.5%Au/TiO ₂ (Supplied from world gold council)	200	0	0
	220	0	0
	240	0	0
	250	0.09	0
	270	0.07	0
	300	0.08	0
	320	0.20	38.2
	350	0.7	21.4
2%Au/TiO ₂	200	0	0
	220	0	0
	240	0	0
	250	0.08	0
	270	0.12	0
	300	0.18	0
	320	0.84	30.1
	350	1.9	12.3
2%Au/regular ZnO	200	0.0	0
	220	0.08	72
	240	0.18	70.5
	250	0.24	68.7
	270	0.35	62.5
	300	0.96	50
	320	1.2	35.6
	350	2.1	20
2%Au/ZnO nanopowder	200	0.0	0.0
	220	0.0	0.0
	240	0.08	77.0
	250	0.10	76.1
	270	0.17	61.5
	300	0.34	56.0
	320	0.45	41.8
	350	0.89	32.2

Table 5.15. Results for propene epoxidation over uncalcined Au supported on Al₂O₃ catalysts

Catalyst	Temp (°C)	Conversion (%)	Sel of PO (%)
2%Au/regular α -Al ₂ O ₃	200	0	0
	220	0	0
	240	0	0
	250	0	0
	270	0.09	45.3
	300	0.21	38.7
	320	0.30	32.5
	350	0.92	14.0
2%Au/regular γ -Al ₂ O ₃	200	0	0
	220	0	0
	240	0	0
	250	0.08	19.7
	270	0.15	15.5
	300	0.23	10.2
	320	0.37	7.1
	350	1.04	3.0
2%Au/ Al ₂ O ₃ nanopowder-1	200	0	0
	220	0	0
	240	0	0
	250	0.09	37.4
	270	0.13	34.6
	300	0.26	28.9
	320	0.41	20.2
	350	1.2	8.3
2%Au/ Al ₂ O ₃ nanopowder-2	200	0	0
	220	0	0
	240	0	0
	250	0.10	40.1
	270	0.16	34.5
	300	0.37	26.8
	320	0.52	20.3
	350	1.1	9.8

Table 5.16. Results for propene epoxidation over uncalcined Au supported on SiO₂**and CeO₂ catalysts**

Catalyst	Temp (°C)	Conversion (%)	Sel of PO (%)
2%Au/regular SiO ₂	200	0	0
	220	0	0
	240	0	0
	250	0	0
	270	0	0
	300	0	0
	320	0.08	Trace
	350	0.23	Trace
	2%Au/SiO ₂ nanopowder	200	0
220		0	0
240		0	0
250		0	0
270		0	0
300		0.05	7.2
320		0.10	3.1
350		0.34	Trace
2%Au/ regular CeO ₂		200	0
	220	0	0
	240	0	0
	250	0.17	18.7
	270	0.63	11.1
	300	1.8	8.3
	320	3.3	2.9
	350	5.7	Trace
	2%Au/ CeO ₂ nanopowder-2	200	0
220		0.97	0
240		1.1	0
250		7.8	0
270		8.6	0
300		9.2	0
320		9.3	0
350		9.6	0

Table 5.17. Results for propene epoxidation over calcined Au catalysts

Catalyst	Temp ($^{\circ}$ C)	Conversion (%)	Sel of PO (%)
2%Au/TiO ₂ (Calcination at 450 $^{\circ}$ C in air for 2h)	200	0	0
	220	0	0
	240	0	0
	250	0.14	0
	270	0.26	0
	300	0.39	0
	320	0.98	10.5
	350	2.2	0.2
2%Au/TiO ₂ (Calcination at 450 $^{\circ}$ C in 5%H ₂ /Ar for 2h)	200	0	0
	220	0	0
	240	0	0
	250	0.11	0
	270	0.22	0
	300	0.34	0
	320	0.67	7.1
	350	1.5	0.3
2%Au/regular ZnO (Calcination at 450 $^{\circ}$ C in air for 2h)	200	0.0	0
	220	0.09	60.1
	240	0.15	54.8
	250	0.22	49.3
	270	0.35	38.6
	300	0.84	22.3
	320	1.1	17.5
	350	1.8	4.6
2%Au/regular ZnO (Calcination at 450 $^{\circ}$ C in 5%H ₂ /Ar for 2h)	200	0.0	0
	220	0.07	55.3
	240	0.12	52.7
	250	0.19	47.4
	270	0.27	40.1
	300	0.72	23.2
	320	1.0	13.0
	350	1.7	7.1

Continued Table 5.17. Results for propene epoxidation over calcined Au catalysts

Catalyst	Temp ($^{\circ}$ C)	Conversion (%)	Sel of PO (%)
2%Au/ZnO nanopowder (Calcination at 450 $^{\circ}$ C in air for 2h)	200	0.0	0
	220	0.08	59.2
	240	0.13	55.6
	250	0.21	48.7
	270	0.37	37.6
	300	0.80	23.1
	320	0.96	15.3
	350	1.7	3.2
2%Au/ZnO nanopowder (Calcination at 450 $^{\circ}$ C in 5%H ₂ /Ar for 2h)	200	0.0	0
	220	0.07	54.1
	240	0.14	50.2
	250	0.26	45.3
	270	0.38	39.7
	300	0.79	20.5
	320	1.0	13.8
	350	1.5	2.8
2%Au/regular α -Al ₂ O ₃ (Calcination at 450 $^{\circ}$ C in air for 2h)	200	0	0
	220	0	0
	240	0	0
	250	0	0
	270	0.07	47.2
	300	0.23	35.6
	320	0.39	27.4
	350	1.3	10.6
2%Au/regular α -Al ₂ O ₃ (Calcination at 450 $^{\circ}$ C in 5%H ₂ /Ar for 2h)	200	0	0
	220	0	0
	240	0	0
	250	0	0
	270	0.06	32.1
	300	0.16	24.3
	320	0.33	12.5
	350	0.97	2.4

Continued Table 5.17. Results for propene epoxidation over calcined Au catalysts

Catalyst	Temp ($^{\circ}$ C)	Conversion (%)	Sel of PO (%)
2%Au/SiO ₂ nanopowder (Calcination at 450 $^{\circ}$ C in air for 2h)	200	0	0
	220	0	0
	240	0	0
	250	0	0
	270	0	0
	300	0.08	0
	320	0.13	0
	350	0.31	0
2%Au/SiO ₂ nanopowder (Calcination at 450 $^{\circ}$ C in 5%H ₂ /Ar for 2h)	200	0	0
	220	0	0
	240	0	0
	250	0	0
	270	0	0
	300	0.05	0
	320	0.09	0
	350	0.23	0
2%Au/regular CeO ₂ (Calcination at 450 $^{\circ}$ C in air for 2h)	200	0	0
	220	0	0
	240	0	0
	250	0.12	10.3
	270	0.78	5.6
	300	2.5	0.7
	320	3.8	Trace
	350	6.7	Trace
2%Au/regular CeO ₂ (Calcination at 450 $^{\circ}$ C in 5%H ₂ /Ar for 2h)	200	0	0
	220	0	0
	240	0	0
	250	0.23	6.5
	270	0.69	2.2
	300	2.4	0.3
	320	4.1	Trace
	350	7.3	Trace

Continued Table 5.17. Results for propene epoxidation over calcined Au catalysts

Catalyst	Temp ($^{\circ}$ C)	Conversion (%)	Sel of PO (%)
2%Au/regular SiO ₂ (Calcination at 450 $^{\circ}$ C in air for 2h)	200	0	0
	220	0	0
	240	0	0
	250	0	0
	270	0	0
	300	0	0
	320	0.05	0
	350	0.14	0
2%Au/regular SiO ₂ (Calcination at 450 $^{\circ}$ C in 5%H ₂ /Ar for 2h)	200	0	0
	220	0	0
	240	0	0
	250	0	0
	270	0	0
	300	0	0
	320	0.12	0
	350	0.57	0
2%Au/regular γ -Al ₂ O ₃ (Calcination at 450 $^{\circ}$ C in air for 2h)	200	0	0
	220	0	0
	240	0	0
	250	0.07	14.2
	270	0.14	13.3
	300	0.26	9.7
	320	0.42	4.1
2%Au/regular γ -Al ₂ O ₃ (Calcination at 450 $^{\circ}$ C in 5%H ₂ /Ar for 2h)	200	0	0
	220	0	0
	240	0	0
	250	0.06	15.4
	270	0.18	10.6
	300	0.29	7.8
	320	0.46	3.4
350	1.1	0.6	

5.3.5 Propene oxidation over supported Au-Cu catalysts

In many cases, supported bimetallic catalysts can provide enhanced selectivity toward some given reactions. For example, Hutchings' research group has shown that Au-Pd/TiO₂ can exhibit significant activity and selectivity for alcohol oxidation in the absence of solvents [33]. The highest turn over frequency (TOF) has been achieved when using such a TiO₂-supported Au-Pd catalyst. STEM and XPS analysis demonstrated that this catalyst features a core-shell microscopic structure with Au located at the core and Pd on the outside. Thus, it can reasonably be proposed that Au affects the electronic structure of Pd and consequently leads to a special catalyst. In addition, Hutchings' group has shown that supported Au-Pd is also an active catalyst for hydrogen peroxide (H₂O₂) synthesis [34-37]. Compared to supported Au or Pd catalyst, Au-Pd catalyst can give the highest productivity of H₂O₂. These results suggest that there could be a broad scope to explore propene epoxidation over supported bimetal alloy catalysts.

During the initial studies, supported Au-Cu catalysts have been investigated. **Table 5.18** lists the data for propene oxidation over supported Au-Cu catalysts prepared by a two-step method. Namely, a deposition-precipitation method is used to first prepare an Au catalyst. Then, Cu is added to the as-prepared Au catalyst by an impregnation method. Interestingly, it has been found that these supported Au-Cu catalysts are active for propene epoxidation. For α -Al₂O₃, ZnO and TiO₂-supported Au-Cu catalysts, the results show that they provide much higher selectivity than supported Au or Cu catalysts

respectively. When using the nanopowder-ZnO-supported Au-Cu catalyst, very high selectivity, *ca.* 96-60%, has been achieved at propene conversions, *ca.* 0.15-3% (**Table 5.18** and **Figure 5.22**). The PO selectivity observed over ZnO-supported Au-Cu catalyst is significantly higher than other catalysts reported so far with respect to propene epoxidation using only molecular oxygen as oxidant. On the other hand, it should be noted that the regular-ZnO-supported Au-Cu catalyst exhibits similar activity to the nanopowder-ZnO-supported Au-Cu catalyst. This can be reasonably understood by the little difference observed between the regular ZnO support and nanopowder ZnO support. XRD and SEM images show that these two ZnO supports have analogous surface morphology and the same crystalline phase composition; the only difference is the particle size of the nanopowder ZnO support which is smaller than that of the regular ZnO support. Consequently, by careful control during the preparation of Au-Cu catalysts, these two ZnO-supported Au-Cu catalysts should show similar catalytic performance.

In addition, the Au-Cu supported on CeO₂ prepared from a supercritical dioxide process has also been tried. However, the results show that this catalyst is totally unselective for propene epoxidation, but a very good catalyst for total oxidation of propene. Blank experiments have demonstrated that the support CeO₂ itself is intrinsically highly active for combustion of propene, even at low temperature. These results exclude the use of CeO₂ as a potential support to prepare Au-Cu catalysts for propene epoxidation.

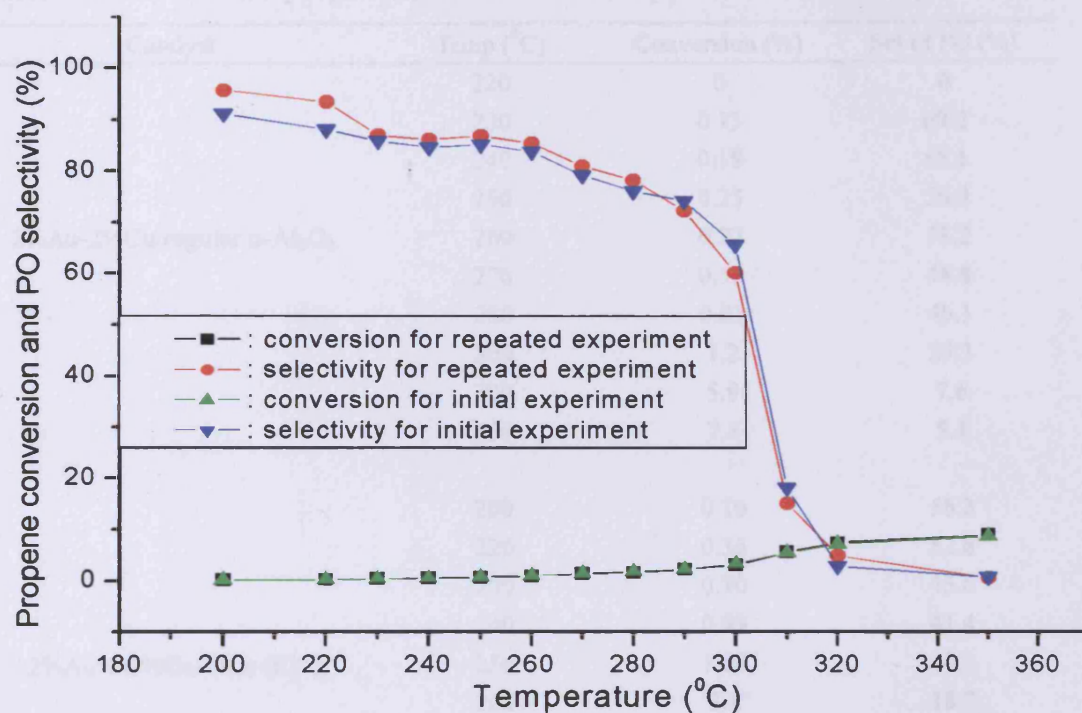


Fig.5.22 Catalytic activity for Au-Cu/ZnO nanopowder catalyst prepared by a two-step method

Table 5.18. Results for propene epoxidation over supported Au-Cu catalysts ^a

Catalyst	Temp (^o C)	Conversion (%)	Sel of PO (%)
2%Au-2%Cu/regular α -Al ₂ O ₃	220	0	0
	230	0.13	69.2
	240	0.18	65.1
	250	0.25	56.0
	260	0.27	53.2
	270	0.35	48.8
	280	0.53	46.1
	300	1.2	25.3
	320	5.9	7.6
	350	7.8	5.1
	2%Au%-2%Cu/TiO ₂ (P25)	200	0.16
220		0.36	52.8
230		0.70	45.6
240		0.89	41.4
250		1.03	40.3
260		3.8	18.7
270		7.9	4.8
300		8.9	1.1
320		9.4	0.8
350		10.1	0.2
2%Au-2%Cu/regular γ -Al ₂ O ₃	200	0	0
	220	0	0
	230	0	0
	240	0	0
	250	0.11	25.3
	260	0.23	20.6
	270	0.55	14.9
	300	2.3	10.1
	320	4.5	2.3
350	7.9	0.2	

^a catalysts prepared by a two-step method.

Continued Table 5.18. Results for propene epoxidation over supported Au-Cu catalysts ^a

Catalyst	Temp (°C)	Conversion (%)	Sel of PO (%)
2%Au-2%Cu/regular ZnO	220	0.25	88
	230	0.5	84.1
	240	0.71	80.3
	250	0.98	79.6
	260	2.16	75.4
	270	3.82	49
	280	6.6	17.2
	300	7.8	9.6
	320	8.5	7.7
	350	9.9	5.0
2%Au%-2%Cu/ZnO nanopowder	200	0.14	95.8
	220	0.25	93.6
	230	0.39	87.2
	240	0.52	86.3
	250	0.68	87.0
	260	0.93	85.6
	270	1.45	81.1
	280	1.60	78.3
	290	2.19	72.4
	300	3.01	60.3
	310	5.6	15.2
2%Au-2%Cu/CeO ₂ nanopowder-2 ^b	320	7.4	5.0
	350	8.4	0.9
	180	6.1	0
	200	7.5	0
	210	8.2	0
	230	8.8	0
	250	9.2	0

^a catalysts prepared by a two-step method.

^b CeO₂ prepared using a supercritical carbon dioxide process.

Continued Table 5.18. Results for propene epoxidation over supported Au-Cu catalysts ^a

Catalyst	Temp (°C)	Conversion (%)	Sel of PO (%)
2%Au-2%Cu/Al ₂ O ₃ nanopowder-2	220	0	0
	230	0	0
	240	0	0
	250	0	0
	260	0.12	28.7
	270	0.29	23.6
	280	0.48	20.1
	300	1.0	13.5
	320	4.2	8.5
	350	7.9	2.4
2%Au%-2%Cu/regular SiO ₂	200	0	0
	220	0.08	36.6
	230	0.15	34.3
	240	0.41	29.8
	250	0.89	17.5
	260	1.8	14.1
	270	2.9	8.6
	300	4.7	3.4
	320	6.8	0.7
	350	8.3	0.1
2%Au-2%Cu/SiO ₂ nanopowder	200	0	0
	220	0.14	42.3
	230	0.29	37.1
	240	0.56	28.2
	250	0.78	20.3
	260	1.1	17.2
	270	2.1	11.6
	300	4.2	6.3
	320	6.7	2.4
	350	8.8	0.3

^a catalysts prepared by a two-step method.

For the most selective catalyst of Au-Cu/ZnO nanopowder, the stability of catalytic performance under the reaction conditions has been tested. The data for testing the activity of Au-Cu/ZnO nanopowder from low temperature to high temperature and from high temperature to low temperature have been plotted in **Figure 5.23**. Apparently, such a Au-Cu/ZnO nanopowder catalyst exhibits high selectivity as well as stable catalytic activity toward propene epoxidation. The composition of Au-Cu catalyst is probably almost unchanged during the reaction.

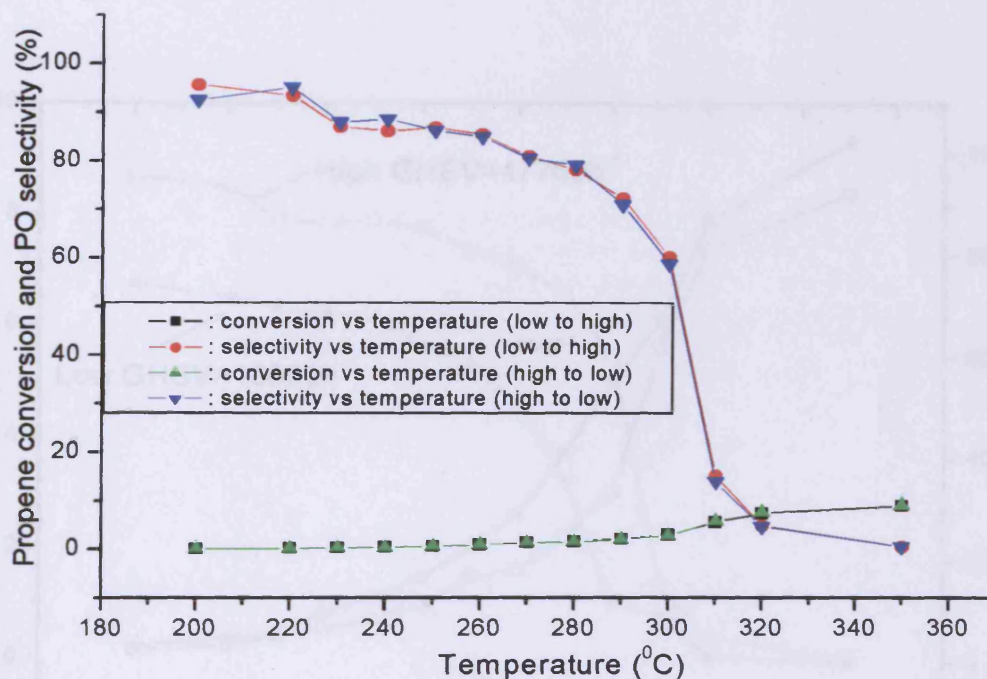


Fig.5.23 Catalytic activity and stability of Au-Cu/ZnO nanopowder catalyst prepared by a two-step method for propene epoxidation

To see if the high selectivity can be maintained when the conversion of propene is increased, the catalytic performance of Au-Cu/ZnO nanopowder catalyst for propene epoxidation with a lower GHSV has been studied; the results are displayed in **Figure 5.24**. It can be seen that conversion has been improved by increasing the contact time of the reactant on the catalyst surface under the condition of low GHSV. However, at the same time, the PO selectivity has been decreased. Therefore, high PO selectivity can only be observed under the condition of high GHSV. Increasing the contact time of the reactant on the catalyst surface will promote the total oxidation of propene with a loss of PO selectivity.

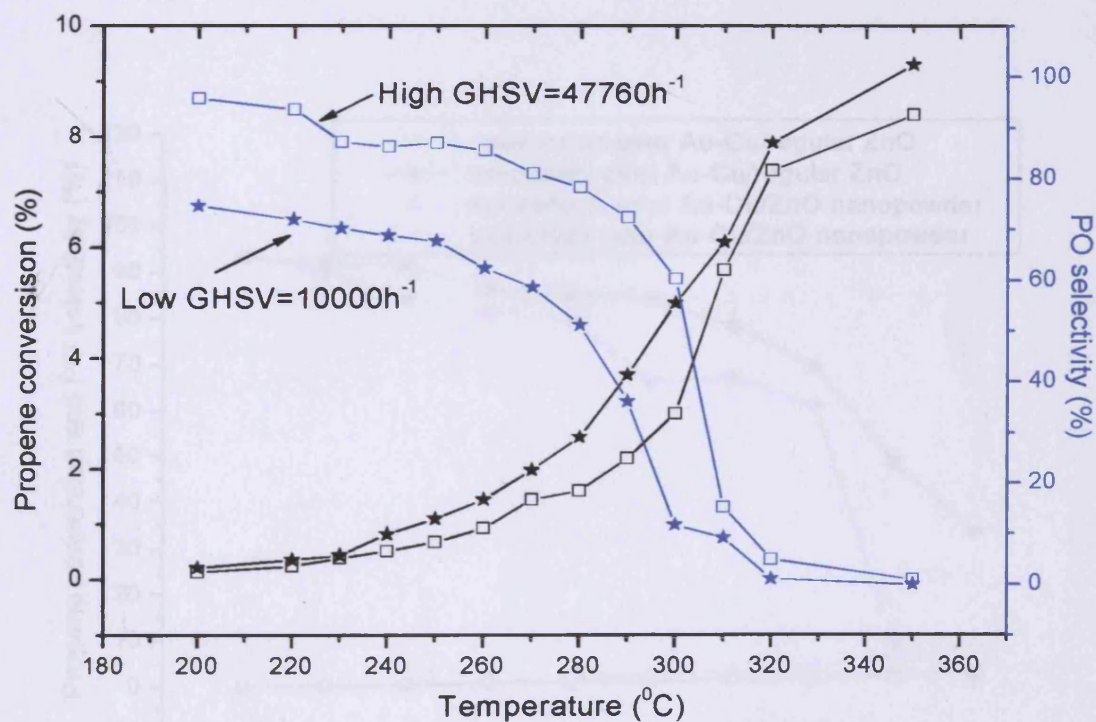


Fig.5.24 Propene epoxidation over Au-Cu/ZnO nanopowder catalyst prepared by a two-step method under the conditions of high and low GHSV

In order to consider the effect of preparation method on the performance of as-prepared catalysts, a simple wet impregnation method has been used to prepare ZnO-supported Au-Cu catalysts. Quite interestingly, it has been found that a ZnO-supported Au-Cu catalyst prepared by a wet impregnation method, followed by calcination at 450°C in air for 2h, can provide comparable activity (Figure 5.22) with respect to the catalyst prepared by a two-step method (Figure 5.25 and Table 5.19). This suggests that, for the ZnO support, preparation methods seem not to be the key factor influencing the catalyst performance. In the meantime, it could be reasoned that perhaps regular and nanopowder ZnO-supported Au-Cu catalysts may feature the similar composition structure.

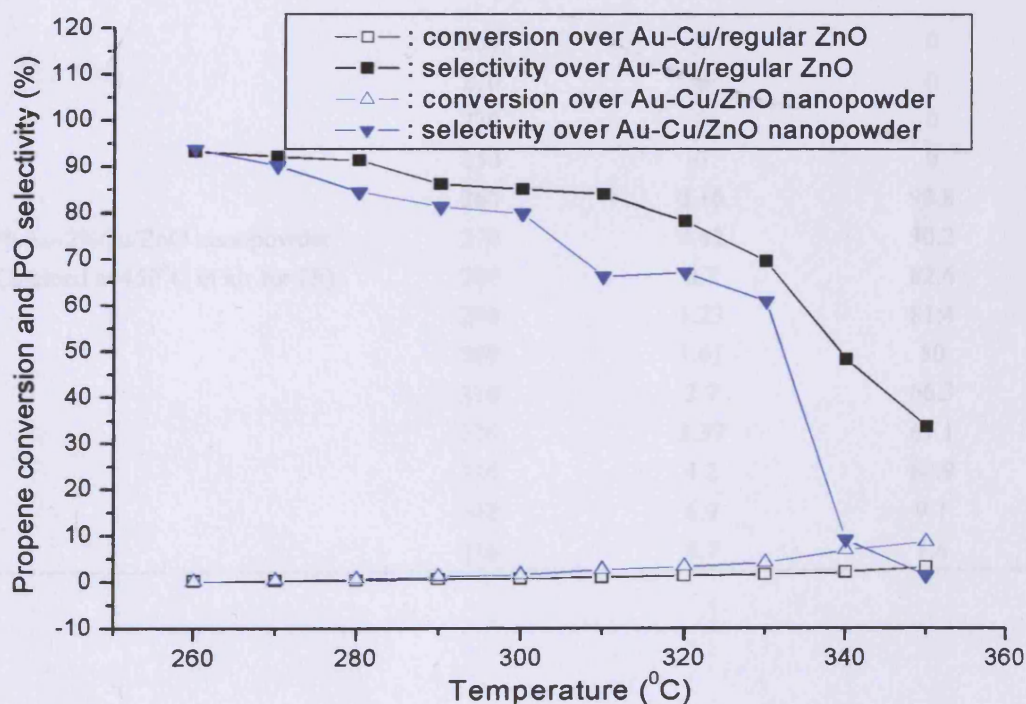


Fig.25 Catalytic activity for Au-Cu/ZnO catalyst prepared by an impregnation method followed by calcination at 450°C in air for 2h

Table 5.19. Results for propene epoxidation over supported Au-Cu/ZnO catalysts prepared by impregnation method

Catalyst	Temp ($^{\circ}$ C)	Conversion (%)	Sel of PO (%)
2%Au-2%Cu/regular ZnO (Calcined at 450 $^{\circ}$ C in air for 2h)	200	0	0
	220	0	0
	230	0	0
	240	0	0
	250	0	0
	260	0.18	93.2
	270	0.29	92.1
	280	0.39	91.3
	290	0.65	86.2
	300	0.73	85.1
	310	1	84
	320	1.34	78.2
	330	1.62	69.5
	340	2.1	48.3
	350	3.2	33.7
2%Au-2%Cu/ZnO nanopowder (Calcined at 450 $^{\circ}$ C in air for 2h)	200	0	0
	220	0	0
	230	0	0
	250	0	0
	260	0.16	93.8
	270	0.42	90.2
	280	0.7	82.6
	290	1.23	81.4
	300	1.61	80
	310	2.7	66.3
	320	3.37	67.1
	330	4.2	60.9
	340	6.9	9.1
	350	8.7	1.4

In addition, the catalytic activity of ZnO-supported Au-Cu catalysts without calcination or with calcination at 450⁰C in 5%H₂/Ar for 2h have been studied, and the data are shown in **Table 5.20**. It is clear that the PO selectivity obtained is much lower than the catalyst calcined at 450⁰C in air for 2h.

Table 5.20. Results for propene epoxidation over supported Au-Cu/ZnO catalysts prepared by impregnation method

Catalyst	Temp (⁰ C)	Conversion (%)	Selectivity (%)
2%Au-2%Cu/ ZnO nanopowder (Calcined at 450 ⁰ C in 5%H ₂ /Ar for 2h)	200	0	0
	220	Trace	0
	230	0.11	35.4
	240	0.34	42.0
	250	0.66	50.5
	270	1.34	46.0
	280	2.0	38.1
	290	3.1	21.4
	300	4.9	17.3
	320	5.8	11.2
2%Au-2%Cu/ZnO nanopowder (Catalyst without calcination)	350	7.9	7.5
	200	0	0
	220	0	0
	230	0.06	66.7
	240	0.09	65.8
	250	0.1	50.1
	270	0.35	45.7
	280	0.58	42.2
	290	0.82	29.1
	300	1.06	24
320	3.3	8.7	
350	7.7	1.4	

In view of the fact that Au-Cu/ZnO prepared by a simple co-impregnation method followed by calcination at 450⁰C in air for 2h can exhibit the comparable activity to that prepared by a two-step method, the co-impregnation method has also been used to prepare Au-Cu catalysts supported on other supports Al₂O₃, TiO₂, SiO₂ and CeO₂. The data for these catalysts performance are listed in **Table 5.21**.

Clearly, unlike Au-Cu/ZnO catalyst, these supported Au-Cu catalysts exhibit different catalytic performance from those prepared by a two-step method. For example, over the Au-Cu/TiO₂ catalyst prepared by a two-step method, PO selectivity, *ca.*40-56%, has been achieved at propene conversion, *ca.*0.2-1.0%. However, in distinct contrast, when using the Au-Cu/TiO₂ catalyst prepared by impregnation method followed by calcination in air at 450⁰C for 2h, only a trace of PO has been observed. These results suggest the preparation method can influence the catalytic performance of Au-Cu catalysts supported on different metal oxides. Nevertheless, it should be mentioned, for these Au-Cu catalysts prepared by an impregnation method, systematic optimization of heat treatment has not been tried. Presumably, with an appropriate heat treatment, these Au-Cu catalysts supported on Al₂O₃, TiO₂, SiO₂ and CeO₂ could exhibit similar catalytic activity to those prepared by a two-step method.

Fortunately, it has been found that the most selective Au-Cu/ZnO catalyst can be prepared by a simple one-step impregnation method followed by heat treatment in air. Moreover, using such an impregnation method to prepare Au-Cu/ZnO offers the advantage of straightforward preparation. Also, it provides a convenient platform for

reproducible catalyst performance.

Table 5.21. Results for propene epoxidation over Au-Cu/Al₂O₃, TiO₂, SiO₂ and CeO₂ catalysts ^a

Catalyst	Temp (°C)	Conversion (%)	Sel of PO (%)
2%Au-2%Cu/ regular α -Al ₂ O ₃ (Calcined at 450°C in air for 2h)	200	0	0
	220	0	0
	230	0	0
	240	0	0
	250	0.14	22.4
	270	0.64	23.6
	300	3.0	21.7
	320	5.1	9.9
2%Au-2%Cu/regular γ -Al ₂ O ₃ (Calcined at 450°C in air for 2h)	200	0	0
	220	0	0
	230	0	0
	240	0	0
	250	0.14	22.3
	270	0.62	21.7
	300	3.0	16.8
	320	6.4	1.6
2%Au-2%Cu/SiO ₂ nanopowder (Calcined at 450°C in air for 2h)	200	0	0
	220	0.1	58.0
	230	0.27	51.9
	240	0.38	48.3
	250	0.51	41.2
	270	1.1	36.3
	300	5.3	22.5
	320	6.8	17.4
350	8.5	11.7	

^a catalysts prepared by a single impregnation method

Continued Table 5.21. Results for propene epoxidation over Au-Cu/Al₂O₃, TiO₂, SiO₂ and CeO₂ catalysts ^a

Catalyst	Temp (°C)	Conversion (%)	Sel of PO (%)
2%Au-2%Cu/TiO ₂ (P25) (Calcined at 450 ⁰ C in air for 2h)	200	0.16	0
	220	0.32	0
	230	0.98	0
	240	2.2	Trace
	250	4.9	Trace
	270	5.6	Trace
	300	7.8	Trace
	320	8.4	Trace
	350	9.3	Trace
2%Au-2%Cu/regular CeO ₂ (Calcined at 450 ⁰ C in air for 2h)	200	0	0
	220	0	0
	230	0	0
	240	0.11	40.2
	250	0.23	37.1
	270	0.66	30.7
	300	1.7	22.6
	320	6.2	5.4
	350	8.7	0.5
2%Au-2%Cu/regular SiO ₂ (Calcined at 450 ⁰ C in air for 2h)	200	0.06	30.5
	220	0.18	28.2
	230	0.44	21.4
	240	0.67	15.2
	250	1.2	10.8
	270	2.3	7.3
	300	4.5	2.1
	320	6.9	0.8
	350	8.8	0.2

^a catalysts prepared by a single impregnation method

5.3.6 Propene oxidation over supported Cu-Ag catalysts

In this section, a series of supported Cu-Ag catalysts prepared by the one-step impregnation method have been studied. The data are summarized in **Table 5.22**. It has been found that only TiO₂-supported Cu-Ag is not selective for PO formation, although this catalyst is active for total oxidation of propene. All other supported Cu-Ag catalysts exhibit significant selectivity for PO formation.

Clearly, supported Cu-Ag catalysts after calcination in air or hydrogen are more selective for PO formation than those without calcination. Among these catalysts, Cu-Ag/ZnO and Cu-Ag/SiO₂ nanopowder catalysts, after calcination at 450⁰C in 5%H₂/Ar for 2h, provide very high selectivity to PO at low temperature (**Figure 5.26**). For example, PO selectivity, *ca.* 58-82%, has been achieved at propene conversion, *ca.* 0.1-2.4%, when using Cu-Ag/regular ZnO catalyst after calcination at 450⁰C in 5%H₂/Ar for 2h. In addition, it should be noted that similar catalytic activity has also been obtained over Cu-Ag/ZnO nanopowder catalyst after calcination at 450⁰C in 5%H₂/Ar for 2h. This is quite reasonable since regular ZnO support has very similar surface morphology compared to ZnO nanopowder support. Thus, the same preparation procedures should lead to the catalysts with similar catalytic activity for regular ZnO-supported Cu-Ag catalyst and nanopowder ZnO-supported Cu-Ag catalyst. Analogous catalytic activity has been observed for ZnO-supported Cu, Ag and Au-Cu catalysts, as has been shown above.

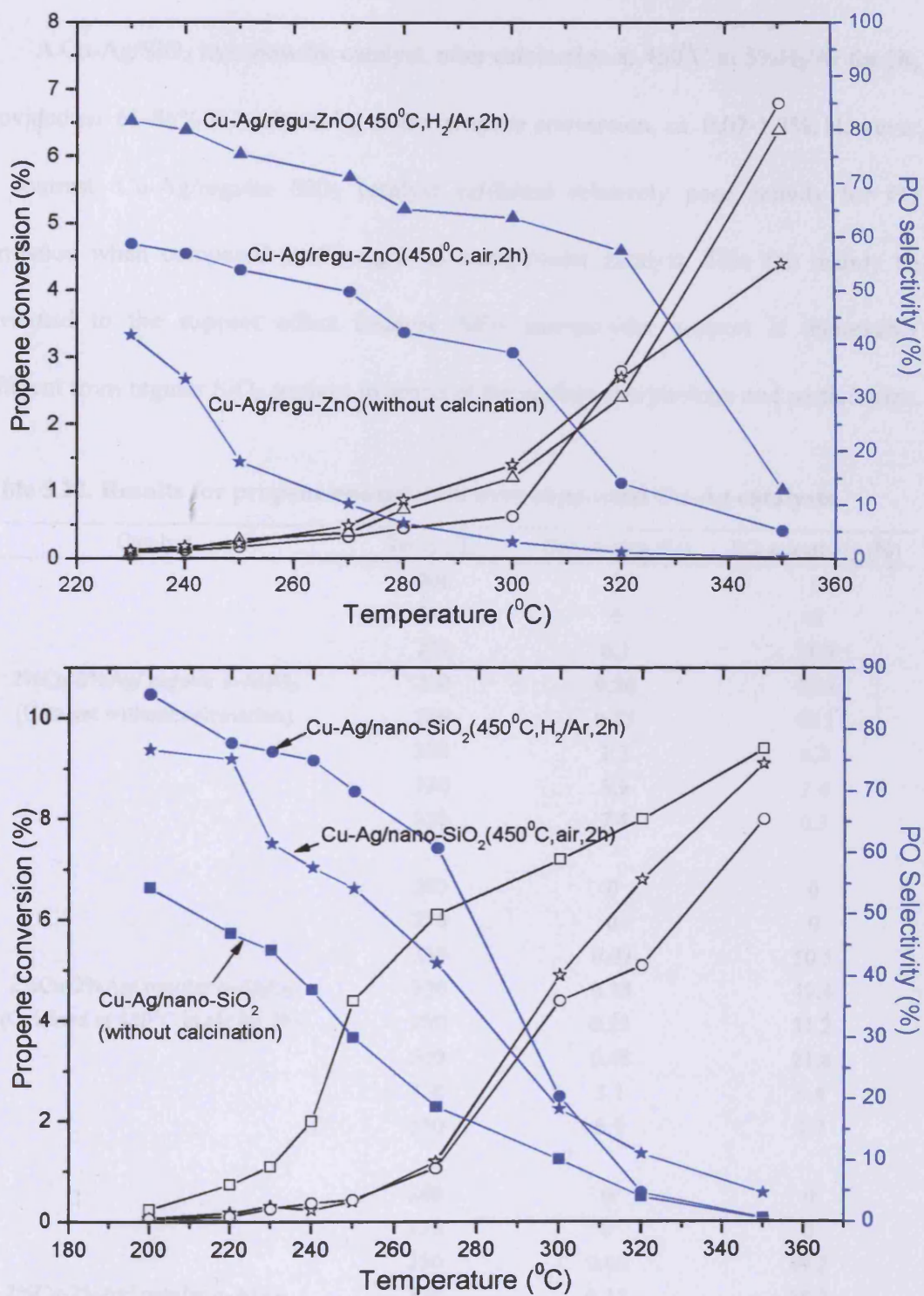


Fig.5.26 Results for catalytic activity of Cu-Ag/regular ZnO and Cu-Ag/SiO₂ nanopowder treated in different ways for propene epoxidation

A Cu-Ag/SiO₂ nanopowder catalyst, after calcination at 450⁰C in 5%H₂/Ar for 2h, provided *ca.* 61-86% PO selectivity at low propene conversion, *ca.* 0.07-1.2%. However, in contrast, Cu-Ag/regular SiO₂ catalyst exhibited relatively poor activity for PO formation when compared to Cu-Ag/SiO₂ nanopowder catalyst. This can mainly be attributed to the support effect because SiO₂ nanopowder support is remarkably different from regular SiO₂ support in terms of the surface morphology and particle size.

Table 5.22. Results for propene epoxidation over supported Cu-Ag catalysts

Catalyst	Temp (⁰ C)	Conversion (%)	PO selectivity (%)
2%Cu-2%Ag/ regular α -Al ₂ O ₃ (Catalyst without calcination)	200	0	0
	230	0	0
	250	0.1	21.3
	270	0.26	15.4
	280	0.55	10.1
	300	1.3	6.3
	320	3.9	2.4
	350	7.4	0.3
2%Cu-2%Ag/ regular α -Al ₂ O ₃ (Calcined at 450 ⁰ C in air for 2h)	200	0	0
	230	0	0
	250	0.09	50.5
	270	0.18	49.4
	280	0.25	31.2
	300	0.48	21.8
	320	3.1	9.4
	350	6.5	2.7
2%Cu-2%Ag/ regular α -Al ₂ O ₃ (Calcined at 450 ⁰ C in 5%H ₂ /Ar for 2h)	200	0	0
	230	0	0
	250	0.08	49.2
	270	0.15	25.2
	280	0.34	22.1
	300	0.55	18.2
	320	4.2	10.8
	350	7.6	6.4

Continued Table 5.22. Results for propene epoxidation over supported Cu-Ag catalysts

Catalyst	Temp ($^{\circ}$ C)	Conversion (%)	PO selectivity (%)
2%Cu-2%Ag/ regular γ -Al ₂ O ₃ (Catalyst without calcination)	200	0	0
	230	0	0
	250	0.12	28.6
	270	0.32	20.3
	280	0.78	12.4
	300	1.7	7.6
	320	3.8	1.7
	350	7.9	0.2
2%Cu-2%Ag/ regular γ -Al ₂ O ₃ (Calcined at 450 $^{\circ}$ C in air for 2h)	200	0	0
	230	0	0
	250	0.1	52.6
	270	0.3	49.1
	280	0.74	33.5
	300	2.2	19.4
	320	3.9	7.2
	350	8.1	0.3
2%Cu-2%Ag/ regular γ -Al ₂ O ₃ (Calcined at 450 $^{\circ}$ C in 5%H ₂ /Ar for 2h)	200	0	0
	230	0	0
	250	0.15	47.8
	270	0.48	27.3
	280	1.2	20.1
	300	2.8	13.4
	320	4.3	8.1
	350	8.6	0.2

Continued Table 5.22. Results for propene epoxidation over supported Cu-Ag catalysts

Catalyst	Temp ($^{\circ}$ C)	Conversion (%)	PO selectivity (%)
2%Cu-2%Ag/ Al ₂ O ₃ nanopowder-2 (Catalyst without calcination)	200	0	0
	230	0	0
	250	0.08	25.4
	270	0.16	20.3
	280	0.66	15.6
	300	1.5	8.2
	320	3.4	2.1
	350	6.9	0.8
2%Cu-2%Ag/ Al ₂ O ₃ nanopowder-2 (Calcined at 450 $^{\circ}$ C in air for 2h)	200	0	0
	230	0	0
	250	0.09	50.2
	270	0.15	47.2
	280	0.64	34.1
	300	1.3	17.3
	320	3.1	7.9
	350	6.2	0.2
2%Cu-2%Ag/ Al ₂ O ₃ nanopowder-2 (Calcined at 450 $^{\circ}$ C in 5%H ₂ /Ar for 2h)	200	0	0
	230	0.1	0
	250	0.16	45.2
	270	0.27	40.2
	280	0.96	18.7
	300	2.0	9.2
	320	3.8	3.6
350	7.7	0.1	

Continued Table 5.22. Results for propene epoxidation over supported Cu-Ag catalysts

Catalyst	Temp ($^{\circ}$ C)	Conversion (%)	PO selectivity (%)
2%Cu-2%Ag/ regular ZnO (Catalyst without calcination)	200	0	0
	230	0.12	41.7
	240	0.18	33.4
	250	0.22	18.1
	270	0.49	10.2
	280	0.87	6.6
	300	1.4	3.1
	320	2.7	1.2
	350	4.4	0.3
2%Cu-2%Ag/ regular ZnO (Calcined at 450 $^{\circ}$ C in air for 2h)	200	0	0
	230	0.09	58.7
	240	0.12	56.9
	250	0.17	53.9
	270	0.32	49.8
	280	0.45	42.2
	300	0.63	38.4
	320	2.8	14.1
	350	6.8	5.2
2%Cu-2%Ag/ regular ZnO (Calcined at 450 $^{\circ}$ C in 5%H $_2$ /Ar for 2h)	200	0	0
	230	0.09	81.7
	240	0.14	80
	250	0.28	75.5
	270	0.38	71.2
	280	0.73	65.3
	300	1.2	63.6
	320	2.4	57.5
	350	6.4	12.8

Continued Table 5.22. Results for propene epoxidation over supported Cu-Ag catalysts

Catalyst	Temp ($^{\circ}$ C)	Conversion (%)	PO selectivity (%)
2%Cu-2%Ag/ZnO nanopowder (Catalyst without calcination)	200	0	0
	230	0.11	43.5
	240	0.16	35.3
	250	0.22	19.6
	270	0.52	12.0
	280	0.90	8.6
	300	1.3	3.5
	320	2.8	1.5
	350	4.7	0.5
2%Cu-2%Ag/ZnO nanopowder (Calcined at 450 $^{\circ}$ C in air for 2h)	200	0	0
	230	0.1	59.5
	240	0.12	57.8
	250	0.15	54.6
	270	0.34	50.7
	280	0.48	43.4
	300	0.68	36.5
	320	2.7	16.3
	350	6.9	6.1
2%Cu-2%Ag/ZnO nanopowder (Calcined at 450 $^{\circ}$ C in 5% H_2 /Ar for 2h)	200	0	0
	230	0.1	80.8
	240	0.16	79.2
	250	0.29	76.8
	270	0.43	73.1
	280	0.79	65.8
	300	1.4	61.2
	320	2.8	55.8
	350	7.0	10.2

Continued Table 5.22. Results for propene epoxidation over supported Cu-Ag catalysts

Catalyst	Temp ($^{\circ}$ C)	Conversion (%)	PO selectivity (%)
2%Cu-2%Ag/SiO ₂ nanopowder (Catalyst without calcination)	200	0.25	54.3
	220	0.74	46.9
	230	1.1	44.2
	240	2	37.8
	250	4.4	30.1
	270	6.1	18.8
	300	7.2	10.2
	320	8	4.1
	350	9.4	0.6
2%Cu-2%Ag/SiO ₂ nanopowder (Calcined at 450 $^{\circ}$ C in air for 2h)	200	0.07	76.7
	220	0.11	75.2
	230	0.26	61.5
	240	0.38	57.6
	250	0.44	54.2
	270	1.07	42.1
	300	4.4	18.4
	320	5.1	11.1
	350	8	4.7
2%Cu-2%Ag/SiO ₂ nanopowder (Calcined at 450 $^{\circ}$ C in 5%H ₂ /Ar for 2h)	200	0.07	85.7
	220	0.18	77.8
	230	0.31	76.4
	240	0.24	75
	250	0.4	70
	270	1.2	60.8
	300	4.9	20.5
	320	6.8	4.8
	350	9.1	0.6

Continued Table 5.22. Results for propene epoxidation over supported Cu-Ag catalysts

Catalyst	Temp ($^{\circ}$ C)	Conversion (%)	PO selectivity (%)
2%Cu-2%Ag/regular SiO ₂ (Catalyst without calcination)	200	0	0
	220	0	0
	230	0.12	41.7
	250	0.22	18.1
	270	0.49	10.2
	300	1.1	4.8
	350	2.6	0.7
2%Cu-2%Ag/ regular SiO ₂ (Calcined at 450 $^{\circ}$ C in air for 2h)	200	0	0
	220	0	0
	230	0	0
	250	0	0
	270	0	0
	300	0.13	46.8
	350	0.38	34.2
2%Cu-2%Ag/ regular SiO ₂ (Calcined at 450 $^{\circ}$ C in 5%H ₂ /Ar for 2h)	200	0	0
	220	0	0
	230	0	0
	250	0	0
	270	0	0
	300	0.11	56.5
	350	0.26	39.7

Continued Table 5.22. Results for propene epoxidation over supported Cu-Ag catalysts

Catalyst	Temp ($^{\circ}$ C)	Conversion (%)	PO selectivity (%)
2%Cu-2%Ag/TiO ₂ (P25) (Catalyst without calcination)	220	0.06	0
	230	0.1	0
	240	0.13	0
	250	0.24	0
	260	2.1	0
	270	5.2	0
	300	7.3	0
	320	8.4	0
	350	8.9	0
2%Cu-2%Ag/TiO ₂ (P25) (Calcined at 450 $^{\circ}$ C in air for 2h)	220	0.06	0
	230	0.8	0
	240	1.7	0
	250	3.7	0
	260	4.9	0
	270	5.2	0
	300	6.9	0
	320	7.9	0
	350	8.8	0
2%Cu-2%Ag/TiO ₂ (P25) (Calcined at 450 $^{\circ}$ C in 5%H ₂ /Ar for 2h)	220	0.12	0
	230	1.4	0
	240	3.1	0
	250	6.1	0
	260	6.9	0
	270	8.2	0
	300	8.9	0
	320	9.2	0
	350	9.4	0

Recently, Barteau's research group reported a density functional theory (DFT) study on the design of Cu-Ag bimetallic catalysts for ethene epoxidation; they suggested that Cu-Ag catalysts should be much more selective for ethene epoxidation than Ag catalyst alone [38]. This prediction has been confirmed by subsequent research work on the direct ethene epoxidation using molecular oxygen over Cu-Ag bimetallic catalysts prepared by an impregnation method [39,40].

In view of these results, it is interesting to compare the catalytic activity of the present Cu-Ag catalysts for propene epoxidation with monometallic supported Ag or Cu catalysts. Cu-Ag catalysts supported on regular ZnO and SiO₂ nanopowder have been selected as typical cases in comparison with Ag or Cu catalyst alone, because these two supported Cu-Ag catalysts provide very highly selective activity for PO formation. Supported Ag or Cu catalysts were prepared by an impregnation method, followed by calcination in 5%H₂/Ar at 450⁰C for 2h, similar to that for Cu-Ag catalysts supported on regular ZnO and SiO₂ nanopowder. Comparative data over supported Cu, Ag and Cu-Ag catalysts are shown in **Figure 5.27**. Clearly, under the same reaction conditions, a supported Cu-Ag catalyst is much more selective than a supported Cu or Ag catalyst alone. Furthermore, it can be seen that the supported Cu catalyst is more selective compared to the supported Ag catalyst. These results demonstrate that there is a great scope to design and optimize supported Cu-Ag bimetallic catalysts for direct propene epoxidation, because they exhibit very promising catalytic performance for PO formation.

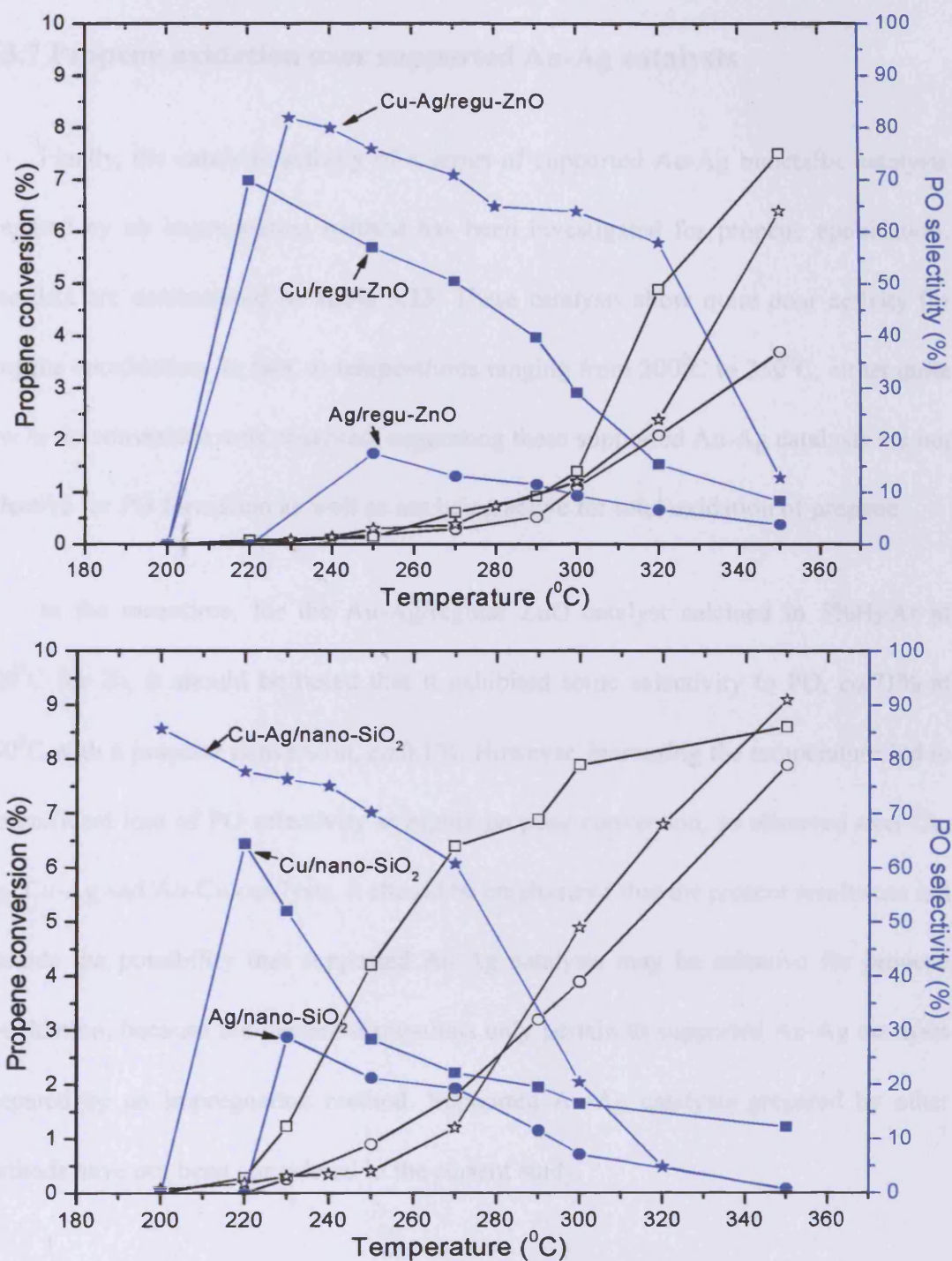


Fig.5.27 Comparison of catalytic activity of Cu-Ag/regular ZnO and Cu-Ag/SiO₂ nanopowder catalysts with supported Cu or Ag catalysts; these catalysts were prepared by similar impregnation methods followed by calcination in 5%H₂/Ar at 450°C for 2h

5.3.7 Propene oxidation over supported Au-Ag catalysts

Finally, the catalytic activity of a series of supported Au-Ag bimetallic catalysts prepared by an impregnation method has been investigated for propene epoxidation. The data are summarized in **Table 5.23**. These catalysts show quite poor activity for propene epoxidation. In fact, at temperatures ranging from 200⁰C to 350⁰C, either quite low or no conversion was observed, suggesting these supported Au-Ag catalysts are not selective for PO formation as well as not being active for total oxidation of propene.

In the meantime, for the Au-Ag/regular ZnO catalyst calcined in 5%H₂/Ar at 450⁰C for 2h, it should be noted that it exhibited some selectivity to PO, *ca.*71% at 350⁰C with a propene conversion, *ca.*0.1%. However, increasing the temperature led to a significant loss of PO selectivity at higher propene conversion, as observed over Cu, Ag, Cu-Ag and Au-Cu catalysts. It should be emphasized that the present results can not exclude the possibility that supported Au-Ag catalysts may be selective for propene epoxidation, because the present discussions only pertain to supported Au-Ag catalysts prepared by an impregnation method. Supported Au-Ag catalysts prepared by other methods have not been considered in the current study.

Table 5.23. Results for propene epoxidation over supported Au-Ag catalysts

Catalyst	Temp ($^{\circ}$ C)	Conversion (%)	PO selectivity (%)
2%Au-2%Ag/regular α -Al ₂ O ₃ (Catalyst without calcination)	200	0	0
	220	0	0
	230	0	0
	250	0	0
	270	0	0
	300	0	0
	320	0	0
	350	Trace	0
2%Au-2%Ag/regular α -Al ₂ O ₃ (Calcined at 450 $^{\circ}$ C in air for 2h)	200	0	0
	220	0	0
	230	0	0
	250	0	0
	270	0	0
	300	0	0
	320	Trace	0
	350	Trace	0
2%Au-2%Ag/regular α -Al ₂ O ₃ (Calcined at 450 $^{\circ}$ C in 5%H ₂ /Ar for 2h)	200	0	0
	220	0	0
	230	0	0
	250	0	0
	270	0	0
	300	0.05	0
	320	0.8	0
	350	3.8	0

Continued Table 5.23. Results for propene epoxidation over supported Au-Ag catalysts

Catalyst	Temp ($^{\circ}$ C)	Conversion (%)	PO selectivity (%)
2%Au-2%Ag/regular ZnO (Catalyst without calcination)	200	0	0
	220	0	0
	230	0	0
	250	0	0
	270	0	0
	300	0	0
	320	0	0
	350	0	0
2%Au-2%Ag/regular ZnO (Calcined at 450 $^{\circ}$ C in air for 2h)	200	0	0
	220	0	0
	230	0	0
	250	0	0
	270	0	0
	300	0	0
	320	0	0
	350	Trace	0
2%Au-2%Ag/regular ZnO (Calcined at 450 $^{\circ}$ C in 5%H $_2$ /Ar for 2h)	200	0	0
	220	0	0
	230	0	0
	250	0	0
	270	0	0
	300	0	0
	320	0	0
	350	0.13	71.2
370	0.26	54.5	
400	1.2	18.3	

Continued Table 5.23. Results for propene epoxidation over supported Au-Ag catalysts

Catalyst	Temp ($^{\circ}$ C)	Conversion (%)	PO selectivity (%)
2%Au-2%Ag/TiO ₂ (P25) (Catalyst without calcination)	200	0	0
	220	0	0
	230	0	0
	250	0	0
	270	0	0
	300	0	0
	320	0	0
	350	0.17	0
2%Au-2%Ag/TiO ₂ (P25) (Calcined at 450 $^{\circ}$ C in air for 2h)	200	0	0
	220	0	0
	230	0	0
	250	0	0
	270	0	0
	300	0	0
	320	0.07	0
	350	0.48	0
2%Au-2%Ag/TiO ₂ (P25) (Calcined at 450 $^{\circ}$ C in 5%H ₂ /Ar for 2h)	200	0	0
	220	0	0
	230	0	0
	250	0	0
	270	0	0
	300	0	0
	320	0.12	0
	350	0.74	0

Continued Table 5.23. Results for propene epoxidation over supported Au-Ag

catalysts

Catalyst	Temp ($^{\circ}$ C)	Conversion (%)	PO selectivity (%)
2%Au-2%Ag/SiO ₂ nanopowder (Catalyst without calcination)	200	0	0
	250	0	0
	270	0	0
	300	0	0
	320	0	0
	350	0	0
2%Au-2%Ag/SiO ₂ nanopowder (Calcined at 450 $^{\circ}$ C in air for 2h)	200	0	0
	250	0	0
	270	0	0
	300	0	0
	320	0.21	0
	350	0.96	0
2%Au-2%Ag/SiO ₂ nanopowder (Calcined at 450 $^{\circ}$ C in 5%H ₂ /Ar for 2h)	200	0	0
	250	0	0
	270	0	0
	300	0.23	0
	320	0.88	0
	350	1.5	0
2%Au-2%Ag/regular CeO ₂ (Catalyst without calcination)	250	0	0
	270	0	0
	300	0.12	0
	320	0.23	0
	350	0.87	0
2%Au-2%Ag/ regular CeO ₂ (Calcined at 450 $^{\circ}$ C in air for 2h)	250	0	0
	270	0.11	0
	300	0.26	0
	320	0.78	0
	350	1.9	0
2%Au-2%Ag/ regular CeO ₂ (Calcined at 450 $^{\circ}$ C in 5%H ₂ /Ar for 2h)	250	0	0
	270	0.08	0
	300	0.19	0
	320	0.35	0
	350	1.2	0

5.4. Conclusions

In summary, the heterogeneous catalytic oxidation of propene to PO has been investigated over supported Ag, Cu and Au catalysts, and bimetallic (Au-Cu, Cu-Ag and Au-Ag) catalysts using only molecular oxygen as oxidant. Several important conclusions can be drawn.

Supported Ag catalysts generally provide low PO selectivity, typically lower than 40%; only for Ag/SiO₂ nanopowder catalyst, a high selectivity to PO, *ca.* 74%, has been obtained. Supported Ag catalysts with calcinations in air or hydrogen lead to catalysts with decreased PO selectivity, suggesting a high oxidation state of Ag favors PO formation.

Supported Cu catalysts are active for selective propene epoxidation and can exhibit either comparable or better catalytic performance than Ag catalysts. The most selective catalyst (*ca.* 81% PO selectivity) is Cu supported on SiO₂ nanopowder. This suggests that there is a broad scope to explore Cu-based materials as inexpensive potential catalysts for propene epoxidation. In addition, it has been found that supported Cu catalysts calcined in hydrogen exhibit lower PO selectivity than those without calcination or with calcination in air. This suggests that the primary active phase should be cationic Cu rather than metallic Cu. In contrast, supported Au catalysts generally provide poor PO selectivity when using only molecular oxygen as oxidant.

Among supported bimetallic catalysts, Au-Cu/ZnO can provide stable and high selectivity to PO, *ca.* 93%, at low temperature. The catalytic performance is much better than supported Cu or Au alone. Supported Cu-Ag catalysts are able to exhibit better performance than supported Ag or Cu catalyst alone. However, supported Au-Ag catalysts are poorly active for propene epoxidation. These results suggest that there is a broad scope to design and optimize supported bimetallic catalysts with high PO selectivity.

Finally, it should be noted that the intrinsic instability of PO leads to the observation of high selectivity for all these catalysts only at low temperature.

5.5. References and notes

- [1] Lambert, R. M.; Williams, F.; Copley, R. L.; Palermo, A. *J. Mol. Catal. A* **2005**, 228, 27.
- [2] Barteau, M. A. *Topic. Catal.* **2003**, 22, 3.
- [3] Sinha, A. K.; Seelan, S.; Tsubota, S.; Haruta, M. *Topic. Catal.* **2004**, 29, 95.
- [4] Xi, Z.; Zhou, N.; Sun, Y.; Li, K. *Science* **2001**, 292, 1139.
- [5] Trent, D. L. *Propene oxide. In Kirk-Othmer: Encyclopedia of Chemical Technology*, Wiley, New York, 2001.
- [6] Ainsworth, S. J. *Chem. Eng. News* **1992**, 9.
- [7] McCoy, M. *Chem. Eng. News* **2001**, 19.
- [8] Clerici, M. G.; Bellussi, G.; Romano, U. *J. Catal.* **1991**, 129, 159.
- [9] Tullo, A. Dow. *Chem. Eng. News* **2004**, 82, 15.
- [10] Pennington, B. T.; Fullington, M. C. U.S. Patent No. 4943643, 1990.
- [11] Iwasawa, Y.; Nakamura, T.; Takamatsu, K.; Ogasawara, S. *J. Chem. Soc. Faraday Trans., 1* **1980**, 79, 939.
- [12] Ananieva, E.; Reitzmann, A. *Chem. Eng. Sci.* **2004**, 59, 5509.
- [13] Panov, G. T.; Sheveleva, G. A.; Kharitonov, A. S.; Romannikov, V. N.; Vostrikova, L. A. *Appl. Catal. A* **1992**, 82, 31.
- [14] Wang, X.; Zhang, Q.; Guo, Q.; Lou, Y.; Yang, L.; Wang, Y. *Chem. Commun.* **2004**, 1396.
- [15] Wang, X.; Zhang, Q.; Yang, S.; Wang, Y. *J. Phys. Chem. B* **2005**, 109, 23500.
- [16] Hayashi, T.; Tanaka, K.; Haruta, M. *J. Catal.* **1998**, 178, 256.

- [17] Sinha, A. K.; Seelan, S.; Tsubota, S.; Haruta, M. *Angew. Chem. Int. Ed.* **2004**, 43, 1546.
- [18] Nijhuis, T. A.; Weckhuysen, B. M. *Chem. Commun.* **2005**, 48, 6002.
- [19] Nijhuis, T. A.; Visser, T.; Weckhuysen, B. M. *J. Phys. Chem. B* **2005**, 109, 19309.
- [20] Vaughan, O. P. H.; Kyriakou, G.; Macleod, N.; Tikhov, M.; Lambert, R. M. *J. Catal.* **2005**, 236, 401.
- [21] Lu, J.; Luo, M.; Lei, H.; Bao, X.; Li, C. *J. Catal.* **2002**, 211, 552.
- [22] Chu, H.; Yang, L.; Zhang, Q.; Wang, Y. *J. Catal.* **2006**, 241, 225.
- [23] Bengter, H.; Tengroth, C.; Jacobsson, S. P. *J. Raman Spectroscopy* **2005**, 36, 1015.
- [24] Lu, G.; Zuo, X. *Catal. Lett.* **1999**, 58, 67.
- [25] Lu, J.; Bravo-Suárez, J. J.; Takahashi, A.; Haruta, M.; Oyama, S. T. *J. Catal.* **2005**, 232, 85.
- [26] Lu, J. Q.; Luo, M. F.; Lei, H.; Li, C. *Appl. Catal. A* **2002**, 237, 11.
- [27] Palermo, A.; Husain, A.; Tikhov, M. S.; Lambert, R. M. *J. Catal.* **2002**, 207, 331.
- [28] Akimoto, M.; Ichikawa, K.; Echigoya, E. *J. Catal.* **1982**, 76, 333.
- [29] Lambert, R. M.; Williams, F. J.; Copley, R. L.; Palermo, A. *J. Mol. Catal. A* **2005**, 228, 27.
- [30] Copley, R. L.; Williams, F. J.; Urquhart, A. J.; Vaughan, O. P. H.; Tikhov, M. S.; Lambert, R. M. *Surf. Sci.* **2005**, 578, L85.
- [31] Copley, R. L.; Williams, F. J.; Vaughan, O. P. H.; Urquhart, A. J.; Tikhov, M. S.; Lambert, R. M. *J. Am. Chem. Soc.* **2005**, 127, 6069.
- [32] Hayashi, T.; Tanaka, K.; Haruta, M. *J. Catal.* **1998**, 178, 566.

- [33] Enache, D. T.; Edwards, J. K.; Landon, P.; Solsona, B. E.; Carley, A. F.; Herzing, A. A.; Watanabe, M.; Kiely, C. J.; Knight, D. W.; Hutchings, G. J. *Science* **2006**, 311, 362.
- [34] Edwards, J. K.; Solsona, B.; Landon, P.; Carley, A. F.; Herzing, A.; Kiely, C. J.; Hutchings, G. J. *J. Catal.* **2005**, 236, 69.
- [35] Edwards, J. K.; Solsona, B.; Landon, P.; Carley, A. F.; Herzing, A.; Watanabe, M.; Kiely, C. J.; Hutchings, G. J. *J. Mater. Chem.* **2005**, 15, 4595.
- [36] Landon, P.; Collier, P. J.; Papworth, A. J.; Kiely, C. J.; Hutchings, G. J. *Chem. Commun.* **2002**, 2058.
- [37] Landon, P.; Collier, P. J.; Carley, A. F.; Chadwick, D.; Papworth, A. J.; Burrows, A.; Kiely, C. J.; Hutchings, G. J. *Phys. Chem. Chem. Phys.* **2003**, 5, 1917.
- [38] Linic, S.; Jankowiak, J.; Barteau, M. A. *J. Catal.* **2004**, 224, 489.
- [39] Jankowiak, J.; Barteau, M. A. *J. Catal.* **2005**, 236, 366.
- [40] Jankowiak, J.; Barteau, M. A. *J. Catal.* **2005**, 236, 379.

Chapter Six

Summary, Conclusion and Future Work

6.1. Summary and conclusion

In this thesis, heterogeneous selective oxidation of hydrocarbons, both in liquid phase and gas phase, has been investigated in detail. Summarizing the results, the main conclusions can be drawn as the following:

(a) For liquid phase reactions, it has been found that supported Au catalysts can provide tuneable activity for selective oxidation of cyclohexene and cis-cyclooctene. Over supported nano-crystalline gold catalysts with a small amount of TBHP as initiator, selective oxidation reactions to target oxygenated products can be readily kick-started.

By choosing the appropriate solvent, the selectivity to partial oxidation products can be finely tailored. In particular, extremely high selectivity, *ca.* 98%, for partial oxidation products with significant conversion has been obtained using a Bi-modified gold catalyst for selective oxidation of cyclohexene. XPS analysis has shown that only a small amount of Bi is needed for the most selective Au catalyst. An analogous effect of enhancing selectivity for partial oxidation products has been found over supported gold catalyst modified by Sn, Sb or Pb. This suggests that there is a significant scope to design and optimize supported gold catalysts with appropriate promoters in order to obtain highly selective supported gold catalysts for selective oxidation.

For cis-cyclooctene oxidation, similar tuning behaviour has also been found in the presence of solvents over supported Au catalysts. More interestingly, high selectivity to partial oxidation products has also been achieved at a high rate of reaction, without the use of solvent, which is a major tenet of green chemistry. Such a gold catalyst is also very highly selective for oxidation of cyclohexane to cyclohexanol and cyclohexanone under mild conditions. However, the selectivity to cyclohexanol and cyclohexanone observed is solely a function of conversion, which in turn is a function of reaction time.

(b) The gas-phase epoxidation of propene to propene epoxide (PO) has been studied over a series of supported Ag, Cu, Au and bimetallic (Au-Cu, Cu-Ag and Au-Ag) catalysts using only molecular oxygen as oxidant.

A support effect has been found on catalyst performance for selective propene epoxidation. With respect to supported Ag catalysts, PO selectivity is typically lower than 40%. However, a highly selective catalyst is Ag supported on a SiO₂ nanopowder, which can provide the selectivity to PO, *ca.* 74%. Calcination in air or hydrogen leads to a poorly selective catalyst for propene epoxidation and this indicates that Ag in a highly oxidized state favours PO formation. Supported Cu catalysts are also active for selective propene epoxidation and can exhibit either comparable or better catalytic performance than Ag catalysts. The most selective catalyst (*ca.* 81% PO selectivity) is Cu supported on a SiO₂ nanopowder followed by calcination in air. This suggests that there is a broad scope to explore Cu-based materials as inexpensive potential catalysts for propene epoxidation. On the other hand, it has been found that supported Au catalysts generally

provide poor activity for propene epoxidation.

Among supported bimetallic catalysts, Au-Cu/ZnO can provide stable performance and high selectivity to PO, *ca.* 93%, at low temperature. The catalytic performance is much better than supported Cu or Au alone. Supported Cu-Ag catalysts are able to give higher yields for propene epoxidation compared to supported Ag or Cu catalysts alone. Similarly, an analogous effect of improved selectivity has been observed in the literature with respect to oxidation of ethene to ethene oxide (EO) over supported Cu-Ag catalysts as compared to supported Ag catalyst alone. A support effect has been found for supported Au-Cu and Cu-Ag catalysts for propene epoxidation, which is similar to supported Ag and Cu catalysts. Nevertheless, supported Au-Ag catalysts are poorly active for propene epoxidation. These results suggest that there is a broad scope to carry out further studies on selective oxidation of propene to PO over supported bimetallic catalysts. Information derived would be valuable for designing supported bimetallic catalysts with optimal activity and selectivity for propene epoxidation.

Finally, it should be noted that the intrinsic instability of PO leads to the observation of high selectivity for all these catalysts only at low temperature. Increasing the temperature leads to higher propene conversion but less selectivity for propene epoxidation.

6.2. Future work

The work in this thesis has demonstrated that supported Au catalysts could be used as potential and promising heterogeneous catalysts for selective oxidation of hydrocarbons under mild conditions. It could be expected that supported Au catalysts may find their novel and unique applications in many respects in the coming years given the current significant interest in gold catalysis. In particular, the field of catalysis by Au is just beginning to open up. Apart from the well documented oxidation of CO that is often used as a testing model reaction to understand active sites of supported gold catalysts, it could be expected that a rich redox chemistry of gold can make it a choice for many chemical reactions, such as selective oxidation, total oxidation, hydrogenation and dehydrogenation.

Supported Cu, Au-Cu and Cu-Ag catalysts can be very selective for one-step direct heterogeneous oxidation of propene to PO using only molecular oxygen as oxidant. In addition to traditional Ag catalysts for ethene oxidation, Cu catalysts can be used as an alternative for propene epoxidation. The results in this thesis have shown that supported Cu catalysts after calcination in air exhibit better catalytic activity than supported Ag catalysts. On the other hand, the results suggest that supported bimetallic catalysts could be used as another choice for propene epoxidation because they exhibit more selective catalytic performance as compared to supported Ag or Cu alone.

However, there is still a lot of work worthy of further systematic exploration in order to achieve catalysts with improved activity and selectivity and understand the

nature of active sites of catalysts. Following the work in this thesis, interesting studies on future work are proposed as the following:

- (a) A detailed study on the preparation and optimisation of supported Au catalysts with promoters in order to achieve optimal Au catalysts. This will help to obtain a more selective catalyst for partial oxidation of alkenes and cyclohexane to target oxygenated products. Meanwhile, the study on this aspect will contribute to find appropriate promoters for designing rational Au catalysts that exhibit specific and highly selective activity toward other chemical processes.
- (b) Further studies on the role of nano-crystalline Au particles in activating molecular oxygen for the selective oxidation of alkenes under mild conditions. This will tell us how nano-crystalline Au particles activate molecular oxygen under mild conditions and how Au particles play their role in the selective oxidation of alkenes. Consequently, it will provide us with a valuable roadmap for pursuing green and sustainable chemistry through control of the reactivity of oxygen.
- (c) Study of supported Au catalysts using different supports such as TiO_2 , ZnO and Fe_2O_3 for the selective oxidation of alkenes and cyclohexane, since a support effect has been well known for Au catalysts. Investigations on this aspect will aim to look at the support effect and the interface effect between gold nanoparticles and support. This will help us to understand how Au

nanoparticles work for selective oxidation reactions and the role of support during the reaction.

- (d) Study of preparation methods for supported Cu, Cu-Ag and Au-Cu catalysts regarding the selective epoxidation of propene to PO in order to consider the effect of preparation methods on the catalytic performance of catalysts. In the current work, impregnation methods are primarily tested. Presumably, other preparation methods would lead to more active and selective catalysts for propene epoxidation. Since a catalyst prepared by different methods feature a specific microscopic structure, it would exhibit different catalytic activity toward propene epoxidation. Investigations in this regard not only help to find more selective catalysts for propene epoxidation, but also contribute to establish a general relationship between catalyst structure and catalytic reactivity.
- (e) Optimization of the formulation of supported bimetal catalysts, mainly supported Cu-Ag and Au-Cu catalysts, which aims to improve the activity and selectivity of catalysts for propene epoxidation. This is a very important factor for influencing the catalytic activity of supported bimetallic catalysts.
- (f) For propene epoxidation, it is worthwhile to study the effect of different volume ratios of helium:propene:oxygen for propene epoxidation. In addition, it is interesting to study reaction profiles with different GHSV. Studies on this aspect would contribute to optimize the reaction conditions

for propene epoxidation. The appropriate choice of reaction conditions is a key factor for the function of catalyst because, even for a good catalyst, improper reaction conditions can lead to an observation of poor selectivity for PO formation.

- (g) A detailed study on the effect of calcination on the catalytic performance for propene epoxidation. In this thesis, catalysts are only calcined in air or hydrogen/helium at 450⁰C for 2h. Other calcination conditions have not been considered. Since heat treatment is a key factor for influencing the catalytic performance for heterogeneous catalysts, detailed studies on this aspect could be very crucial to obtain a stable, durable and highly active catalyst for propene epoxidation. For example, it has been mentioned in the introduction section that an Au/Fe₂O₃ catalyst after two-step heat pretreatment can be used as an excellent catalyst for CO oxidation under fuel-cell conditions. Au/Fe₂O₃ catalysts have been widely studied previously; however, it has not been found that this catalyst can be very efficient for CO oxidation under fuel-cell conditions until recently.
- (h) Study on the nature of active sites of supported Cu catalysts for propene epoxidation. Although recently several works have suggested supported Cu catalysts can be used as inexpensive materials for propene epoxidation using only molecular oxygen as oxidant, the active sites of supported Cu catalysts are still unclear. Earlier work proposed that metallic Cu may be the active

phase; however, the latest work suggests that cationic Cu may be the active phase.

- (i) To characterize the microscopic structure of the most selective Au-Cu catalysts by means of TEM and XPS analysis. The information gained from TEM and XPS analysis would help to understand the geometric and electronic structure of Au-Cu catalysts, and the microscopic composition of catalysts. As a result, this will help to understand the relationship between structure and activity for selective oxidation of propene to PO, and in turn to design catalysts with superior performance for propene epoxidation.

- (j) Another worthy aspect of major importance with respect to the direction of future work is the nature of the factors that are responsible for limiting the selectivity to target partial oxidation products as conversion increases. Although factors related to this fundamental issue are well known to be very complicated in heterogeneous catalysis reactions, their identification will be crucial if we are to make substantial progress in selective oxidation. This issue has been attracting the attention of chemists in heterogeneous catalysis for many years, but there has been only limited progress to date. One reason for this is that when conversion increases, other competitive reactions, such as total oxidation, isomerization and rearrangement reactions also occur simultaneously, because generally the increase in conversion is obtained by using higher temperatures. However, two important strategies could be

worthy of exploration in order to overcome this issue. One is to try to learn what are active sites for total oxidation and what are active sites for selective oxidation. This will help to design better catalysts with more selective active sites. The other is to try to design multi-component catalysts with other dopants and in particular dopants that can block non-selective sites and promote the selective oxidation processes.

